ISAS - INTERNATIONAL SCHOOL
FOR ADVANCED STUDIES

Thesis submitted for the degree of
"Magister Philosophiae"

Evolution of massive stars with diffusive mixing

CANDIDATE:
Licai Deng

SUPERVISOR:
Prof. D. Sciama
CO-SUPERVISOR
Prof. C. Chiosi

Academic Year 1990/91
ISAS/SISSA

TRIESTE

SISSA - SCUOLA
INTERNAZIONALE
SUPERIORE
I STUDI AVANZATI
TRIESTE
Strada Costiera 11

Thesis submitted for the degree of
"Magister Philosophiae"

Evolution of massive stars with diffusive mixing

CANDIDATE:
Licai Deng

SUPERVISOR:
Prof. D. Sciama
CO-SUPERVISOR
Prof. C. Chiosi

Academic Year 1990/91
ISAS/SISSA

Contents

Chapter 1

Introduction

In this thesis, evolutionary tracks for 15, 20, 30 $M_{\odot}$ stellar models under different mixing assumptions are computed with the code of PADOVA stellar evolution group. Furthermore, some attempts are made using Xiong's (1985) method to treat stellar convection for intermediate mass stars also during this work. Finally a comparison between Xiong's hydrogen burning models of 15 $M_{\odot}$ is presented

As the evolution of massive stars depends very much on the chemical profiles built up by nuclear reactions and convective mixing in stellar interior, the treatment of mixing is a very critical point. Mixing of chemicals inside the convective cores, overshooting regions and semiconvective regions is important because it determines the chemical distributions, therefore affects evolutionary scenarios. Mixing may be treated separately by assuming its form and degree, or treated together with convection. Because the convective zones depend on what theory is to be accepted, the adopted theory of convection may explain the differences among theoretical models. Different convection theories give different descriptions of the thermodynamical properties of the convective regions, and more importantly, the different ways and different degrees of mixing which greatly affect the evolution of stars.

Conventionally, mixing is taken as an instant process in convective regions and mixing

there is complete. We also have some regions in stars, which are not stable against perturbations, such as the region outside the retreating convective cores of massive stars during the hydrogen burning phase. This requires some partial mixing in those regions as found for the first time by Schwarschild & Harm (1958), and was termed by *semiconvection*, for massive stars this was first studied by Chiosi & Summa (Case B in the work, 1970). The true physical reasons for this finding are not yet clear even at present time. One way to treat this mystery phenomenon was to acquire the fulfillment of some local convection criteria, either Schwarzschild's or Ledoux's as done by Chiosi & Summa, and compute chemical distribution under this condition. Partial mixing was also accepted as a diffusion process (cf. Simpson 1971, Eggleton 1972, Langer 1985), provided the diffusion coefficient by either chosen explicitly with some prescription (Langer 1985, Weaver 1978) or computed in each zone by checking the neutral stability condition adopted (Simpson 1970). Diffusion is a quite good way of treating all the mixing processes in stars if the diffusion coefficient is well chosen. Large enough value of the coefficient gives short mixing time scale and perfect flat profile as found in fully convective regions, while small coefficient could mimic the chemical profiles for partial mixing cases. And this treatment is a rather simple way to get the chemical distributions in stars and to reveal the problems related to mixing.

In this thesis I will assess the problem of mixing with diffusion for different cases.

Chapter 2 is mainly about the current major developments to the study of massive stars.

In chapter 3 I discuss the Mixing Length Theory and present some comments. Xiong's method and results on massive star evolution are summarized. A comparative study with the present method is presented here.

Chapter 4 describes diffusion process and the numerical treatment which is used for this work.

Based on the method described in chapter 4, the evolution of 20, 30 $M_{\odot}$ models are

computed. Chapter 5 is deserved to description of input physics used in this work, and discussions of the numerical results of the models. Conclusions of the present work and possible extensions are given in chapter 6.

The figures related to each chapter are put in the end of the chapter.

Chapter 2

Evolution of Massive Stars

Massive stars are defined as stars whose cores never go to a degenerate regime and burn all nuclear fuels quiescently. The minimum mass for this category of stars is 10-12 $M_{\odot}$ according to the standard model, the exact value depending on the chemical composition. The evolution of the stars in this mass interval is affected by many physical factors. These include mass loss from the surface through a stellar wind as observed, the mixing treatment and the extent of mixing. Different ways of taking into account these factors may produce very different evolutionary scenarios. The observation of supergiant stars gives us much information to help understand the evolution of massive stars. (see recent review by Chiosi et al 1991). Observation of luminous (massive) stars ($M_b < -7$) in the solar vicinity (within 2.5 Kpc from the sun) and in the Large Magellanic Cloud (LMC) highlight some evidence which offer constraints on the evolution theory of massive stars (Humphreys 1978, Humphreys & Davison 1979, Gamany et al 1982).

Humphreys & Davison (1979) pointed out for the first time that the most luminous blue stars are about a factor of six brighter than the most luminous red stars. This fact defines a luminousity boundary in the HR diagram (fig.5). Because stars evolves away from the main sequence to red side in the HR diagram at almost constant luminosity, this boundary may imply that either the evolution of these stars is so fast that we have hardly

hardly any opportunity to find them or that the most luminous stars never go to red but directly evolve into WR stars. The highest mass loss rates are found along this boundary (de Jager et al 1979), and the boundary itself is marked by some luminous blue variables. This implies that the evolution of stars should include heavy mass loss to account for the observational facts.

Another problem revealed by those observations is presented by the stars found in the blue Hertzsprung gap. A large number of stars is found in the region just to the red of the main sequence, while the theoretical expectation is that this region should be unpopulated because of the fast evolution of stars in this region . Some observational uncertaintities may be the cause for this problem such as the distance of individual galatic supergiants, individual reddening and colour excesses for LMC stars, which make the comparison between theory and observation less clear. On the other hand, the observations may also imply, besides the observational uncertainties, that the main sequence band has to be widened to reduce the gap. Dispersion in the initial chemical compostition may also affect the red edge of the main sequence band and the blue edge of the helium burning band, and makes the gap filled. It is clearly seen, with the help of the published evolutionary models with different compositions (Maeder 1990), that this effect cannot eliminate the gap completely.

A 'ledge' of blue stars found in the above observations, is clearly seen in the HR diagram of LMC supergiant stars (fig.5). The star density in the range $3.9 \leq log\mathrm{T}_{eff} \leq 4.2$, decreases redwards and forms a diagonal line (Fitzpatrik & Gamany 1990). Explanation of the ledge is that stars with intial mass 40-50 $M_{\odot}$ either perform an extended loop short before core helium exhaustion (case A of Chiosi & Summa [1970], semiconvection and mass loss of Langer [1990]), or slowly move redwards while burning helium in the core (Brunish & Truran 1982 a,b). Models with core overshoot and mass loss (Maeder and Meynet 1987, 88, 89, Maeder 1990) cannot be used here, because these models spend the whole core helium burning time in the red. The ledge and even the stars found in the

middle of the HR diagrams raise a problem for models with overshoot.

The ratio of red to blue supergiant stars in the luminosity range $-9.5 \leq M_b \leq -6.5$ is about 1:10 (Humphreys & McElroy 1984). As the link between blue supergiant stars and red supergiant stars is generally accepted, evolutionary models must acount for both the blue stars and red stars. Evolution theory should give the life-time ratio implied by the star counts, either through the blue-red-blue scenarios as most popularly viewed (Chiosi & Summa 1970), or blue-red ones (Brunish & Truran 1982 a,b).

The red Hertzsprung gap does not make particular difficulties to evolutionary models, the time to cross this gap is fairly short for all schemes. A lack of the massive stars close to zero age main sequence is found in the HR diagrams of supergiants. This is explained by the fact that stars are not observable during the first 20% of their core hydrogen burning life time, because they are located in the circumstellar gas from which they formed. As this period is at least comparable to the total life time of post main sequence stages, this point together with photometric incompleteness make a big uncertainty to the comparison of theoretical results to observed star frequencies.

Star counts in different areas of the HR diagram of supergiant stars (Meylan & Maeder 1982, Bertelli et al 1984) suggests that there must be an extension of the main sequence band. Theoretical aspects for this extension are mass loss by stellar wind and its effects on the atmosphere, core convective overshoot, and the underestimate of radiative opacity in the CNO ionization region (Bertelli et al 1984). The observed shape of the main sequence band serves as an important constraint on the core overshoot models, as argued by many authors. (Chiosi et al 1978, Bressan et al 1981, Bertelli et al 1984, Maeder & Meynet 1987)

The observation of supergiant stars offers many opportunities to test evolutionary models. To account for all the observed properties, much theoretical effort has to be made. Among all the recent theoretical approaches to the evolution of massive stars, mass loss (which is a directly observed phenomenon), overshoot from convective core and

semiconvection are the most discussed topics. For the present work I will be concentrating on these factors.

2.1 Semiconvection

In this mass region, the evolution of stars is affected by the problem of semiconvection, which was first recognized by Schwarzschild & Härm (1958). In these stars during central hydrogen burning, the convective cores retreat, leaving behind a certain chemical profile. The radiative gradient ∇_{rad} in the region outside the core, where the hydrogen content grows outwards, starts to rise and soon exceeds the adiabatic gradient ∇_{ad}. This makes the region dynamically unstable. This problem is removed if we introduce some partial mixing, which equalizes the above two gradients (temperature neutrality condition, related to standard Schwarzschild criterion). Noting the existence of a gradient of molecular weight, Sakashita & Hayashi (1958, 1961) argued that neutrality should be taken with a density criterion, which is proposed by Ledoux (1947). Kato (1966) using a local analysis, pointed out that the density condition should be applied with the presence of a gradient in molecular weight. Langer et al (1983) developed a method to treat this partial mixing with diffusion. They found that, in a region with

$$\nabla_{ad} < \nabla_{rad} < \nabla_L (= \nabla_{ad} + \frac{\beta}{4-3\beta} \frac{\mathrm{d}ln\mu}{\mathrm{d}lnP}) \tag{2.1}$$

the medium is vibrationally unstable. A slightly displaced mass will start to oscillate with slowly growing amplitude and penetrate more and more into regions of different chemical composition, leading to a rather slow mixing mechanism. A way of choosing the diffusion coefficient is offered in this treatment which will be discussed in chapter 3 & 4.

We have no clear knowledge of the mechanism of semiconvective mixing. One way to treat semiconvection is to calculate the hydrogen profile by keeping the neutrality condition fulfilled. Because of electron scattering dominant opacity ($\kappa \propto [1+X]$), this is

easily done with the dependance of radiative temperature gradient on opacity. Existing models critically depend on what condition is to be used (Chiosi and Summa 1970). The density condition, namely the Ledoux criterion, is a stronger condition favouring stability compared to a temperature condition.

Semiconvection will not happen if mass loss by a stellar wind and/or overshooting are taken into account (Chiosi and Nasi 1974, Chiosi et al 1978). In Xiong's (1985) point of view, semiconvection is not a physical phenomenon which is most probably due to local treatment of convection and disappears if a correct treatment is used.

The explosion of SN1987A brought a lot of studies on the evolution of massive stars, aimed at reproducing a blue progenitor with the evolutionary models. Models with semi-convection work very successfully for this purpose (Langer 1989, Woosley 1988, Weiss 1989). But as a general treatment, the same method should be able to account, at the same time, for the whole population of massive stars unless we could prove that the SN1987A progenitor is an exceptional case.

2.2 Evolution with mass loss by stellar wind

During their evolution, massive stars lose matter through stellar winds. This marks a very important property of evolution of stars, which greatly improves our understanding of these stars as reviewed by Chiosi & Maeder (1986). Evolution incorporating mass loss shows substantial differences from the constant mass case. In practice, to avoid the enormous task of self-consistency between the wind properties and the underlying stellar structure, mass loss is achieved by some empirical formulation from mass loss theory (Castor et al 1975, Abbott 1982, Pauldrach et al 1986, De Jager et al 1988). No self consistent model which offers mass loss rates as a result of physical properties of stars is available up to now.

During the main sequence phase, the effect of mass loss may be summarized as follows,

- Convective cores decrease more rapidly than constant mass evolution, but the fractional mass of the cores is larger as a result of stripping matter off from the envelope;
- Stars evolve at lower luminosity, but are over-luminous for their mass. The extension of intermediate semiconvective and/or full convective regions is reduced. The semiconvective zone is removed if a very heavy mass loss rate is to be accepted;
- The life time on the main sequence is longer due to the fact that the lower luminosity overwhelms the effects of smaller cores and the weakened semiconvective feeding of fuel into the core;
- The main sequence band is wider for moderate rates and narrower for high rates. Very large rates may make stars stay forever in the high effective temperature region (blue side) of the HR diagram;
- Mass loss may give a lower age of clusters and make the line of constant mass in the HR diagram steeper, which leads to a systematic variation in the determination of stellar mass by means of evolutionary tracks. This point is especially true for more massive (higher rates) and highly evolved (long history of losing mass) stars;
- Helium cores at the end of the core H-burning phase are smaller than for constant mass evolution.

Subsequent phases after H-burning are more complicated to explain. The running of the tracks during He-burning is affected by many physical properties of the structure. The behaviour in HR diagram is determined by several competing factors: 1) classical mirror expansion corresponds to core contraction; 2) the increasing size of the core mass, absolutely by shifting of the H-burning shell and relatively by mass loss, favours a redwards motion up to some critical point and then bluewards; 3) large intermediate convective zones will homogenize the envelope and tend to limit the growth in stellar radius; 4) large luminosity to mass ratio favours envelope expansion.

After the He-burning phase, the evolutionary time scale becomes very short. Then the mass loss is small and unlikely to be important for those stages.

The evolutionary tracks for massive stars with mass loss is shown in figure 6.

2.3 Effects of convective overshooting

The physical ground of convective overshoot is simple indeed but the treatment of this phenomenon has resulted in a variety of proposed models. Generally speaking, with the inclusion of overshoot, stars go to lower effective temperatures, and run at higher luminosities. Stars live longer due to the enlargement of the convective core, which overwhelms high luminosity. This general feature holds for simple methods (Bressan et al 1981) as well as the most sophisticated one of Xiong's (1985). Models taking into account core overshoot produces life time ratios which fit observed colour magnitude (C-M) diagrams of (LMC) very well (Chiosi 1989, Maeder & Meylan 1989, Bertelli et al 1990). Also, the weak point of these models, the morphology of tracks on the HR diagram, is improved by including envelope overshoot (Alongi et al 1991). In another sense, because of the consistent treatment of envelope overshoot with that of the core, this finding could imply that overshoot may general exists in all convective zones in stellar interiors.

As a classical tool for testing stellar evolution theory, C-M diagrams and luminosity functions offer strong diagnostic and calibration means for overshoot and imposed parameters. Lots of studies aimed at this purpose can be found in the literature.

Compared with classical models, evolution incorporating core overshooting shows the following character: 1) Much wider main sequence bands; 2) Older ages when determined from turn-off, red star clump and AGB luminosity; 3) Larger ratios of main sequence stars to evolved stars; 4) Higher luminosities of core He-burning models, but much narrower loops; 5) Absence of luminous C & M stars in clusters with turn-off mass greater than $M_{up} \approx 5M_{\odot}$ (instead of $M_{up} \approx 8.9M_{\odot}$); 6) Lower turn-off mass in the mass (age) range

which shows the transition from clusters exhibiting a well developed RGB to those which do not. All above features become more apparent for increasing overshoot extent.

Also, overshoot models brings into agreement the discrepancy between evolutionary mass and pulsational mass (Chiosi 1991), this being one of the long standing problems in this field. Models including overshoot improved the explanation of galactic clusters (Mermiloid & Maeder 1986).

As for the problems revealed by the HR diagrams of galactic and LMC supergiant stars, new models are presented by Bertelli et al (1991), which takes into account mass loss, both core and envelope overshoot and revised opacities. The result suggests that convective overshoot and opacity change play dominant roles. As convective overshoot receives so much emphasis, I will try to approach this phenomenon by taking into account overshoot from all possible convective regions, with the method of Bressan et al (1981) developed for the overshoot velocity field and the treatment of diffusion. Mass loss and semiconvection will also be considered.

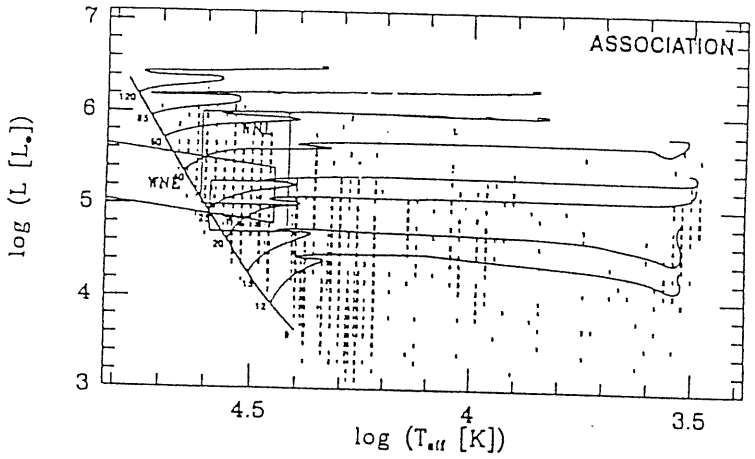

The HRD for luminous stars within 3 Kpc of the Sun. The evolutionary tracks are from Maeder and Meynet (1987). Reproduced from Blaha and Humphreys (1989).

Fig 5

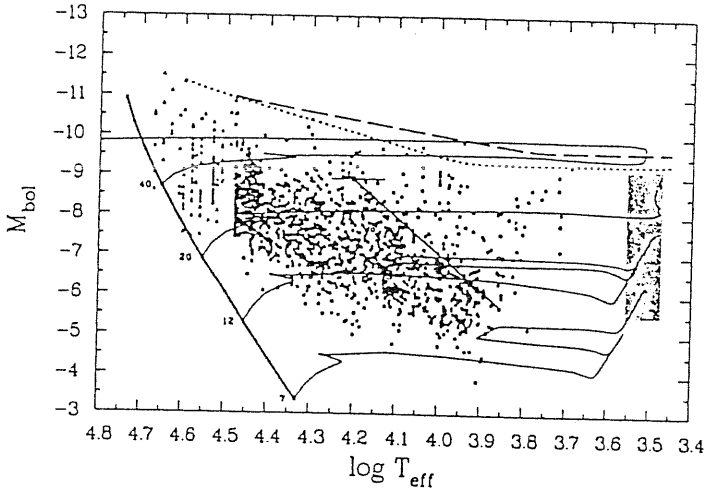

The HRD for luminous stars in the LMC. The evolutionary tracks are from Maeder and Meynet (1988). The ledge is shown by the solid diagonal line. The dotted and dashed lines are the luminosity boundary from Garmany et al (1987) and Humphreys (1987). The shaded area shows the region of red supergiants. Reproduced from Fitzpatrick and Garmany (1990).

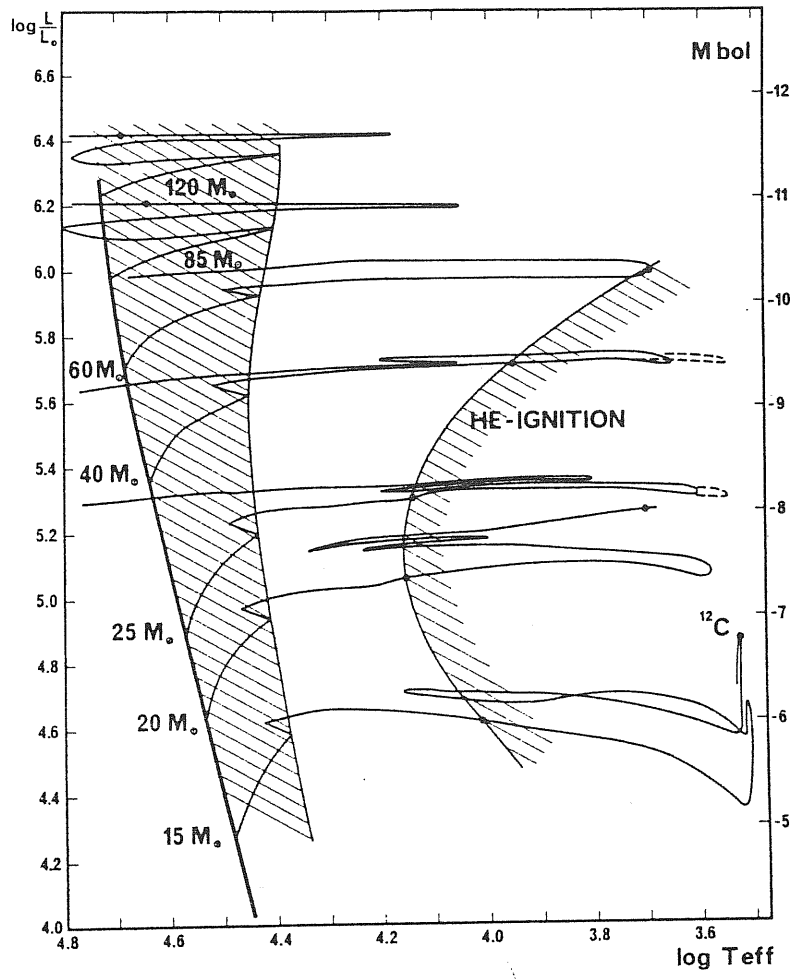

Figure 3 Evolutionary tracks in the HR diagram of massive stars with initial composition $X = 0.73$, $Z = 0.02$ evolved with mass loss by stellar winds. The hatched areas indicate the main sequence band and the beginning of He-burning, which is spent according to the repartition given in the last two columns of Table 2. The first dot along each track indicates the beginning of the He-burning phase. The second dot (if present) indicates the beginning of the C-burning phase. The mass loss rates for OB stars are from Garmany et al. (98); for red supergiants, the expression by Schönberner (225) scaled on the results by van der Hucht et al. (112) is used; and for WR stars, results by Barlow et al. (24) and Nussbaumer et al. (202) are adopted. These models were computed with Schwarzschild's criterion for convection and no convective overshooting. The evolutionary tracks indicated by the solid lines have been computed with mixing length in the outer convection equal to 0.3 × density scale height (171). The dashed lines show the effect of a different treatment of the outer convection (that is, of a mixing length equal to 1.5 × pressure scale height).

Fig 6

Chapter 3

On stellar convection theory

A long standing open problem and probably the most disputed point of stellar physics is convection which occurs in stars for almost every mass interval and every stage of evolution. Even at the present time, when it is generally believed that the main features of the structure of stars and the evolutionary scenarios are well understood, we are still facing the lack of a satisfactory theory of convection. This is a source of uncertainty in understanding the nature of stars. Thanks to the progress in other aspects in this field, and better observational data available to constrain our theoretical results, the uncertainty induced by convection is becoming more apparent than it was in the past.

Historically, our understanding of convection, comes from laboratory experiments (a good review was given by Spiegel 1971,1972), where the Boussinesq approximation is always acceptable. The basic idea of the Boussinesq approximation is that the vertical extension of the fluid is much less than its density and pressure scale heights, allowing the state quantities to be treated as constants. And another approximation is usually assumed, i.e. the inelastic approximation which was used in astrophysical convection (Gough 1969, Xiong 1986). The underlying physics of this approximation is to filter out high frequency phenomena such as sound waves, which are believed to be not important to transport processes in stars. The Boussinesq approximation is adequate for laboratory

convection, but not true for convection in stars, where the thermodynamic quantities vary considerably inside convective zones. Nevertheless, the usually used mixing length theory for stars is in fact a Boussinesq theory, as reviewed by Spiegel. His argument was that all those assumptions are valid implicitly for the mixing length. This is seen in the derivation of the mixing length theory

3.1 Mixing Length Theory

The commonly used stellar convection theory is the one developed by Böhm-Vitense (1958). The basic idea is to model the complicated motion of convective elements by some average elements. In reality, convective elements may have sizes varying from as small as the molecules to as large as the dimension of the whole field. These fictitious elements all possess the same physical properties if generated at a given radial distance r from the center. Each of the elements will travel, on average, a distance Λ (defined as the mixing length) through the medium due to the buoyancy force, and at the end it will mix with its surroundings, therefore losing its identity. By assumption, the dimension of the average elements are set to be the same as Λ, the mixing length, and the shapes of the elements are not specified. This is surely an extremely simple picture for stellar convection, and the mixing length theory constructed on this simple picture greatly simplifies our description. Here, we have two characteristic lengths: the mixing length and the dimension of the element (in mixing length theory, they are set to be the same, but if the problem of overshooting comes in, we will have another length scale in mixing length framework), usually set to be proportional to local the pressure scale height, with the coefficient being a free parameter. The determination of these lengths may have considerable consequences to stellar evolution. The same problem of parameterization of these lengths exists also in some sophisticated theory for stellar convection (cf. Xiong 1985,1986). This parameterization will have basically the same effects, if they use the

same quantity (pressure scale height), as will be shown in section 3.3 for Xiong's case. This might be an intrinsic problem of all current convection theories. The theory should give, instead of require, a measure of the dimensional lengths, this is why the theories are non satisfactory.

Besides the crudity of the mixing length theory, stellar models constructed on the basis of mixing length theory do not show any obvious contradictions with observations. Some attempts were made for refined theories of convection (cf. Spiegel 1960), and some non-mixing length theories (Faulkner et al 1965, Unno 1967, Xiong 1985) were also proposed. But it is not clear yet whether or not these theories are superior to classical the mixing length theory. Although mixing length theory is now a conventional way of treating stellar convection, this does not mean its weak points are ignored. Precisely the contrary, great efforts have been made to control the uncertainties within tolerable margins. While the main lines of stellar evolution given by mixing length theory is believed to be correct, the most apparent weakness, that of overshoot, could be attacked also with this treatment (Maeder 1975,Bressan et al 1981). Again, the parameterization introduced by this way of extension of the theory should be calibrated with observations. Recent studies show that these approaches give a very good improvement over the classical models. (Chiosi & Maeder 1986, Chiosi et al 1991).

For the purpose of stellar evolution, the main task of a convection theory is to give expressions for the transport of energy by convection. In the framework of mixing length theory, the expression turns out to be very simple. I will follow Cox and Giuli's description. In a convective zone, we assume complete pressure equilibrium between the convective elements and their surrounding matter, and the hydrostatic equilibrium always holds at each level. Consider a convective element which begins to rise at a position of radial distance r from the center possessing an initial temperature $T'(r)$ which is assumed to be the same as the value of the field. After moved a distance δr from the original position, the temperature will change $\delta T' = \frac{\mathrm{d}T'}{\mathrm{d}r}\delta r$, while the corresponding change of the

temperature of the average field is, $\mathrm{d}T = \frac{\mathrm{d}T}{\mathrm{d}r}dr$. So the difference between the element and the surrounding at the new position $r + dr$ is

$$\Delta T(\delta r) = \delta T' - dT = \delta r(\frac{\mathrm{d}T'}{\mathrm{d}r} - \frac{\mathrm{d}T}{\mathrm{d}r}) \tag{3.1}$$

Using Schwarzschild's notation (Schwarzschild 1958), $\nabla\Delta T = [(-\mathrm{d}T/\mathrm{d}r) - (-\mathrm{d}T'/\mathrm{d}r)]$, we have

$$\Delta T(\delta r) = \delta r \nabla \Delta T \tag{3.2}$$

Supposing here that the temperature will not change drastically within δr, and setting $T' \approx T$ along the path of the element in δr, we can write,

$$\Delta T = \delta r T[(-\mathrm{d}lnT/\mathrm{d}r) - (-\mathrm{d}lnT'/\mathrm{d}r)] = -\frac{\mathrm{d}lnP}{\mathrm{d}r}\delta r T[(\frac{\mathrm{d}lnT}{\mathrm{d}lnP}) - (\frac{\mathrm{d}lnT'}{\mathrm{d}lnP})] \tag{3.3}$$

or, with the definition of local pressure scale height: $\lambda_p = -\frac{\mathrm{d}r}{\mathrm{d}lnP}$

$$\nabla\Delta T(\delta r) = \frac{T}{\lambda_p}(\nabla - \nabla') \tag{3.4}$$

where $\nabla = \frac{\mathrm{d}lnT}{\mathrm{d}lnP}$ is the usual notation for the temperature gradient (with respect to pressure), the prime means the same quantity for the rising element.

This gives the excess in temperature after the element has traveled a distance δr. This distance is going to be replaced by our mixing length Λ, which measures for an average eddy the distance between the starting point and the ending one, where it is supposed to mix with the field. Substitution of this distance with Λ is direct under our assumptions, and this is the implicit entry of the Boussinesq approximation, because doing this substitution requires Λ being very small within which T, ρ, P etc... are approximately constant. But calibration of this length scale gives that Λ is nearly one pressure scale height (Schwarzschild et al 1957, Sears 1959, Demarque et al 1964). This is one of the main self-inconsistencies of mixing length theory. The same idea will be used for the derivation of the convective flux, the mean convective velocity, (see below).

The motion of this element with excess in temperature will lead to an energy flux, which is easily written as,

$$\mathrm{F}_c = \frac{1}{2}\rho v c_p \delta r \nabla \Delta T \tag{3.5}$$

where, ρ is the density, v is the speed of the element which will be given later, and c_p is the specific heat at constant pressure. The reason for using c_p is the pressure equilibrium we assumed at the beginning. The numerical factor is due to the consideration of only the upwards moving element, the descending ones are cooler than the average field which will absorb energy during its motion, therefore leading to an outward energy flux. A similar expression could be given for sinking elements. Equation (3.5) gives the total flux with the factor replaced by one.

To give the actual flux of convection, mixing length theory uses an average over all possible δr. This is done by replacing δr with Λ, the mixing length. And all other factors in the right hand side of equation (3.5) should be thought of as averaged over the distance as well as the sphere of each level r along the path. With this idea, the flux is written as,

$$\mathrm{F}_c = \frac{1}{2}\rho \bar{v} c_p \Lambda \nabla \Delta T \tag{3.6}$$

where $\bar{v}$ is the averaged speed of convecting elements. With the help of equation (3.4) we may write the expression for convective flux in a more convenient form for the interest of stellar evolution, which is

$$\mathrm{F}_c = \frac{1}{2}\rho \bar{v} c_p T \frac{\Lambda}{\lambda_p}(\nabla - \nabla') \tag{3.7}$$

Now, we have an expression for convective flux which is suitable for stellar structure equations. But one thing is still missing: the average velocity of convective elements. To find this, lets consider the equation of motion for an element. Because of the excess in temperature of the element under consideration with respect to the medium, and the pressure equilibrium we have supposed, the element will have a different density from the

surroundings. Let $\Delta\rho$ being the difference. The equation of motion is written as,

$$\ddot{r} = -g - \frac{1}{\rho}\frac{\partial P}{\partial r} \tag{3.8}$$

Write $\rho = \rho_0(1 + \Delta\rho/\rho)$, where ρ_0 is the equilibrium value. And noting the hydrostatic equilibrium supposed at the beginning and droping out the subscription for equilibrium values, we have,

$$\ddot{r} = -g\Delta\rho/\rho \tag{3.9}$$

This expression corresponds to a net force (buoyancy force minus gravitational force): $f = -g\Delta\rho$. At the starting point, there is no excess both in temperature and density, so this force is virtually zero there. The above equation gives actually the force at some new position after a displacement of δr. Suppose the gravitational acceleration does not change in this small distance, then the work done by the net force through a finite distance, Δr, is,

$$W(\Delta r) = \int_0^{\Delta r} f(\delta r)\mathrm{d}(\delta r) = -g\int_0^{\Delta r} \Delta\rho(\delta r)\mathrm{d}(\delta r) = -\frac{1}{2}g\Delta\rho(\Delta r)\Delta r \tag{3.10}$$

where in the last equality, we have supposed $\Delta\rho$ varies linearly with Δr. This expression of work done on the element should be averaged over all possible Δr with the same idea for convective flux, which is replacing Δr by the mixing length Λ, and introduce a numerical factor. We write,

$$\bar{W}(\Lambda) = \frac{1}{4}W(\Lambda) = -\frac{1}{8}g\Delta\rho(\Lambda)\Lambda \tag{3.11}$$

During the motion of the element up to its dissolving, there must be some energy changes with the field due to friction, heat loss and transfer of kinetic energy to surrounding matters. This is treated with a parameter concerning the efficiency of convection. For the moment we assume one half of the work will become eddy's kinetic energy, so we have,

$$\overline{\frac{1}{2}\rho v^2} \approx \frac{1}{2}\rho\bar{v}^2 = -\frac{1}{16}g\Delta\rho(\Lambda)\Lambda$$

which gives the following velocity which will be used in the expression for convective flux,

$$\bar{v}^2 = -\frac{1}{8}\frac{g}{\rho}\Delta\rho(\Lambda)\Lambda \tag{3.12}$$

Using the equation of state, we can replace the density in the above equation by temperature, bearing in mind the pressure equilibrium, it can be written as,

$$\Delta ln\rho = -Q\Delta lnT$$

where

$$-Q \equiv (\frac{\partial ln\rho}{\partial ln\mu})_{P,T}(\frac{\partial ln\mu}{\partial lnT})_P + (\frac{\partial ln\rho}{\partial lnT})_{\mu,P} \tag{3.13}$$

For a perfect gas, $Q = 1 - (\partial ln\mu/\partial lnT)_P$, while for a more general case, with the medium being a mixture of perfect gas and blackbody radiation field, $Q = \frac{4-3\beta}{\beta} - (\frac{\partial ln\mu}{\partial lnT})_P$

In any case, with eq. (3.12), the mean squared velocity can be written as,

$$\bar{v}^2 = \frac{1}{8}gQ\frac{\Lambda^2}{T}\Delta\nabla T \tag{3.14}$$

At last we have the final expression for convective flux,

$$\mathrm{F}_c = \frac{1}{4\sqrt{2}}g^{1/2}Q^{1/2}\frac{\rho}{T^{1/2}}c_p\Lambda^2(\Delta\nabla T)^{3/2} \tag{3.15}$$

It is this expression which goes into the energy equation for stellar evolution and structure, whenever the medium is found to be unstable against convection. The equation for energy transport is based on a lot of simplifying assumptions. The frequently used idea of average for expressions of temperature difference, velocity, and energy flux brings in this theory some crudity. This difficulty is regulated by adjusting the ratio of mixing length to pressure height. The resulting formulations depend only on the local thermodynamical quantities, which is not true in reality, because the convective element has some memory of its past formation and previous interactions with the environment. A more realistic description is a NON-local version of mixing length theory. This is related to the problem of overshooting which is discussed in the next section.

3.2 Treatment of overshooting

The determination of the boundaries of stellar convective regions is a subject which deserves a lot of attention. Classically, the borders are defined by the so-called Schwarzschild criterion, which actually gives the point where the acceleration of the convective elements vanishes. But the elements may still move, due to their inertia, further into the stable region outside the convective zones. This is the problem of overshooting. Overshooting is very important to stellar evolution, because it will change the size of the core, if it is supposed to occur for convective cores, therefore affecting the lifetime because of more fuel is available, and the subsequent stages. Besides overshooting from convective cores, we may take convection from all other convective regions (intermediate and envelope) consistently the same way as for core convection. The effects of envelope overshoot is studied by Alongi et al (1991). The extent of overshoot, and even the existence is now subjected to a lot of studies in this field, as reviewed by Renzini (1987)

The way to treat overshooting is different from work to work, the results are quite different and sometimes even contrary. Among the pioneer works in this topic, Saslaw and Schwarzschild (1965) found the overshoot distance negligibly small, while Shaviv and Salpeter's (1973) work gives very large distance. Determination of the boundary for convective cores is not an easy thing to do. With mixing length theory, this is achieved by introducing another parameter to describe the extent of overshooting (Maeder 1975, Bressan et al 1981). The criterion proposed by Roxburgh (1975), which is claimed to be parameter free, has been convincingly criticized (Bressan 1984, Baker and Kuhfub 1986) for its consistency. According to Renzini's argument, the overshooting zone is small if the temperature gradient is radiative there, large if adiabatic. On the contrary, in Xiong's treatment, very large and radiative overshooting regions can exist at the border of convective cores of massive stars. This will be studied in the future.

Local mixing length theory is inadequate for the study of this problem, because velocity

become zero when the element reaches the border defined by Schwarzschild criterion. A non-local description of the element has to be developed. There are several ways to do this (Maeder 1975a, Cloutman & Whitaker 1980, Bressan et al 1981). The one I used for this thesis is developed by Bressan et al (1981). I will introduce it in the following, and extend it to general case to account for envelope and intermediate convective zones.

This treatment is based on the assumption that the temperature is adiabatic up to the point where the velocity becomes zero (see fig 1). A non-local description of the motion of a convective element is established in the framework of mixing length theory. Write the equation of motion (eq. [3.9]) as

$$v\frac{\partial v}{\partial r} = -g\frac{\Delta\rho}{\rho}. \tag{3.16}$$

Now $\Delta\rho$ will not be approximated as done in eq.(3.10), but given by integration of the change along its path from the original position r_1 to its present position r,

$$\Delta\rho = \int_{r_1}^{r}[\frac{\partial\rho'}{\partial x} - \frac{\partial\rho}{\partial x}]\mathrm{d}x \tag{3.17}$$

And the expression of convective flux will not be the same as eq (3.15), because the temperature difference eq(3.2) is to be expressed the same way as density, so we have

$$\Delta T = \int_{r_1}^{r}[\frac{\partial T'}{\partial x} - \frac{\partial T}{\partial x}]\mathrm{d}x. \tag{3.18}$$

Correspondingly the flux in this case becomes

$$F_1 = kc_p\rho v\int_{r_1}^{r}[\frac{\partial T'}{\partial x} - \frac{\partial T}{\partial x}]\mathrm{d}x \tag{3.19}$$

where k is a numerical factor, which is set to 2 to take into account both the rising and descending elements. For the expression of velocity, after some mathematical evaluation, and ignoring the contribution of the molecular gradient term in equation (6) of their paper, they give,

$$\frac{1}{3}v^3 = \frac{1}{k}\int_{r_1}^{r}\frac{g}{T}\frac{X_T}{X_\rho}\frac{F_c}{c_P\rho}\mathrm{d}x \tag{3.20}$$

where the convective flux is determined by subtracting radiative flux from the total flux, both of which are known throughout the whole star. The above equation is numerically integrated from the starting level r_1, up $r = r_1 + l$. where $l = \lambda H_p$, and H_p is pressure scale height, λ is mixing length parameter. The behaviour of the element within l is the same as in local mixing length theory and, at the end, the element will dissolve and lose its identity. This integration is done for all elements originated in the range between the r and $r - l$. Because elements created in this range may arrive at r with different velocities, the maximum is take for the velocity field at this position. The border of the convective core is defined at which the velocity determined by this method becomes zero.

This equation if derived for a chemically homogenous convective core. The dropped term concerning the molecular weight gradient may be several orders of magnitude higher than the temperature term, which forms the barrier for convective penetration if some discontinuity is present. But there is some argument for this point: this barrier might be removed by convective overshooting from unstable regions on a very short time scale and further extension is then possible (Castellani et al 1971, Maeder 1975b, Renzini 1977). As the purpose of the present work is to explore the possibility of treating overshooting with diffusive mixing, I assume here the same way of evaluating the velocity field is also suitable for envelope and intermediate zones if they happen during evolution. Then, for those convective zones, we will treat the rising and descending elements separately. As the sinking elements are cooler than the environment, they will make a negative flux with respect to is direction of motion. In this case, the expression of velocity for rising element will be the same as eq (3.20) except the k is cancelled. For the descending elements we have

$$\frac{1}{3}v^3 = -\frac{1}{k}\int_{r_1}^{r} \frac{g}{T}\frac{X_T}{X_\rho}\frac{F_c}{c_P\rho}\mathrm{d}x \tag{3.21}$$

Here, the minus sign appears because the element is sinking, $r < r_1$. The same idea for mixing and scale length is valid for these elements. Again, take the maximum of all

possible values of the velocity for the velocity field of sinking elements. For all element, we take the larger value of the two as the convective velocity.

The physics of this treatment is not discussed here in this thesis. But this way of proceding is consistent with the treatment of convective core. I will take it here as an assumption.

3.3 Xiong's Treatment

As a special case of non-MLT, Xiong's theory (Xiong 1985,1986) turns out to be probably the most complicated treatment as far as stellar evolution is concerned. As a theory for stellar convection, its present form is only a proto-type, in the sense that its application is limited to a medium made up of two chemical components. More precisely, it is only suitable for the hydrogen burning phase, where H and He dominate the chemical evolution in the core. I will first give a very simple description about its basic ideas and assumptions involved to give the final formulation of the scheme. More details are found in Xiong (1986), second I will present partial results. Unfortunately, this method has been abandoned due to enormous numerical difficulties.

This theory starts with the basic dynamical equations of fluids with two component mixture (cf. Landau and Lifshitz). To describe the turbulent convection, a normal way of studying turbulence is used. Quantities are written as a mean value plus its fluctuation. Equations for fluctuational variables are given by subtracting the mean equations from the original equations. Then the equations for correlation functions are constructed using the resulting equations. In the deduction, the following assumptions are used

- In the stellar interior, molecular diffusion flux and molecular viscosity is always small compared with turbulent diffusion and radiative conduction;
- Turbulent convection is supposed to be subsonic, therefore relative fluctuations in

temperature and density are negligible;

- High Reynolds number is a character of stellar convection, the dimension of eddies for which viscous dissipation become important is much smaller than the dimension of mean field;
- The inelastic approximation is accepted to filter out the sound waves;
- The fluctuation in gravitational potential is neglected;
- Turbulence is quasi-isotropic;
- Turbulent motion is quasi-steady, because the time scale of turbulent motion is much less than that of evolution;
- The third order correlation functions are approximation by a gradient form of the second order ones

All the assumptions except the last one seem to work well while the last one is not very-well studied, and one of the two parameters which measuring non-local effects and its relation to overshoot comes in to the equations at this point. This makes the theory some what uncertain.

3.3.1 Results for Massive Stars

Models for massive stars evolving on the main sequence are presented by Xiong (1986) with his statistical theory of convection. Some other attempts with this approach to the study of variable stars (Xiong 1980, 1982) and helioseismology were also made. For the first case, as massive stars evolve away from main sequence, the convective core shrinks, leaving the convective region being chemically homogeneous because complete mixing is found there. In the second case, since we deal with a chemically homogeneous envelope, the complications from abundances are removed, which greatly simplifies the problem.

From the point of view of simplifying Xiong's method, the above points also suggest a way of simplifying this theory, which is to move the problem related to chemical abundances from the equations of dynamical quantities, and treat them by means of other simpler methods. Diffusion, for example is a good candidate, and the link mentioned above will be the diffusion coefficient. If loss of physics could be controlled in a tolerable fashion, this would be a solution for the problem.

For massive stars, the main results for this theory maybe outlined as follows,

- With this theory, the semiconvection does not occur.
- the evolutionary tracks run at higher luminosity than in classical treatment. The difference depends on the choice of the convection parameters c_1,c_2 (two numerical parameters in Xiong's model which regulate the transport efficiency and mixing extension) and becomes larger for lower masses.
- the life time of the burning phase is much longer because the core is enlarged by a considerable amount, this also depends on the parameters.
- evolution occurs at much lower T_{eff}, which makes the main sequence band of this mass range wider.
- A simple criterion does not exist, i.e. neither Schwarzschild's nor Ledoux's criterion is verified. The actual behaviour is closer to Schwarzschild criterion. The boundary of the convective core is defined by the convective flux which changes its sign when pass through the boundary.
- The turbulent kinetic energy flux is less than 1% of the total, so it never has any influence on internal structure.
- The temperature gradient approaches the radiative temperature gradient, instead of adiabatic in the overshooting region, as a result of a negligible turbulent flux in

this region.

- The mass of the convective core is almost unchanged in H-burning phase, but the overshooting region shrinks.

The above results can be understood in the following way. Actually, the first four of the above points are general results of models with overshoot as reviewed by Chiosi et al (1991). With overshoot alone, using the PADOVA code, Xiong's results (Xiong 1986) could be modeled with a large overshooting region (Λ=2.5, 1.5 where Λ is overshoot parameter of Bressan et al 1981). Two tracks with different Λ for a 15 solar mass star were constructed for this purpose. As we can see from figure 2, the lowest effective temperature in the hydrogen burning phase is lower at increasing Λ. All the tracks run at higher luminosity than the classical model. Concerning the positions of the ZAMS, we find some difference between Xiong's models and ours which is mainly due to the opacity used. The opacity in use in our models is by Huebner et al (1977), which has a bump in CNO ionization region. The effect of this enhanced opacity is to make the models less luminous and fainter. So, if we attribute the difference of ZAMS position to this reason, and shift Xiong's track to the one with $\Lambda = 2.5$, we find a very good fit. Table 1 gives $log(L/L_{\odot})$, $logT_{eff}$, the central composition, pressure and temperature, and the core mass of our two tracks together with those by Xiong. Note that while the convective core mass for Xiong's case is defined approximately by the Schwarzschild criterion, the mixing region is larger than the value listed there. To conclude, it is clear that the main feature of the behaviour of the models can be very well resembled by larger a parameter, or more precisely, a larger overshoot region.

The last four points reveal severe systematic differences from those of convective overshoot based on the Mixing Length. These points imply a very different internal structure. Therefore, the most interesting aspect of Xiong's work are the results for the internal structure and the criterion of the border for the convective core.

3.3.2 Difficulties

I have made some efforts to apply this theory, using the Xiong code, to intermediate mass stars. The internal structure for stars higher than 2 $M_{\odot}$, with homogeneous chemicals is given. As pointed out by Maeder(1975), and also by Xiong(1985) the ZAMS models are only slightly affected by overshooting. In Xiong's scheme, this is because the energy transport by convection is negligible in the overshooting region. The size of the overshooting region is much larger than in others (Meader 1990, Bressan 1990), Fig 3. This is mainly due to the choice of the convective parameters: by putting $c_1 = c_2 = 1/2$, approximately $2H_p$ is found for the overshoot region. These values were usually adopted in Xiong's calculations. With this value, Xiong's formalism gives the same convective energy transport rate. But this large overshoot region leads to models contradicting the observations (Bertelli et al 1984).

The numerical difficulties in Xiong's scheme encountered in intermediate mass stars is due to the following. When a models evolves away from ZAMS, as the fluctuation for chemicals (here, the hydrogen content) comes into the equation, all the 17 equations (instead of 10 for homogeneous case) must be solved. As pointed out by Xiong(1986), these equations are of Stiff-type, and the problem of spatial oscillation is met in the convective region. The domain of convergence is usually very small for solutions of convective variables. In intermediate mass stars, pressure and density are larger than in high mass stars, and the spatial oscillations make it very difficult to converge the model. A small time step, which means small adjustment in chemical abundance and other quantities, is needed to achieve a stable solution. As the time step became very small, the computing time became so long, that the calculation of numerical models became exceedingly time consuming.

There is another potential, probably bigger difficulty in Xiong's scheme, i.e. the greatly increasing number of equations if more chemicals will be involved. If one more chemical

element is included, four variables and four equations must be added, i.e. the cross-correlation functions with temperature, velocity and the other chemicals, and the auto-correlation function.

All this means that much computational effort has to be spent to reach the the same evolutionary results obtained by means of other treatments. One argument against this theory is that, because of the same dependence on pressure scale height is used to determine the boundary of convective region, Xiong's treatment suffers of the same problem affecting mixing length theory, i.e. the unbound growth of the core. When we go to lower mass stars, the core grows because the pressure scale height becomes large. This trend continues and tend to diverge. As it can be seen from figure 3, Xiong's method gives a larger overshoot region (larger core mass) because a larger parameter is used, whereas the ratio of overshoot mass to the Schwarzschild core mass varies, with respect to the stellar mass, in the same way as in other simple methods. The main results of this method are quite similar to those with other methods, if we allow for difference caused by larger parameters. Therefore, it is clear that such an enormous numerical effort is not compensated by physical improvement with respect to results obtained from the mixing length theory. This is the main reason why I gave up this method and use the PADOVA code.

Xiong's method has no such problems if applied in variable stars, solar oscillations and envelope structure (Xiong 1990). To be used in stellar model calculations, ways out must be found to cope with the above difficulty. The key point are the chemical equations. One possible way out is to treat mixing of chemicals and other processes involving chemicals in diffusion scheme, and treat the structure and dynamic properties of turbulence in a seperate manner. Xiong argued against this possibility (Xiong 1986), in a sense that the chemical contents are strongly coupled with dynamical variables, and preferred to treat them simultaneously. In light of the problems mentioned above, I think it is worth looking back to diffusion. This may not be so ad hoc as it may seem to be. As shown in chapter

4, if we treat convective mixing as a diffusion process, the numerical difficulty in getting the chemical distribution is greatly reduced. If diffusion is properly taken into account, and most important, the diffusion coefficient is carefully chosen, we may get results in agreement with observation. In turn, the observation may constrain the theory and the treatment of diffusion.

Nevertheless, Xiong's method gives a detailed description about the dynamical properties of the turbulent field in the one dimensional case. Xiong's method suggests that the composition profile in the overshooting region is smoothly connected to the outside profile given by the retreating boundary (see figure 4). Xiong's treatment of composition is not a diffusive one, but this profile could be anyway achieved by assuming some diffusion in the overshooting zone. We can take the whole convective zone, the fully convective region (classically defined by Scharzschild criterion) plus the convective penetrative region, as the domain of diffusion.

TABLE (1)

(ovs = 1.5)

MOD	Age	LogL	LogTE	comp	LogTc	LogRHOc	LogPc	M_c.c.
1	0.000	4.1920	4.4362	0.750	7.45975	0.58910	16.23737	0.372
21	5.740	4.3090	4.4671	0.637	7.52174	0.72641	16.40851	0.383
35	9.273	4.4016	4.4623	0.541	7.53029	0.71450	16.37933	0.372
52	12.689	4.5167	4.4492	0.417	7.54471	0.71315	16.35718	0.355
71	14.877	4.6133	4.4272	0.312	7.55956	0.72385	16.35000	0.340
92	16.288	4.6907	4.3966	0.224	7.57427	0.74369	16.35502	0.325
127	17.464	4.7709	4.3426	0.133	7.59452	0.78405	16.38133	0.308
151	18.125	4.8246	4.2831	0.069	7.61357	0.83048	16.42318	0.294

(OVS = 2.5)

MOD	Age	LogL	LogTE	comp	Log Tc	logRHOc	Log Pc	M_c.c.
1	0.000	4.1506	4.4306	0.750	7.45742	0.57601	16.22256	0.457
20	7.054	4.2752	4.4654	0.637	7.51975	0.70789	16.39049	0.450
34	11.492	4.3881	4.4660	0.540	7.52973	0.69224	16.35924	0.443
51	15.601	4.5362	4.4593	0.417	7.54599	0.68814	16.33812	0.430
70	18.111	4.6567	4.4409	0.311	7.56216	0.69418	16.33017	0.421
91	19.672	4.7560	4.4098	0.224	7.57806	0.71006	16.33525	0.410
125	20.912	4.8608	4.3454	0.133	7.59945	0.74575	16.36216	0.394
150	21.559	4.9349	4.2558	0.069	7.62227	0.79726	16.41393	0.380

Table 1c. $M = 15 M_\odot$ $c_1 = c_2 = \frac{1}{2}$

No	t	$\log T_e$	$\log \frac{L}{L_\odot}$	Xc	$\log P_c$	$\log T_c$	$\frac{M_c}{M_o}$
0	0	4.478	4.210	0.750	16.483	7.516	0.356
2	5.683 E6	4.484	4.335	0.637	16.455	7.530	0.370
4	9.462 E6	4.487	4.453	0.540	16.435	7.544	0.390
7	1.302 E7	4.482	4.606	0.415	16.415	7.562	0.403
10	1.515 E7	4.464	4.730	0.310	16.408	7.579	0.417
13	1.648 E7	4.433	4.830	0.224	16.412	7.595	0.423
17	1.754 E7	4.374	4.933	0.133	16.436	7.616	0.430
21	1.815 E7	4.298	5.006	0.069	16.485	7.639	0.430

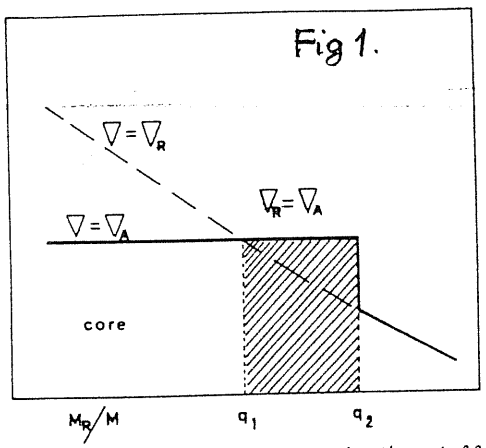

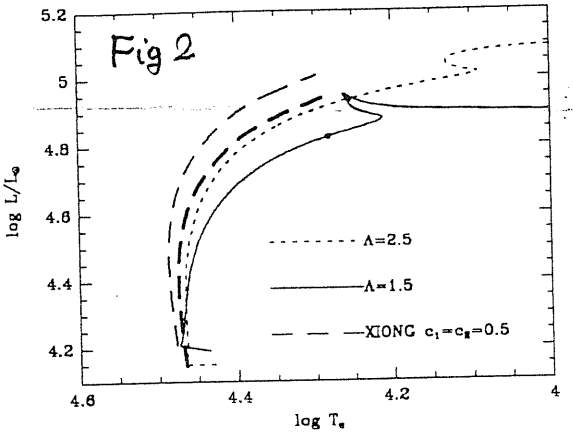

Fig. 1 - Temperature gradients in the stellar models. The shaded area indicates the region of overshooting. The fractionary masses q_1 and q_2 correspond to the level at which acceleration and velocity of the convective elements become zero, respectively.

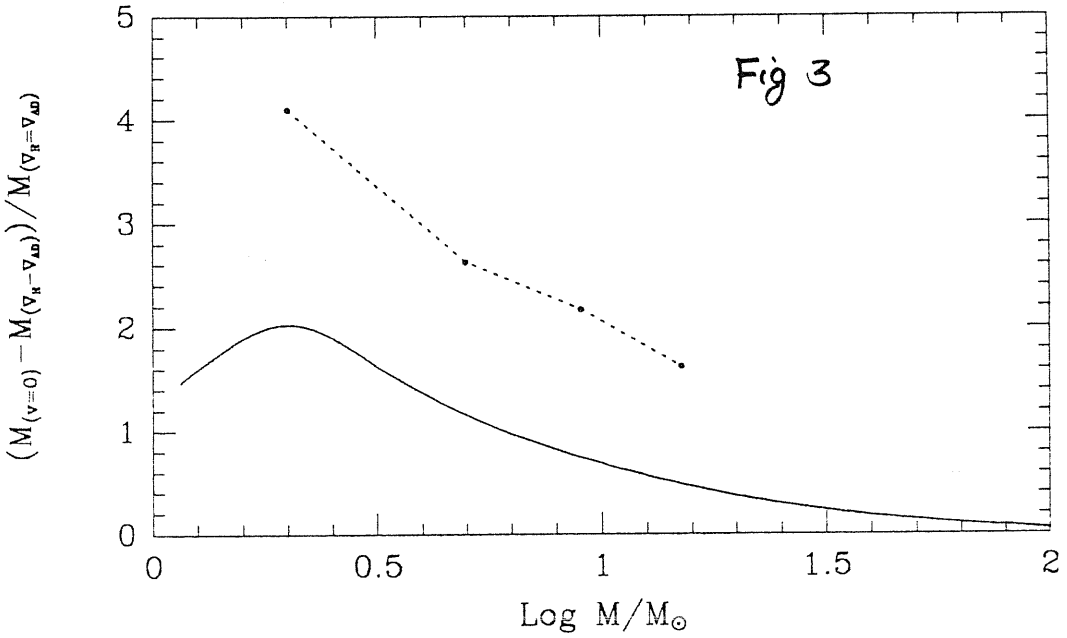

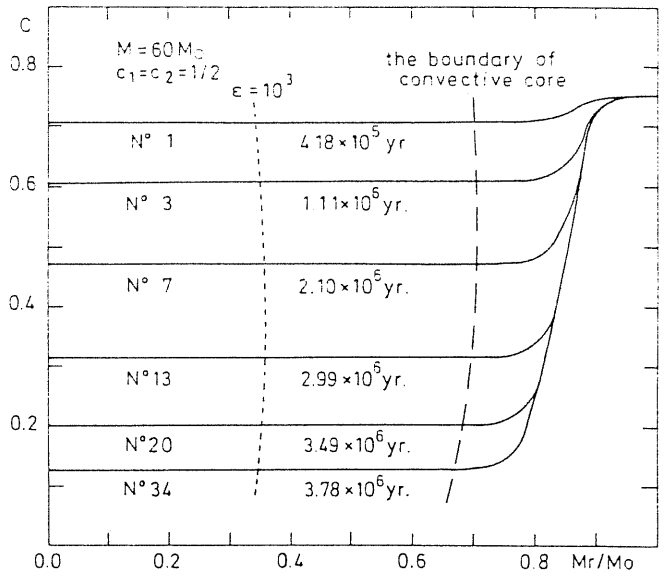

Fig 4.

Fig. 2. The hydrogen distribution in the models of the 60 $M_\odot$ star at various times. The dashed curve and the dotted curve indicate the location of the boundary of the convective core and the nuclear energy-generation rate $\varepsilon = 1000$ erg/cm s., respectively

Chapter 4

The Treatment of Mixing with Diffusion

In the present work, we take the mixing of the chemicals inside convective regions as a diffusive process. This method is used by many authors for stellar evolution calculations. The motivation is to give an expression to some slower mixing processes required by the instability analysis of stellar interiors, such as semiconvection, and to see what is the effect of a molecular weight gradient given by partial mixing in these regions on the evolution of stars. The true physics of the partial mixing is not known at present. People use diffusion to model this complicated phenomenon. Some new points of view are given by these studies, See for example, Eggleton (1971,1972), Simpson (1971), Sreenivasan & Wilson (1977), Langer et al (1983, 1985, 1990), Weaver et al (1978), and for diffusion, see Jost (1960)

In the central convective regions of stars, as the convective mixing is so effective that mixing uccurs on time scale which is much shorter than that of nuclear burning, homogeneous chemical distributions are always found. In the semiconvective case, however, the mixing occurs on a time scale comparable to the nuclear time scale, as discussed by the above authors. Differing from fully convective zones, mixing inside semiconvective

regions give rise to molecular weight gradients as a result of incomplete mixing. These inhomogeneous chemical profiles have some consequences on stellar structure and give a different picture of evolution.

In present the study, the same diffusion scheme for convective mixing is accepted. In a similar way as to treat partial mixing in semiconvective regions, we will take an assumption that a partial instead of complete mixing happens in overshooting regions, the physical reasons for the idea are to be presented later.

4.1 Mathematics of Diffusion

The mathematics of diffusion can simply be described as follows. Suppose we have a medium with some chemical profile. As time goes on, diffusion homogenize the medium. According to Jost (1960), Fick's first law gives,

$$\vec{\mathrm{J}} = -\mathrm{D}\vec{\nabla} C \tag{4.1}$$

where C is the chemical concentration with a dimension $[g\ cm^{-3}]$, and $\vec{\mathrm{J}}$ is the flux (corresponding to concentration diffusion Chapman & Cowling [1970]) of this chemical with a dimension of $[g\ cm^{-2}\ sec^{-1}]$. D is defined as the diffusion coefficient. The diffusion, in this case, happens because of the gradient in concentration, and the effect of diffusion is to reduce this gradient. In general, any gradient of physical parameters in a mixture will lead to transportation of species. A more precise definition of diffusion flux for a two component mixture is found in Laundau & Lifshitz's book on **Fluid Mechanics** (1987), which is the following,

$$\vec{\mathrm{J}} = -\rho \mathrm{D}_{12}(\vec{\nabla} C + k_T \vec{\nabla} ln T + k_P \vec{\nabla} ln P) \tag{4.2}$$

The meaning of the symbols are: D_{12} is the mutual diffusion coefficient, k_T the dimensionless thermal diffusion ratio with its production with D_{12} giving the thermal diffusion

coefficient, and $k_P \mathrm{D}_{12}$ the so-called barodiffusion. If we have convection in our medium, the turbulent mixing is dominant. The physics of this mixing is not yet understood because the nature of turbulence itself is not clear at this moment. We only know that the turbulent motion is so vigorous, which makes the region of full convection completely mixed. A simple picture of convective mixing is that the large eddies get energy from the average field and start the motion with the composition of their original positions, they distribute the kinetic energy to smaller eddies and so on. As this part of the energy is being turned to thermal energy at the level of smallest eddies, the composition will be mixed there with the surrounding. As we can find from the literature, mixing due to convection in a stellar interior, despite being very complicated, could nevertheless be treated as a diffusion process. This is a hypothesis, and the main problem is, if we accept this assumption, to determine the diffusion coefficient. There were some discussions in the literature about the equation of diffusion for the problem (Sreenivasan et al 1977, Cloutman et al 1976). Cloutman et al used a one point correlation function of fluctuations of turbulent velocity and chemical concentration to treat the problem of turbulent mixing, and the gradient approximation is made to the correlation in leading to the equation of diffusion. Langer et al (1983) proposed an equation which is not the same one as the one used later by the authors. Actually, we can arrive at the final equation as the one used by Weaver et al (1978), and Langer (1985), by making assumptions to the flux of the diffusion. Noting the form of the definition of diffusion flux (eq. 4.2), we assume that the diffusion flux due to turbulence can be written formally, being proportional to the gradient of fractional abundance of the diffused chemical, with all physical details contained in the coefficient. This is actually the Boussenisq approximation. So the total flux of the convective region is

$$\vec{\mathrm{J}} = -\rho \mathrm{D}(\vec{\nabla} C + k_T \vec{\nabla} ln T + k_P \vec{\nabla} ln P) - \rho \mathrm{D}_c \vec{\nabla} C \tag{4.3}$$

where D_c is the coefficient due to convection.

All the terms except the last one in the above equation describe the contribution of molecular diffusion as the results of gradients of chemical concentration, temperature and pressure respectively. Molecular diffusion can be neglected in astrophysical contexts because of its low efficiency or long time scale compared with that of turbulence (Cloutman et al 1976, Xiong 1985, Kippenhanh & Weigert 1991). With this definition, we can derive the equation for diffusion as follows. The mass conservation is always fulfilled

$$\frac{\partial \rho}{\partial t} + \vec{\nabla} \cdot (\rho \vec{\mathbf{v}}) = 0 \tag{4.4}$$

and the equation of *conservation* for species i can be written as

$$\frac{\partial \rho U_i}{\partial t} + \vec{\nabla} \cdot (\rho U_i \vec{\mathbf{v}}) = -\vec{\nabla} \cdot \vec{\mathbf{J}}_i - q_i \tag{4.5}$$

Using equation (4.4), we can write equation (4.5) as

$$\rho \frac{dU_i}{dt} = -\vec{\nabla} \cdot \vec{\mathbf{J}}_i - q_i \tag{4.6}$$

where, $d/dt = \partial/\partial t + \vec{\mathbf{v}} \cdot \vec{\nabla}$ is the Lagrangian time derivative and q_i is the burning rate of the species under consideration.

Putting the flux into the above equation, and taking into account the spherical symmetry of our problem, yields,

$$\frac{dU_i}{dt} = -\frac{q_i}{\rho} + \frac{1}{\rho}\frac{\partial}{\partial r}(r^2 \rho \mathbf{D} \frac{\partial U_i}{\partial r})$$

and writing the spatial derivatives into Lagrangian coordinate, using,

$$\frac{\partial}{\partial m_r} = \frac{1}{4\pi r^2 \rho}\frac{\partial}{\partial r}$$

m_r (mass inside the sphere with radius r), as we use for structures, at last we have,

$$\frac{dU_i}{dt} = -\frac{q_i}{\rho} + \frac{\partial}{\partial m_r}[(4\pi r^2)^2 \rho^2 \mathbf{D} \frac{\partial U_i}{\partial m_r}] \tag{4.7}$$

Equation (4.7) gives the usual diffusion equation to be solved for chemical distributions in stars. We have not gone into any physics of diffusion yet, which is mainly contained in

the diffusion coefficient, and probably the way of approaching this is not so direct. A lot of attempts have been made to study the relation between the choices of the coefficient (or the calculation of it), and its consequences on stellar evolution. Work done on this subject include explicit calculations of the diffusion coefficient (Simpson 1971, Sreenivasan & Wilson) and using prescriptions (Weaver et el 1978, Langer et al 1985). For the present work, we will accept the way of using a prescription for the diffusion coefficient to study the incomplete mixing in stars.

As we can see from the work done in the past about the diffusion models, the evolution of stars depends on what coefficient is to be used. For the fully convective zones, all authors use the same formula for the diffusion coefficient,

$$\mathrm{D}_{FC} = \frac{1}{3} v l_m \tag{4.8}$$

where v is the convective velocity, and l_m is the mixing length, both depend on the convection theory.

This formula could be verified in the following way. Suppose the velocity of a convective element is v. It starts with the concentration of the original place. It is to be mixed at the end when the element dissolves. In mixing length theory, this length traveled by the element is exactly the *mixing length*. The motion of this element will make its contribution to the diffusion flux; for an upward moving element, it is

$$j^+ = \frac{1}{6} C v \delta l = \frac{1}{6} \rho \mathrm{U} v \delta l$$

the numerical factor comes from the average of $\cos^2\theta$ for upward moving element, with θ being the angle between the direction of motion and radius, and δl is some scale distance traveled by our element. Noting that the values of ρ ,v and C (or U) are determined at $(-\delta l)$ (and at $[+\delta l]$ for downward moving elements, taking the current position being 0) we can expand ρ, U and v at $z = 0$, neglecting all terms except linear ones, we have,

$$j^{\pm} = \frac{1}{6}[\rho(0) \mp \frac{\partial \rho}{\partial z}\delta l][v(0) \mp \frac{\partial v}{\partial z}\delta l][\mathrm{U}(0) \mp \frac{\partial \mathrm{U}}{\partial z}\delta l]$$

The net flux is given by $j = j^+ - j^-$, which is

$$j = -\frac{1}{3}[\frac{\partial \mathbf{U}}{\partial z} v\rho\delta l + \frac{\partial(\rho v)}{\partial z}\mathbf{U}\delta l]$$

The second term describes the gradient of mass flow, which corresponds to the variation of density according to mass conservation. For steady state it is negligible. So we write

$$\vec{J}_c = -\frac{1}{3}\rho v\delta l\vec{\nabla}\mathbf{U} = -\mathbf{D}_c\rho\vec{\nabla}\mathbf{U} \tag{4.9}$$

where $\mathbf{D}_c = -\frac{1}{3}\rho v\delta l$ is taken to be the diffusion coefficient if we take the convective mixing as a diffusion. This expression for $\mathbf{D}_c$ in the equation is a qualitative one which suggests a way to evaluate the coefficient in the full convection case.

Now we have the equation (4.7) which was used by researchers with different numerical schemes. Some of them made simultaneous solutions of diffusion with the normal stellar structure equation (Simpson 1971), which means introducing a second order differential equation to our problem. Doing this might improve the accuracy of the problem (Cloutman & Eoll 1976) as the diffusion coefficient becomes very large, but this can also be quite time consuming, the extreme case was found in Xiong's method. Others solved this equation independently (Weaver et al 1978; Langer et al 1985, 1990). There are not any significant differences existing besides the more different ways of choosing the coefficient and the convection treatment involved.

In each convective zone, the diffusion equation is solved to give a chemical profile. The problem of choosing the coefficient is to be discussed latter. A numerical scheme is given here for solving the diffusion equation. The first term in eq.(4.7) can be written as the change rate of abundance of chemical i, which is more convenient for numerical purposes, then we have,

$$\frac{d\mathbf{U}}{dt} = (\frac{\partial \mathbf{U}}{\partial t})_{nucl} + \frac{\partial}{\partial m_r}[(4\pi r^2)^2\mathbf{D}\rho^2\frac{\partial \mathbf{U}}{\partial m_r}] \tag{4.10}$$

The term $(\frac{\partial \mathbf{U}}{\partial t})_{nucl}$ times the time step is the variation of fractional abundance at each mesh point before and after a time step, given as numbers on each mesh through a nuclear reaction routine. Now the equation is ready for discretization.

4.2 Numerical Methods

Our grid is the same as the one used for stellar structure models, with the center being M, which is the total number of mesh points, going down to 1 at the fitting point with atmospheric integral. The left hand side of the equation is discreticized with forward difference,

$$dU_i/dt = (U_i^{n+1} - U_i^n)/\Delta t$$

where Δt is the stepwidth in time, the superscripts give the chemical concentration at time t^{n+1}, and time t^n. The subscripts stand for the mesh m_i.

To discreticize the right hand side, we have to consider the stability of our scheme. There are many schemes for this kind of parabolic equation (e.g. Crank 1986). In our case, as the mesh is not a equal-spaced one, the scheme turns out to be slightly different from others usually found in numerical books. For a general discussion, we use a weighted mean scheme as follows. For simplicity, we first make the following substitution,

$$D_i = [\mathbf{D}_i(4\pi r^2)^2\rho^2]_i \tag{4.11}$$

So the second term on the right hand side of our equation is discreticized in the following way. The first step is to make a centre space difference of the second derivative with respect to mass, at two intermediate points, $P_{+\frac{1}{2}}:\frac{1}{2}(m_{i-1}-m_i)$, and $P_{-\frac{1}{2}}:\frac{1}{2}(m_i-m_{i+1})$ with half stepwidth in mass which gives,

$$\frac{2}{(m_{i-1}-m_{i+1})}[(D\partial U/\partial m)_{P_{+\frac{1}{2}}} - (D\partial U/\partial m)_{P_{-\frac{1}{2}}}]$$

The second step is to make the difference for the first derivative, again with center space difference, which yields,

$$\frac{2}{(m_{i-1}-m_{i+1})}\{(1-\alpha)[\frac{1}{(m_{i-1}-m_i)}\frac{(D_{i-1}+D_i)}{2}(U_{i-1}-U_i)] - [\frac{1}{(m_i-m_{i+1})}\frac{(D_i+D_{i+1})}{2}(U_i-U_{i+1})]\}^{n+1} \tag{4.12}$$

where $0 \leq \alpha \leq 1$ is the weight constant, which is to take into account contributions from different epochs. With $\alpha = 1$ gives an complete explicit scheme, $\alpha = 0$ complete implicit scheme, $\alpha = 1/2$ the well known Crank-Nicolson scheme which has second order of accuracy both in time and space. The superscript in the above equation defines quantities at different times.

Some comments should be made here about the above scheme. For any problem of this kind, with α different from 1, the above discreet form for our diffusion equation are unconditionally stable. Of course some specific value of α will be chosen; we will come to this point later. Now to simplify the above difference equation, we make some substitutions:

$$A_i = \frac{(D_{i+1} + D_i)}{(m_{i-1} - m_{i+1})(m_i - m_{i+1})} \tag{4.13}$$

$$C_i = \frac{(D_i + D_{i-1})}{(m_{i-1} - m_{i+1})(m_{i-1} - m_i)} \tag{4.14}$$

$$\begin{aligned} B_i &= A_i + C_i \\ &= \frac{(D_{i-1} + D_i)}{(m_{i-1} - m_{i+1})(m_i - m_{i+1})} + \frac{(D_i + D_{i+1})}{(m_{i-1} - m_{i+1})(m_i - m_{i+1})} \end{aligned} \tag{4.15}$$

And take δU_i to represent the term due to nuclear burning in our equation:

$$\frac{\delta U_i}{\Delta t} = (\partial U_i / \partial t)_{nucl} \tag{4.16}$$

Then we have the following difference equation for our problem:

$$\begin{aligned} &\frac{U_i^{n+1} - U_i^n}{\Delta t} = \delta U_i / \Delta t + \\ &(1 - \alpha)\{A_{i+1} U_{i+1} - B_i U_i + C_{i-1} U_{i-1}\}^{n+1} \\ &+\alpha\{A_{i+1} U_{i+1} - B_i U_i + C_{i+1} U_{i+1}\}^n \end{aligned} \tag{4.17}$$

Suppose there is convection between mesh points N_1 and N_2, equation (4.17) valid for i goes from $N_1 - 1$, to $N_2 + 1$ and give us a set of $(N_1 - N_2 - 2)$ linear equations. Fortunately, as can be seen from the above equation, this set turns out to be *tridiagonal*, which can

be solved with a very effective method. At both boundary points, however, we have to provide other two equations given by the boundary condition of our problem.

4.3 Boundary Conditions

We will assume the diffusion equation is solved for a given model, in this case, the boundary will be wall-like, that means no net mass flows across the boundary. This will have the advantage of keeping easily the conservation of matter in one zone. So, we have,

$$J_{N_1} = J_{N_2} = 0 \tag{4.18}$$

To discreticize the boundary conditions, we also have to write the original equation for the boundary points. To do this, we imagine there is an extra point outside each end of the region $[N_1, N_2]$, and each point set at a distance from the boundary which is the same as the first point inside the zone from the border. Each fictitious point outside the boundary has the same D (defined by (4.11)) as the corresponding inner point. This is just to guarantee eqs (4.18). Then we have:

$$J_k = (U_k - \tilde{U}_k)/2\Delta m = 0$$

which gives:

$$U_k = \tilde{U}_k$$

where subscript k denotes boundary meshes. $\tilde{U}$ means imaginary points.

The equations for boundary points are, for the inner boundary N_1,

$$\begin{aligned} \frac{U_{N_1}^{n+1} - U_{N_1}^n}{\Delta t} &= \delta U_{N_1}/\Delta t \\ &\quad +(1-\alpha)\{\tilde{A}_{N_1}\tilde{U}_{N_1} - B_{N_1}U_{N_1} + C_{N_1-1}U_{N_1-1}\}^{n+1} \\ &\quad +\alpha\{\tilde{A}_{N_1}\tilde{U}_{N_1+1} - B_{N_1}U_{N_1} + C_{N_1-1}U_{N_1-1}\}^{n} \end{aligned} \tag{4.19}$$

and for the upper boundary N_2,

$$\begin{aligned}\frac{U_{N_2}^{n+1}-U_{N_2}^{n}}{\Delta t} &= \delta U_{N_2}/\Delta t \\ &+(1-\alpha)\{A_{N_2+1}U_{N_2+1}-B_{N_2}U_{N_2}+\tilde{C}_{N_2}\tilde{U}_{N_2}\}^{n+1} \\ &+\alpha\{A_{N_2+1}U_{N_2+1}-B_{N_2}U_{N_2}+\tilde{C}_{N_2}\tilde{U}_{N_2}\}^{n} \qquad (4.20)\end{aligned}$$

where the tilde variables mean the quantities of fictitious points.

The above equation also holds if the boundary becomes the center or the surface of the star as in cases of core convection and envelope convection respectively. Using above equations, we arrive at

$$\begin{aligned}\frac{U_{N_1}^{n+1}-U_{N_1}^{n}}{\Delta t} &= \delta U_{N_1}/\Delta t + \\ &(1-\alpha)\{C_{N_1-1}U_{N_1-1}-B_{N_1}U_{N_1}\}^{n+1} \\ &+\alpha\{C_{N_1-1}U_{N_1-1}-B_{N_1}U_{N_1}\}^{n} \qquad (4.21)\end{aligned}$$

$$\begin{aligned}\frac{U_{N_2}^{n+1}-U_{N_2}^{n}}{\Delta t} &= \delta U_{N_2}/\Delta t + \\ &(1-\alpha)\{A_{N_2+1}U_{N_2+1}-B_{N_2}U_{N_2}\}^{n+1} \\ &+\alpha\{A_{N_2+1}U_{N_2+1}-B_{N_2}U_{N_2}\}^{n} \qquad (4.22)\end{aligned}$$

The Fictitious points are cancelled out deducing. and B_{N_1},C_{N_1}, A_{N_2},B_{N_2}, are given below:

$$B_{N_1}=\frac{1}{(m_{N_1-1}-m_{N_1})^2}\frac{(D_{N_1-1}+D_{N_1})}{2}=-C_{N_1}$$

$$B_{N_2}=\frac{1}{(m_{N_2+1}-m_{N_2})^2}\frac{(D_{N_2+1}+D_{N_2})}{2}=-A_{N_2}$$

The above boundary equations, plus the set of equations for interior points form a complete set of tridiagonal system.

We will show below that our numerical scheme together with the accepted boundary conditions gives a conservative finite difference formalism. The variation of chemical U in

a mesh labeled i is,

$$\frac{(U_i^{n+1} - U_i^n)}{\Delta t} = (\frac{\Delta U_i}{\Delta t})_i + \frac{2}{m_{i-1} - m_{i+1}}(\mathbf{F}_{i-1/2} - \mathbf{F}_{i+1/2})$$

where,

$$\mathbf{F}_{i\pm1/2} = \frac{1}{2}(D_i + D_{i\pm1})\frac{\pm U_i \mp U_{i\pm1}}{\pm m_{i\mp1} \mp m_i}$$

Summing up $\frac{(U_i^{n+1} - U_i^n)}{\Delta t}$ over the whole range $[N_1, N_2]$ gives the total variation in this zone, i.e.,

$$\sum_{N_1}^{N_2}\frac{(U_i^{n+1} - U_i^n)}{\Delta t} = \sum_{N_1}^{N_2}\frac{\Delta U_i}{\Delta t} + \frac{2}{m_{N_1-1} - m_{N_1+1}}\mathbf{F}_{N_1+1/2} + \frac{2}{m_{N_2+1} - m_{N_2-1}}\mathbf{F}_{N_2-1/2} \quad (4.23)$$

So the total variation in this region will be the total change due to thermal nuclear reaction, and marginal terms which are flux of matter flowing across the boundary. As our boundary conditions set those terms to zero, this formula give strict conservation of species, i.e. any change of species inside a zone will be completely due to reactions, *if we are free of numerical errors.* As found in the numerical calculations, rounding errors may be important in some circumstances, and we have to find a way to correct them

Some assumptions are to be made here. The coefficients in our difference equations, A_i, B_i, A_i all have superscript, i.e. they are values from different times. This means in order to solve this tridiagonal system, two models of structure should be stored. In practice, we couldn't know a priori the structure quantities for the next epoch, because the structure is to be decided upon our solutions for the chemicals. A possible assumption is that the chemicals diffuse at a given structure, i.e. diffusion will not affect our structure. This of course is not a physical picture, because it would be strange if this happens in real stars. However, this is based on the following considerations. Solving chemical distributions independently will be more convenient, and the results of new chemical profiles will have their consequences on structure. In practice, every time we have a new chemical distribution, just like nuclear burning for each step, we will adjust the structure

to fit the changes in the chemical composition. This adjustment is automatically done by the routines that solve the structure equations. In this case, we will have

$$A_i^n = A_i^{n+1}$$

$$B_i^n = B_i^{n+1}$$

$$C_i^n = C_i^{n+1}$$

This assumption is shown to be acceptable by our numerical experiment, if the time step is well tuned.

4.4 Conservation of chemicals during diffusion

In solving the linear equation in the above section, we have to keep the chemical contents inside our diffusion regions, so as to be conserved. Although the numerical scheme and the boundary conditions of the problem are conservative ones, numerical errors may exist in our system which could be thought of as leakage. That means some small amount of fuel is to be lost or added to the star as if the region had some unexpected thermal nuclear burning going on inside. This will surely affect the age estimate, and possibly affect evolution on later phases. To control this problem, we integrate the abundances in diffusion zones, and check this integral before and after the solution of our linear equations. The integration is done with the following method.

As the mesh is non-equally spaced, we fit two sets of three successive points,

$$(m_{i+1}, m_i, m_{i-1}) \quad (m_i, m_{i-1}, m_{i-2})$$

with two second order parabola, and take simple averages of the two fitted functions to approximate the value of the abundance U in the interval $[m_i, m_{i-1}]$, i.e.

$$U \approx \mathrm{P}_i = \frac{1}{2}[\mathrm{P}_1 + \mathrm{P}_2] \tag{4.24}$$

where

$$\mathrm{P}_1 = a_i x^2 + b_i x + c_i$$

$$\mathrm{P}_2 = a_{i-1} x^2 + b_{i-1} x + c_{i-1}$$

The integral of U is then approximated by the integration of the fitted function P;

$$\int_{m_i}^{m_{i-1}} U dm \approx \int_{m_i}^{m_{i-1}} \mathrm{P} dm = \frac{1}{2} \int_{m_i}^{m_{i-1}} (\mathrm{P}_1 + \mathrm{P}_2) dm \tag{4.25}$$

The final formula of this approximation is

$$\int_{m_i}^{m_{i-1}} \mathrm{P}_i dm = \frac{h_i}{6} (3\,U_i + 3\,U_{i-1} - \frac{L_i + R_i}{2}) \; (i = M-1, M-2, ...3, 2) \tag{4.26}$$

Then, the total integration over the diffusion region, $[N_1, N_2]$ is given by,

$$\int_{m_{N_1}}^{m_{N_2}} U dm = \frac{1}{6} \sum_{i=m}^{2} (3\,U_i + 3\,U_{i-1} - \frac{L_i + R_i}{2}) \tag{4.27}$$

where

$$L_i = \frac{\delta_i^2}{1+\delta_i} U_{i+1} - \delta_i U_i + \frac{\delta_i}{1+\delta_i} U_{i-1}$$

$$R_i = \frac{\lambda_i}{1+\lambda_i} U_i - \lambda_i U_{i-1} - \frac{\lambda_i^2}{1+\lambda_i} U_{i-2}$$

$$h_i = m_{i-1} - m_i$$

$$\delta_i = h_i / h_{i+1}$$

$$\lambda_i = h_i / h_{i-1}$$

$$L_M = R_2 = 0$$

and m_i is the mass inside the sphere of mesh i.

We make the integration with equation (4.27) for every diffusion zone at each time step to check for conservation. If the relative error is greater than some given value (say, 10^{-4}, as I used for this work), then, the difference between the integrations of the two epochs will be attributed to the profile before nuclear burning, and the whole diffusion equation is solved again until the condition is fulfilled.

4.5 About the Diffusion Coefficient

Now, the problem is to choose a proper diffusion coefficient for our problem. Different choices appear in the literature which leads to quite different results. This is easily understood because the evolutionary features depend critically on the chemical profiles. Here I just list in the following a few possible ways to obtain the coefficient from literature. Generally speaking, there are two types. One is to directly calculate the coefficient according to the run of hydrogen to maintain convective neutrality. Since inside the cores of massive stars opacity is dominated by electron scattering, we have $\kappa \propto (1+x)$. Another way is to use some explicit dependence on local thermodynamic quantities of the coefficient.

4.5.1 Numerically calculation of the coefficient

Simpson (1971), Sreenivasan & Wilson (1977) accepted a direct calculation of the coefficient by checking the run of hydrogen content to keep the convective neutrality fulfilled. Then it is assumed that the other chemicals will be dispersed with the same diffusion coefficient. This is carried out in practice by the following. The diffusion coefficient is written in to two first order equations (using Simpson's notation), for the diffusion flux,

$$\phi^s = -\lambda \frac{\partial x^s}{\partial m} \tag{4.28}$$

and for the time variation of the abundance x^s,

$$\frac{\partial x^s}{\partial t} - \theta^s = \frac{\partial \phi^s}{\partial m} \tag{4.29}$$

And the neutrality condition is also specified,

$$(\frac{\partial T}{\partial P})_{ad} - \frac{3\kappa L}{64\sigma G T^3 m} = 0 \tag{4.30}$$

where x^s is the chemical abundance of chemical s, λ is Simpson's diffusion coefficient (corresponding to $4\pi r^2 \rho^2 D$ in our notation), θ^s is the burning rate of chemical s, the

other symbols have the usual meaning. Now the equations (4.28), (4.29) and (4.30) are solved simutaneously. And here x^s is only the hydrogen content which determines the almost purely electron scattering opacity in interior of massive stars. Because the runs of luminosity, temperature, and adiabatic temperature gradient are all known, the diffusion coefficient can be determined, and the same coefficient is then used for solving other chemicals.

4.5.2 Prescriptions of the Diffusion Coefficient

Another way to get the coefficient is to give the coefficient explicitly with some local thermodynamical quantities. This prescription is assigned to all chemical elements.

For the convective core, with the same treatment of diffusion as in slower mixing regions, chemical homogeneity should be achieved. This is done through large diffusion coefficient. This yields a very short time scale for diffusion to homogenize the medium. The following formula, which could be given by a simple dimension argument, is generally accepted for fully convective case (Weaver et al 1978, Langer 1985),

$$D_i = \frac{1}{3} v_i l_i \tag{4.31}$$

where l_i is some local scale length describing the convective mixing which may be thought of as mixing length. Hence, to determine l_i we may use the same treatment of the mixing length. Also, v_i is the convective velocity at the mesh i. This expression for the diffusion coefficient is implied by the derivation of concentration flux in the above text. The physics behind this choice is straightforwardly to be seen, because inside the convective zone, mixing due to turbulent convection is dominant and the other diffusion processes like molecular, thermal or barodiffusion are negligible. The differences in the diffusion coefficient for convective cores among different authors are due to the different treatments of convection, and the different choices of the precise expressions for the convective velocity, as well as different setting of the mixing length. The velocity used in this thesis is given

by the algorithm by Bressan et al (1981).

This prescription of the diffusion coefficient gives a mixing time scale,

$$\tau_D = l^2/D \tag{4.32}$$

where l is the dimension of the convective field. This time scale is of order of a year for the typical convective core of massive stars. Hence it gives perfect mixing. The choice of the coefficient for incomplete mixing such as semiconvection are at variance in the literature.

For semiconvection, Eggleton (1972) used

$$D_{sc} \propto (\nabla_{rad} - \nabla_{ad})^2 \tag{4.33}$$

and Weaver et al (1978) gave

$$D_{sc} \propto \frac{D_c D_r}{D_c + D_r} \tag{4.34}$$

where D_r is the radiative diffusion coefficient. These choices of diffusion coefficient give very convenient numerical treatment, but contain some arbitariness. Langer et al (1983, 1985) proposed a method based on the vabrational stability analysis and a numerical factor was used to scale the efficiency of semiconvective mixing. He took all the mixing in stellar interior as diffusion, for fully convective region, he use the same expression as Weaver et al's and expressed as:

$$D_c = \frac{1}{3}\gamma^{\frac{2}{3}} H_p [\frac{c}{\kappa\rho} g\beta(1-\beta)\nabla_{ad}(\nabla_{rad} - \nabla_{ad})]^{1/3} \tag{4.35}$$

where $\gamma = l_m/\lambda_p$, the other symbols have the usual meaning.

For semiconvective zones, he gave:

$$D_{sc} = \alpha \frac{\kappa_r}{6c_p\rho} \frac{\nabla - \nabla_{ad}}{\nabla_{LED} - \nabla} \tag{4.36}$$

where

$$\kappa_r = 4acT^3/3\kappa\rho$$

is radiative conductivity, the other symbols have the usual meaning. α, is his scaling parameter of the diffusion time scale.

The physical arguments underlying the choice of the diffusion coefficient are connected with our understanding of the nature of convection. As we have no clear judgement on the convection theories, probably we will have no judgement on diffusion process used for chemical distribution.

4.5.3 Diffusion coefficient for overshoot region

To get the goal of we have in mind, we have to specify the diffusion coefficient. The idea is the following. In the properties of elements overshooting into the region outside the convective core, are studied by many authors. The turbulent energy flux becomes very small (Xiong 1986) and the convective flux turns out to be negative (Bressan et al 1981, Meader 1983). And due to the deceleration of the medium in the overshooting regions, the velocity is slowed down and finally turn to be zero, the temperature excess of a element turns to be zero when crossing the boundary and becomes negative (Meader1975). These physical processes may imply that the mixing process there might be gradually slowed down. My assumption of diffusive mixing is based on this simple consideration, and this is also one of the results of Xiong's method (1985). I will further assume that we accept the same method for all convective regions if they are present. Doing this needs more physical considerations, and it is left to be studied later. Within the overshooting region outside each convective zone, I will follow Weaver et al's choice for semiconvective mixing region. The radiative diffusion coefficient is determined in the following way,

$$\mathbf{F}_r = -\frac{16\pi acT^3}{3\kappa\rho}\frac{dT}{dr} \tag{4.37}$$

where $\mathbf{F}_r$ is radiative flux.

Writing the above equation with the gradient of radiative energy density on the right

side, we have

$$\mathbf{F}_r = -\frac{4\pi c}{\kappa\rho}\frac{du_r}{dr} = -D_r\frac{du_r}{dr} \tag{4.38}$$

where D_r defines the diffusion coefficient for radiative energy. This gives an approximate measure of the time scale for some slower or incomplete mixing as inside semiconvection regions. For the present work, we take equation (4.31) for convectively unstable regions. For overshooting zones, we use

$$D_{os} = \alpha_{os}\frac{D_c D_r}{D_c + D_r} \tag{4.39}$$

where the cofficient is adjested to give a time diffusion scale around the current time step.

Because the mixing in real stars is not such a simple diffusion process, any choice for the diffusion coefficient will be somewhat arbitrary. As long as the lack of a satisfactory convection theory exists, using diffusion for chemical mixing in some incomplete mixing regions in stars at least a workable means of treating chemical distribution. This treatment actually introduces an additional parameter to stellar evolution, as is clearly shown by Langer (1985), and the present work. Further work should be determine this coefficient on a more physical ground.

Chapter 5

Numerical results of diffusive mixing stellar models

5.1 A brief introduction of input physics

5.1.1 The code

The code was originally developed by Kippenhahn, Weigert and Hoffmeister (1967). The relaxation method introduced by Henyey (1958) was adopted to solve the normal equations for stellar evolution. This code has been revised by the PADOVA stellar evolution group, mainly concerning the mixing scheme, the new nuclear reaction rates and opacities.

5.1.2 Opacity

Radiative and conductive opacities are taken from the Los Alamos Astrophysical Opacity Library (1977) wich can only be used for $T > 10^4$; for $T \leq 10^4$, the opacity was derived from the tables of Cox and Stewart (1970). The values of the opacity are obtained by bicubic spline interpolations among the tables. The molecular opacity contribution due to CN, CO, H_2O and TiO is considered, utilizing the analytical formula of Bessel et

al (1989,1991). These formula are based on opacity tables including molecular opacity sources computed by Alexander (1975) and Alexander et al. (1983).

5.1.3 Nuclear reaction Rates

Changes in the chemical abundances have been followed in detail using an updated version of the routines employed by Greggio (1984). For the H-burning reactions, the three pp chains and CNO tri-cycle have been considered (cf. Maeder 1983), while the following reactions have been taken into account during Helium burning: 4He(α,γ) 8Be(α,γ) 12C(α,γ) 16O(α,γ)20Ne $--(\alpha,\gamma)$26Mg 14N(α,γ) 18F(e+ν)18O(α,γ)22Ne $<$ $--(\alpha$,n)25Mg. The $C^{12}(\alpha,\gamma)^{16}O$ reaction rate has been taken from Caughlan and Fowler (1988), the latest redetermination lowers the value of Kettner et al. (1982), Langanke and Koonig (1982), Caughlan et al. (1985) almost to the 1972 one by Fowler et al., 1975. Screening factors from Graboske et al. (1973) have been adopted. Beta decays have been treated as instantaneous, as well as the 8Be(α,γ)12C reaction. For the elements 2H, 7Be and 7Li we have considered a depletion rate equal to the supply rate from the beginning of the computation. For the remaining species (1H, 3He, 4He, 12C, 13C, 14N, 16O, 17O, 18O, 20Ne, 22Ne, 25Mg, 26Mg) the evolution has been followed in detail using an explicit scheme of integration. Following the notation by Arnett and Truran (1969), the network equations are written in terms of the abundances Yi = Xi/Ai, where Xi is the mass fraction of the species i and Ai its atomic mass number, and can be expressed as (cf. Maeder 1983): dYi/dt = -[ij]YiYj + [rs]YrYs . Their integration over the time step (Δt), determined on the basis of the structural variations, is covered in several mini time steps (Δt), whose number depend on the temperature at the given mesh point, if convectively stable. In convective regions, however, the length of the mini time step Delta t is controlled by the difference in the results obtained with one integration over the whole Delta t, and that obtained with two successive integrations over $(\Delta t)/2$. In order to save computational time, the variations of the abundances in convective regions are determined

from the mean rates, averaged over the whole region, as in Iben (1964). The variations of the abundance of a species i is determined by $(\Delta Yi) = (dY\ i/dt) * (\Delta t)$, where the derivative is computed evaluating the reaction rates in t + (Δ t)/2, by means of extrapolation from the two preceeding models. During Hydrogen burning, special care has been paid to avoid oscillations in the abundances once equilibrium between supplying and depleting reactions is achieved by any element: the results of the numerical integration are compared to the appropriate equilibrium abundances at each time step, and the equilibrium value is adopted if necessary. The conservation of the total number of CNO nuclei and of the total number of nucleons are secured in the computation of the abundances of 14N and 3He, respectively, once equilibrium of these two elements is achieved.

5.1.4 Mixing algorithm

The numerical method described in chapter 4 is used for all diffusion regions, including full convection, overshoot regions outside each border of full convection zones, and semiconvetion occurring when $\nabla_{ad} < \nabla < \nabla_{LED}$.

When a region is fully convective, i.e. $\nabla_{rad} > \nabla_{ad}$, because of the large diffusion coefficient, the medium up to the point where $\nabla_{rad} = \nabla_{ad}$ is completely mixed. This is exactly the same as instant mixing.

In each overshoot region, the diffusion coefficient is smaller by several orders of magnitude than for convective regions, and the mixing time scale [eq(4.32)] in the overshooting region is comparable to the time step for changing the abundance of chemicals through nuclear reaction. We can adjust the time scale for mixing with the parameter α to test different mixing time scales. The assumed slow mixing process "makes a profile" inside the overshooting zone. For semiconvection, Langer's scheme and coefficient (eqs [4.35],[4.36]) are adopted.

5.1.5 Mass loss rate

Mass loss by a stellar winds is taken into account following the rate of mass loss for radiation pressure driven winds of Castor et al (1975). The mass loss rate is given by,

$$M = \frac{L}{cv_{th}} \frac{\alpha}{\Gamma} \left| \frac{1-\alpha}{1-\Gamma} \right|^{\frac{1-\alpha}{\alpha}} (K\Gamma)^{1/\alpha} \tag{5.1}$$

with L, M being the stellar luminosity and mass, c the speed of light, v_{th} the thermal speed of random motion of absorbing ions, Γ the ratio of the luminosity to Eddington luminosity. The force multiplier parameter α and K are assumed to be 0.83 and 0.01 respectively.

For the case of outer envelope convection, we adopt for atmosphere mixing length, $l_{atm} = 1.5$.

The initial chemical abundances used for all the models is $X = 0.700$ for hydrogen, $Y = 0.280$ for helium, and all other chemical elements heavier than helium (including 3He) is taken as "metal", $Z = 0.02$.

5.2 A description of the models

Based on the assumption we made for the overshoot region from all convective zones in the stellar interior, and using the numerical scheme for diffusion given in chapter 4, the following sequences are computed.

Case IO: $M = 20M_{\odot}$ Instant mixing throughout the whole mixing range, with core overshoot parameter $\lambda_c = 1.0$, and envelope overshoot parameter λ_e=0.7. For intermediate convective zones, boundaries are determinied by the Schwarzschild condition.

Case DO3: $M = 20M_{\odot}$ Diffusive mixing with the diffusion parameter $\alpha_{os} = 10^{-3}$; with all boundaries determined by a velocity criterion.

Case DO4: The same as case **DO3**, except $\alpha_{os} = 10^{-4}$.

Case DO3ML: The same as case **DO3**, except mass loss is considered.

We also computed two tracks for the semiconvective case with Langer scheme.

Case SC30: $M = 30M_{\odot}$ Semiconvection and diffusive mixing: $\alpha_{sc} = 0.01$.

Case SC20: The same as case **SC30**, except $M = 20M_{\odot}$.

For each of the above sequences, I will give a table, and a set of figures. The table is named after the name of the model, and the figures will be named by the name of the coresponding sequence, and an index number.

5.3 Case SC30 Diffusive semiconvection and comparison with Langer's models

Langer's prescription for the diffusion coefficient is used for two models in this study. Employing this model is aimed at testing the routine of diffusive mixing and to make some comparison between the semiconvective diffusion models and our overshooting diffusive ones.

Before going into details, I will put some stress on the difference in input physics and numerical treatments. First of all, convection is differently treated, the one we are using is based on a simple non local description of convection described in chapter 2, while the one used by Langer (1985) is a classical version of mixing length theory. The mixing length parameter l ($l = \Lambda/H_p$) in Langer's models is 1.5. The one we used corresponds to $l = 1$ in classical mixing length theory. Due to some problems in the chemical routine when using diffusion, our model stops at the central helium content of 0.255. This is mainly

due to our treatment of chemical mixing by diffusion. Another thing is that we neglected the energy transport by semiconvection and this brings simplicity to the mixing. This is based on the fact that energy transport by semiconvection is negligible. However, this is also to be included in the future.

Our model Case **SC30** corresponds to case C in Langer (1985), with $\alpha = 0.01$. The HR diagrams and the internal structure map of convective zones of our model are given in fig. SC30(1). The table SC30 shows some quantities of our model, as described in the legend written below the table. The same figure is copied and named as fig. SC30(1L), there are several differences found on comparison,

- The life time of hydrogen burning is 5.70 $10^6 yr$ while Langer's model gives $5.6710^6 yr$. This difference is due to our model having a higher value of core mass;

- Our track runs at about 0.2 magnitudes higher than Langer's, and at the b point (conventionally defined as the lowest effective temperature reached by stars during main sequence, which defines the boundary of main sequence band) our model possesses a lower effective temperature. These are clearly the result of a larger core size.

- Up to the point that our program stops, our model ignites and spends all helium burning in the red-ward side of the HR diagram, while Langer's spends 0.6% of the hydrogen life time of helium burning in the blue, which is 7% of its whole helium burning lifetime. This marks the largest difference between the two models;

- The main feature of the change of structure of convective and semiconvective zones resembles Langer's model. In Langer's figure SC30(1L), during the main sequence phase, one semiconvective zone is formed in the intermediate zone, while ours is disconnected. The distribution of intermediate zones during the crossing of the HR diagram is quite similar. There are some horizontal cuts by semiconvective

thin layers. All these things may understood as the result of the calculation of the diffusion efficiency parameter and mass zoning. As noted by Langer, if α is small, the zones will tend to be connected. As I said at the beginning, we used different mixing length theory and this will affect the value of the diffusion.

As data about the structure of the models is not given by Langer, and because of the numerical problems for this mixing scheme, as mentioned above, further comparison is not presented for the moment. Our models qualitatively reproduce Langer's results. Fig SC30(2-6) shows some information about the mixing. The three panels in each figure give the energy generation rates which affect the chemical profile, and temperature gradients, which defines the region of mixing, and the middle one gives the profiles of hydrogen and helium made by these two factors.

Langer emphasized that one of the important aspects of the efficiency parameter is to make the convective (either fully convective or semiconvective) zones more connected if it is small and vise versa. During our numerical experiment, We found that this could be due to neglecting neutrality condition. Without checking the neutrality condition, the mixing could be at any level. This actually gives a possibility to create new zones if the parameter is large, and, for a small enough parameter, it will not change too much the hydrogen profile.

5.4 A description of the diffusive mixing models

5.4.1 Case: IO Instant mixing scheme

This is the original treatment of mixing in the PADOVA code. This is set to be a standard for testing the diffusive mixing scheme, which is going to be described later, for the present purpose. In this model, convective and overshoot completely eliminate the molecular gradient profile instantly (corresponding to infinitely large diffusion coefficient).

This fixes an upper limit for for degree of mixing in the overshooting region. The lowest degree of mixing is the classical model, which does not mix at all in the regions by the new criterion.

5.4.2 Case DO3 & DO4 overshooting and diffusive mixing

Diffusive mixing is computed for stellar models with two different parameters. The numerical method is described in chapter 4. Our parameter α_{os} works the same as used by Langer, and Weaver et al, so as to regulate the diffusion time scale of the mixing process. It is very interesting to see the effect of incomplete mixing in the overshooting regions. As we will see later, variation of this parameter will have the expected effect, which is that larger values make the model beahave more like case **IO**, and lower values have the oppsite effect.

5.4.3 Case DO3ML: Diffusive overshoot and mass loss

To account for the directly observed features of evolution of massive stars, one model of mass loss with the rate specified above is constructed. Diffusion in this case is included to see how the diffusive mixing treatment will be influenced by mass loss.

5.5 Comparison of the models

5.5.1 General evolutionary features of these models

Central Hydrogen Burning phase. Through this phase, the evolution of all the models **IO, DO3, DO4, DO3ML**, is basically the same. The exception is **DO3ML** which loses some mass, up to the **b** point. The mass of the star is 18.76 $M_{\odot}$, and some deviation from the group is apparent, as shown on fig. 7. The lowest temperature at **b** is given by the model with mass loss.

As can be seen from the table of each sequence, the longest life in central Hydrogen burning phase is given by the case **IO**, the smaller the α the shorter the life time. As for Case **DO3ML**, the effect of mass loss to extend hydrogen burning life time is balanced by this incomplete mixing of overshooting. This is not a surprising result, because this incomplete mixing has the similar effect as some reduction of the core region. Less fuel gives a shorter life time. This difference is bigger than the difference between case A and case B presented by Chiosi & Summa (1970). Of course, this difference could be as big if the parameter is adjusted. The semiconvective model forms an intermediate semiconvective zone from a very early time of hydrogen burning, and this zone goes deeper as the fully convective core retreats. This makes the hydrogen profile more smooth (fig **SC20** 3).

Crossing the HR diagram and Helium ignition. As the stars exhaust the central hydrogen, the core contracts. Only for the case **SC20** does the core become radiative. The others have a very small convective zones remaining round the center. This is due to the very strong release of gravitational energy during contraction. The general structure among all sequences is that, due to the energy source in the shell, some intermediate convective zones develop. For all models with diffusive overshooting, the structure of the intermediate zones are very similar to each other. A single intermediate zone forms at a fractional mass of 0.6, and breaks into two disconnected zones, the upper one reaching 0.75. For the semiconvective sequence, some intermediate layers formed above the thick shell hydrogen source (fig. **SC20** 3). Different from **SC30**, the **SC20** model produces at the inner boundary of these intermediate zones a very thick semiconvective zone (fig. **SC20**). All the models run very fast across the HR diagram after ignition of helium. The intermediate zones disappear at the ignition of helium in the core.

5.5.2 Helium burning phase and the loop

The helium burning phase is quite different among the sequences, and can be seen from the HR diagram of the five tracks (fig.7). The semiconvective case did not go to the end for the same problem as the 30 $M_{\odot}$ case but the helium content is already very low < 0.1, so almost the whole life time of helium burning for this case is spent in the red. In this phase, the track stays at a point ($logT_{eff} = 3.614$, $logL/L_{\odot} = 4.7157$) for quite a long time until the problem of a nonphysical growth in the neon abundance occurs, see fig.(**SC20** 2). Case **IO** and **DO3ML** evolve along the Hayashi limit during the whole He burning phase, but **DO4** & **DO3** make loops to the blue side. This is a very interesting point. Since this is a problem of the models with core overshoot, as seen in chapter 2, it is solved by introducing envelope overshoot (Alongi 1991). For the chemical composition used in this work, case **IO**, even using $\lambda_e = 0.7$, spends the whole helium burning in the red. **DO4**, **DO3** spend respectively about 36%, and 33.5% of their central helium burning life time in this loop, and the highest effective temperature reached by these two models are 3.87 and 3.82 respectively. As a prilimilary understanding, loops made by **DO3** and **DO4** are not likely to be caused only by diffusive mixing. The most contrasting point between the looping sequences and other overshooting ones is that they have used extra mixing in the intermediate zone between hydrogen exhaustion and helium ignition. This extra mixing in the large intermediate zones will have very strong influence on the evolution of the envelope (Chiosi & Summa 1970). Actually, diffusive mixing only slightly influences the evolution, as can be seen from fig 7. On the main sequence, where only the core convection is present, the tracks of the sequences with diffusive mixing follow exactly the same track as **IO**, the difference becoming visible only at the exhaustion of hydrogen.

Life time ratios. The life time ratio is a very important quantity for stellar evolution and is strongly constrained by obervational star counts. Moreover this is ultimately linked to the mixing processes in the stellar interior. The life time ratios of helium burning to

hydrogen burning are

$$\begin{aligned}
\left(\frac{t_{He}}{t_H}\right)_{IO} &= 0.0531 \\
\left(\frac{t_{He}}{t_H}\right)_{DO3} &= 0.0614 \\
\left(\frac{t_{He}}{t_H}\right)_{DO4} &= 0.0617 \\
\left(\frac{t_{He}}{t_H}\right)_{DO3ML} &> 0.0550 \quad \text{(not reach He exhaustion)} \\
\left(\frac{t_{He}}{t_H}\right)_{SC20} &> 0.0550 \quad \text{(problem of chemical routine)}
\end{aligned}$$

The life time ratio is considerably affected by using diffusive mixing but appears not very sensitive to the change in the parameter. The life time on the main sequence for case **DO4** is $4 \cdot 10^4 yrs$ longer than case **DO3**. Probably more numerical tests should be done to find a threshold value for this parameter.

Mass loss Case bf DO3ML The main features of stellar evolution with mass loss is clearly seen in this model. The track runs at lower luminosity on the main sequence, which gives a greater apparent difference than by diffusion only. This model does not show the loop as with **DO3** and **DO4**.

Fig. 7

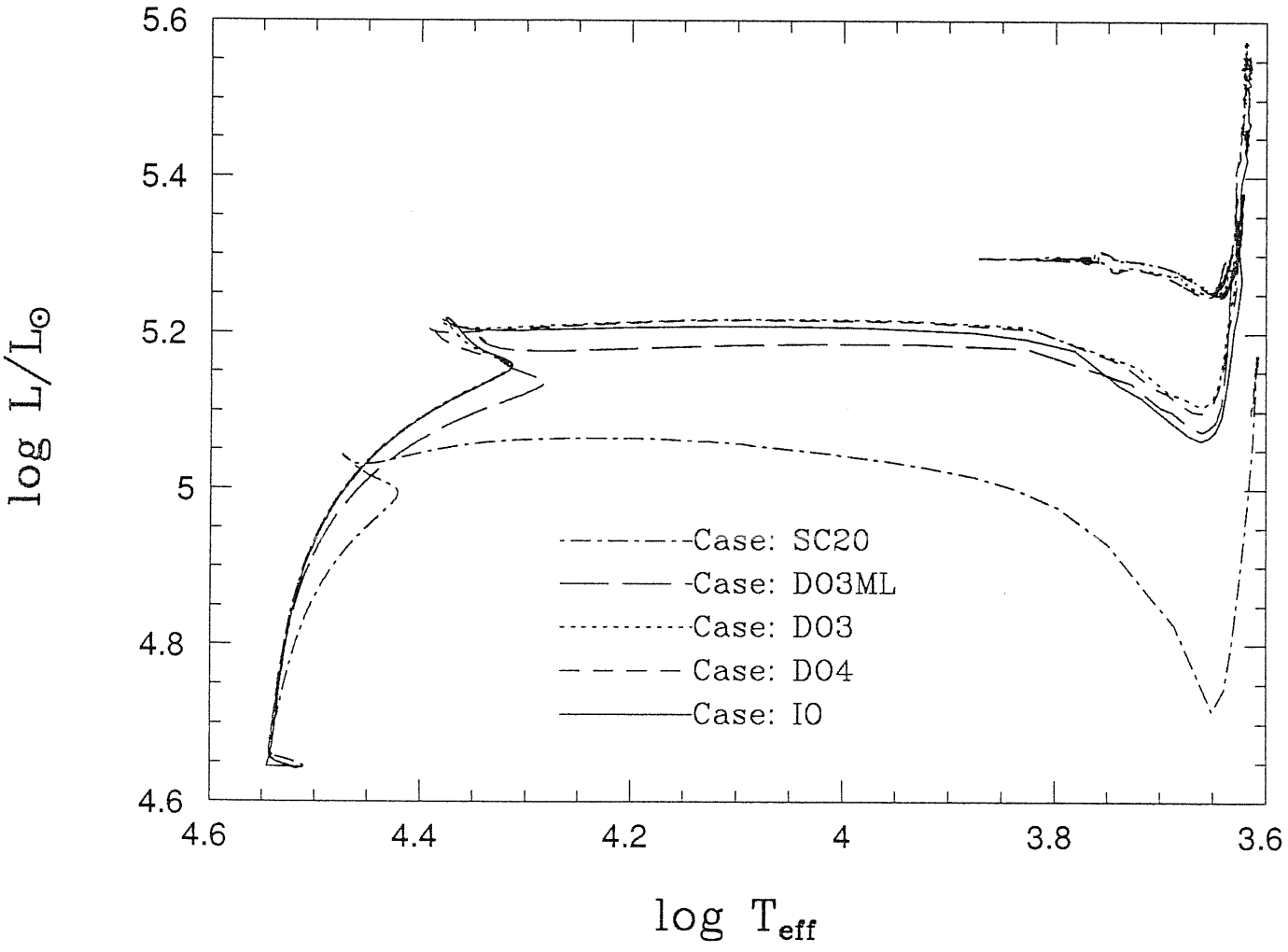
5.6
5.4
5.2
5
4.8
4.6
log L/L⊙
4.6
4.4
4.2
4
3.8
3.6
log T_eff
Case: SC20
Case: DO3ML
Case: DO3
Case: DO4
Case: IO

TABLE ( ) Case: IO

MOD	eta	dt/t	LogL	LogTE	Mbol	gms	rate	comp	Xsup	Ysup	Csup	Osup	Nsup	Conv	qhel	qcarox
At ZAMS:																
1	0.000	0.000	4.6443	4.5102	-6.84	20.00	0.00	0.700	7.00E-01	2.80E-01	4.36E-03	9.63E-03	1.06E-03	5.332	0.000	0.000
2	0.559	0.053	4.6453	4.5458	-6.84	20.00	0.00	0.696	7.00E-01	2.80E-01	4.36E-03	9.63E-03	1.06E-03	5.941	0.000	0.000
At the lowest point on MS:																
166	9.865	0.940	5.1574	4.3126	-8.12	20.00	0.00	0.012	7.00E-01	2.80E-01	4.36E-03	9.63E-03	1.06E-03	4.206	0.000	0.000
At Central H exhaustion:																
166	9.865	0.940	5.1574	4.3126	-8.12	20.00	0.00	0.012	7.00E-01	2.80E-01	4.36E-03	9.63E-03	1.06E-03	4.206	0.000	0.000
216	9.932	0.947	5.2013	4.3622	-8.23	20.00	0.00	0.000	7.00E-01	2.80E-01	4.36E-03	9.63E-03	1.06E-03	2.930	0.000	0.000
At the bottom of RGB:																
234	9.937	0.947	5.2023	4.3097	-8.24	20.00	0.00	0.981	7.00E-01	2.80E-01	4.36E-03	9.63E-03	1.06E-03	0.280	3.616	0.000
At Central He ignition:																
239	9.939	0.948	5.2076	4.1647	-8.25	20.00	0.00	0.981	7.00E-01	2.80E-01	4.36E-03	9.63E-03	1.06E-03	0.131	3.848	0.000
240	9.939	0.948	5.2083	4.1171	-8.25	20.00	0.00	0.980	7.00E-01	2.80E-01	4.36E-03	9.63E-03	1.06E-03	0.216	3.868	0.000
At first Dredge-up:																
268	9.944	0.948	5.3601	3.6227	-8.63	20.00	0.00	0.976	6.54E-01	3.26E-01	3.37E-03	8.22E-03	3.29E-03	2.474	4.126	0.000
269	9.945	0.948	5.3643	3.6231	-8.64	20.00	0.00	0.976	6.54E-01	3.26E-01	3.37E-03	8.21E-03	3.30E-03	2.492	4.135	0.000
At the tip of RGB:																
590	10.488	1.000	5.5560	3.6155	-9.12	20.00	0.00	0.549	6.16E-01	3.64E-01	3.13E-03	7.70E-03	4.04E-03	0.000	4.613	3.529

MOD ---- Model number
Log L ---- log L/Lo
gms ---- current stellar mass
Xsup ---- surface H abundance
Osup ---- surface Oxygen abundance
Conv ---- fractional mass of convective core
Qcarox --- fractional mass of he exhsauted core

eta ---- age in 10**6 year
logTE ---- log (effective temperature)
rate ---- energy generation rate
Ysup ---- surface He abundance

dt/t ---- ratio of (step width in ime/total lifetime)
Mbol ---- bolometric magnitude
comp ---- central abundance (major abundance element)
Csup ---- surface Carbon abundance
Nsup ---- surface Nitrogen abundance
Qhel ---- fractional mass of hygrogen exhausted core

** The same legend is used for the tables of the sequences

Evolution of Central Abundances

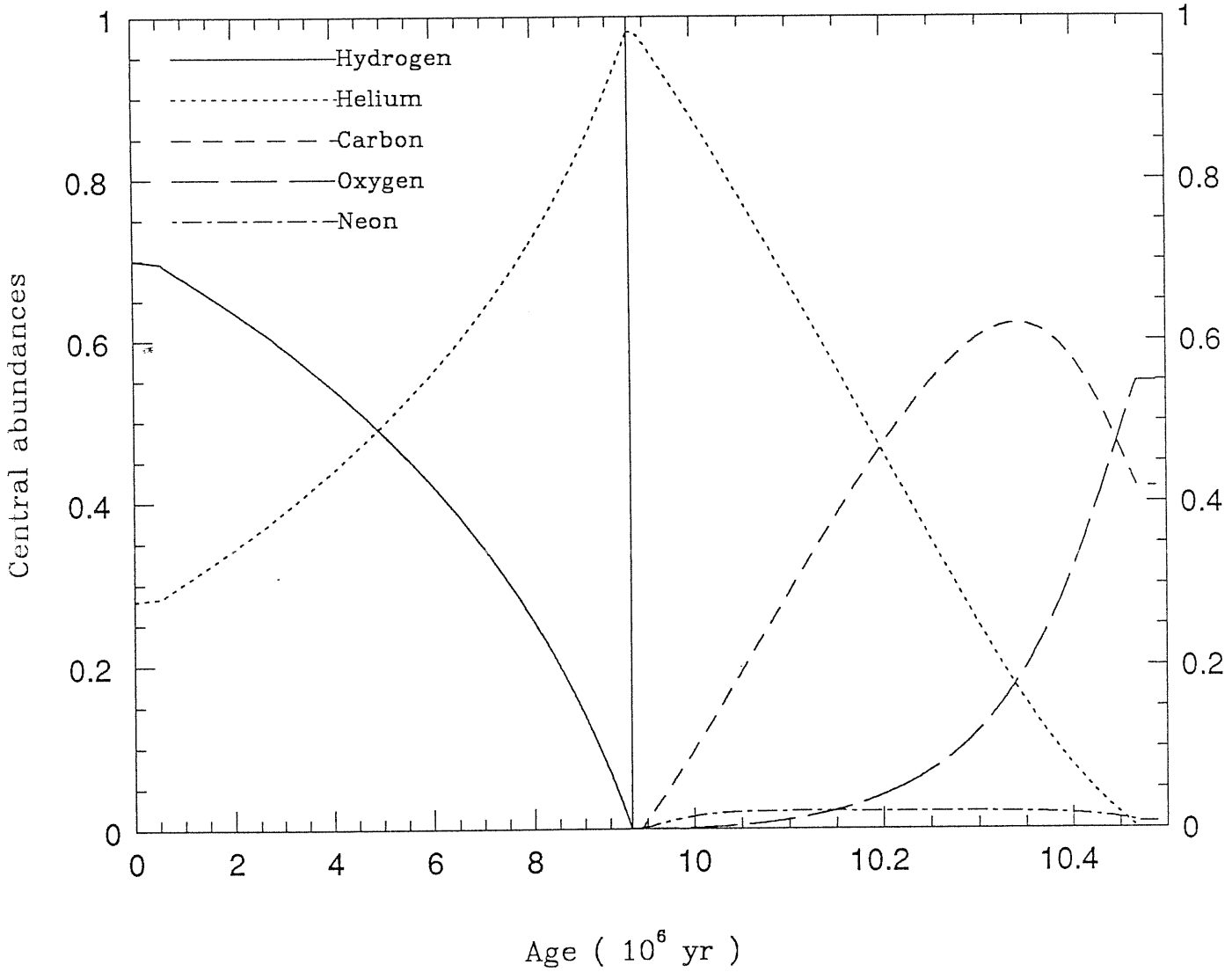

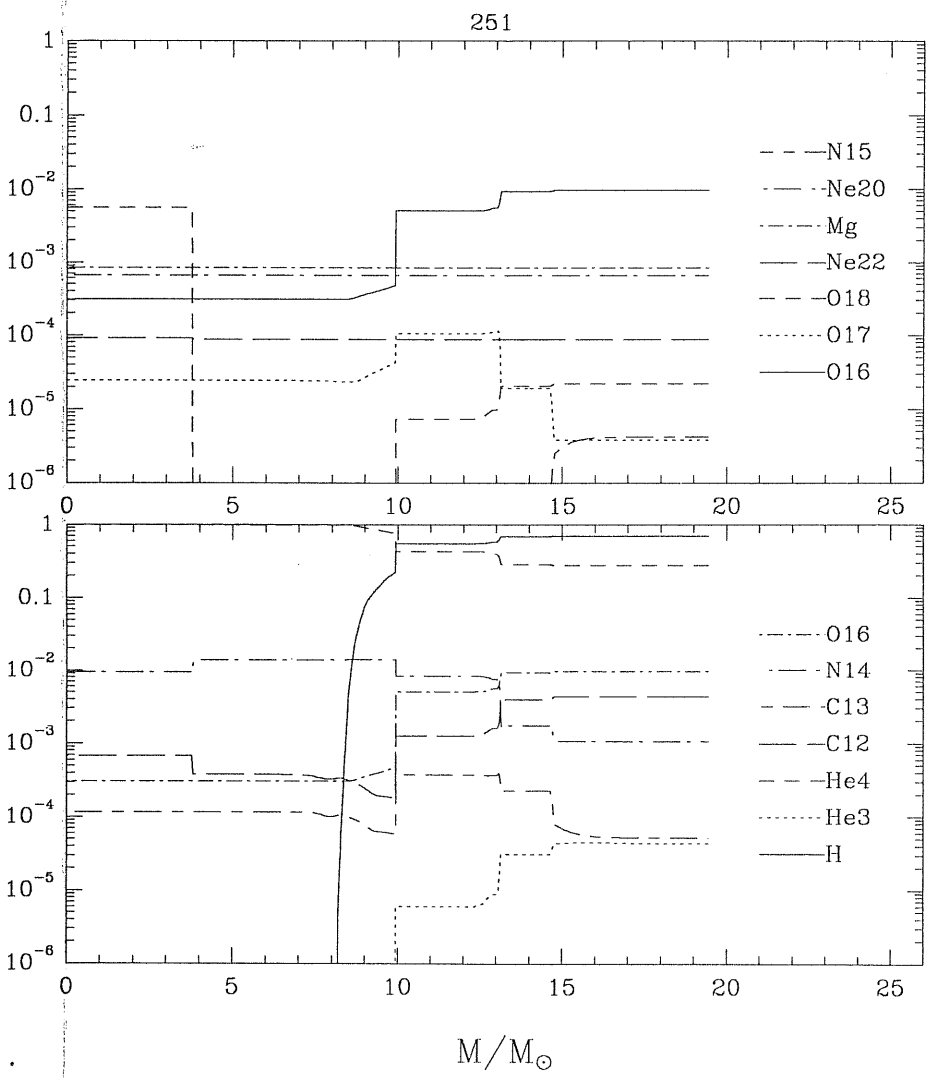
251
N15
Ne20
Mg
Ne22
O18
O17
O16
O16
N14
C13
C12
He4
He3
H
M/M⊙

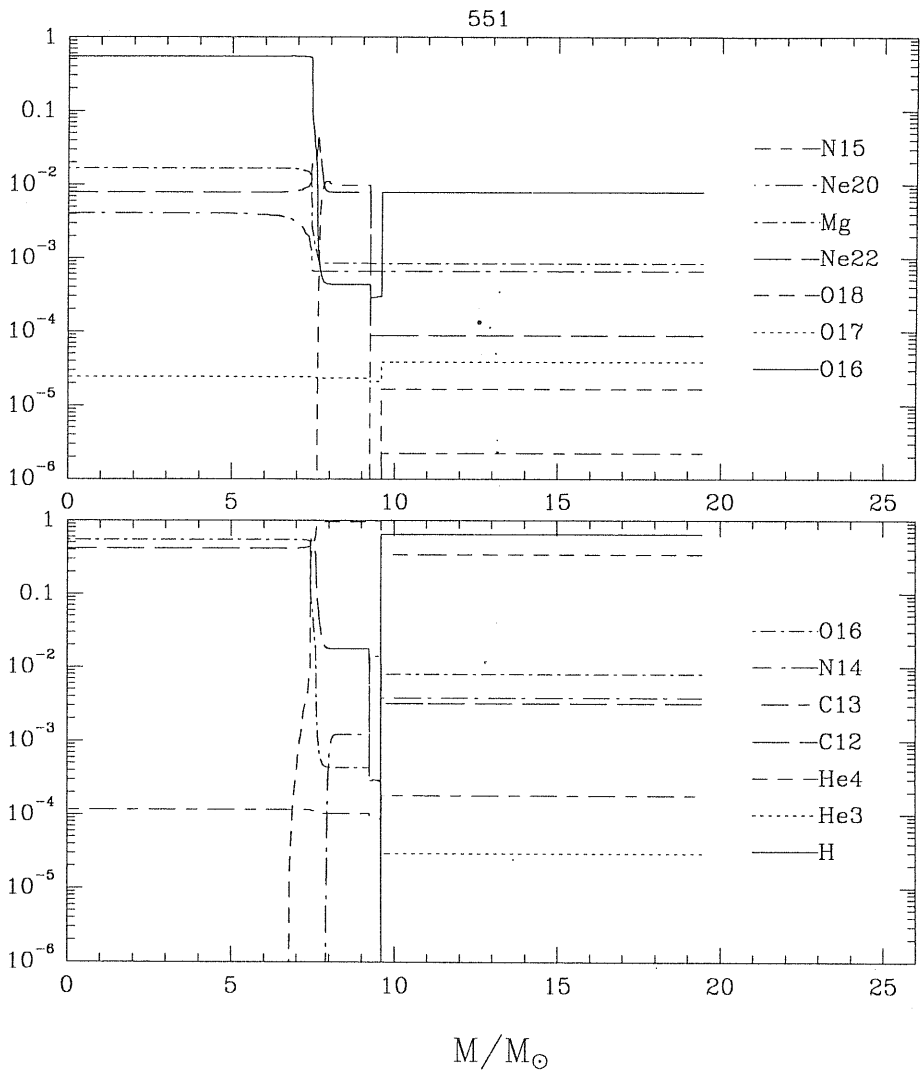
551
N15
Ne20
Mg
Ne22
O18
O17
O16
O16
N14
C13
C12
He4
He3
H
M/M⊙

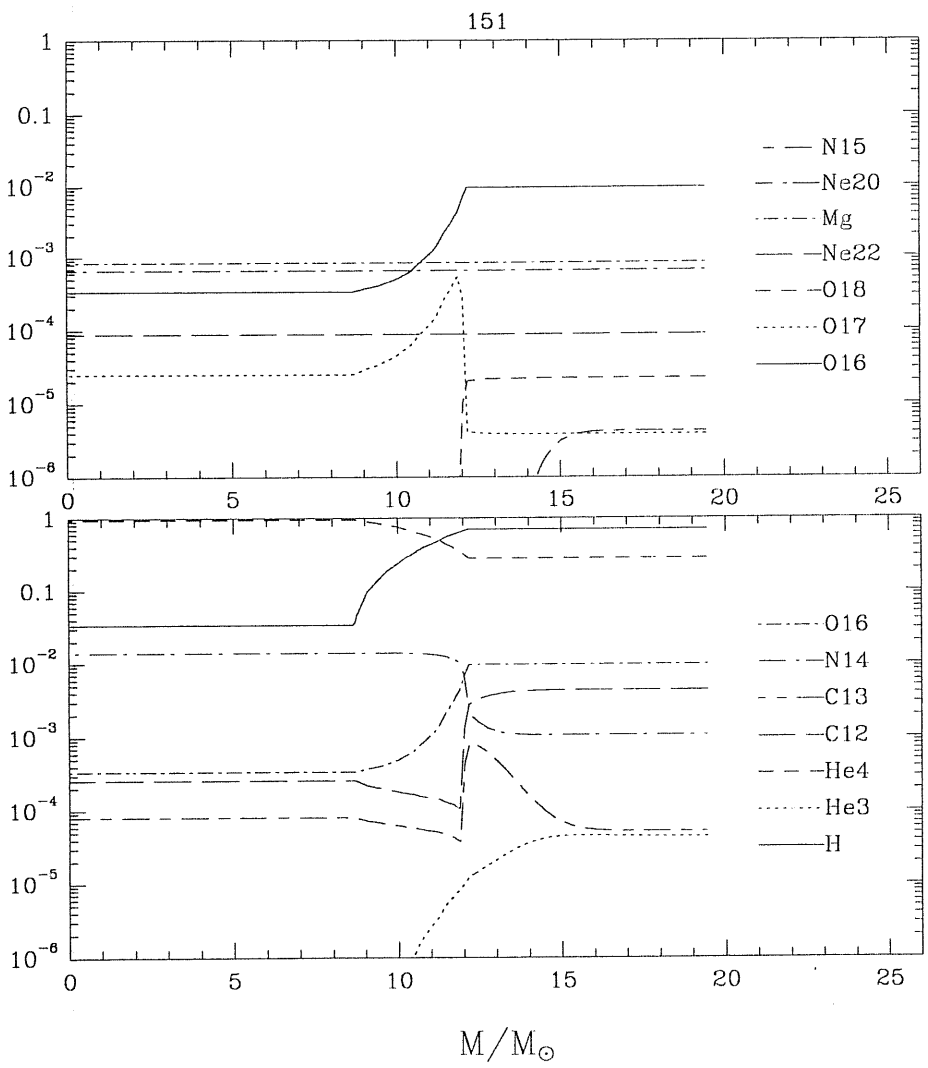
151
N15
Ne20
Mg
Ne22
O18
O17
O16
O16
N14
C13
C12
He4
He3
H
M/M⊙

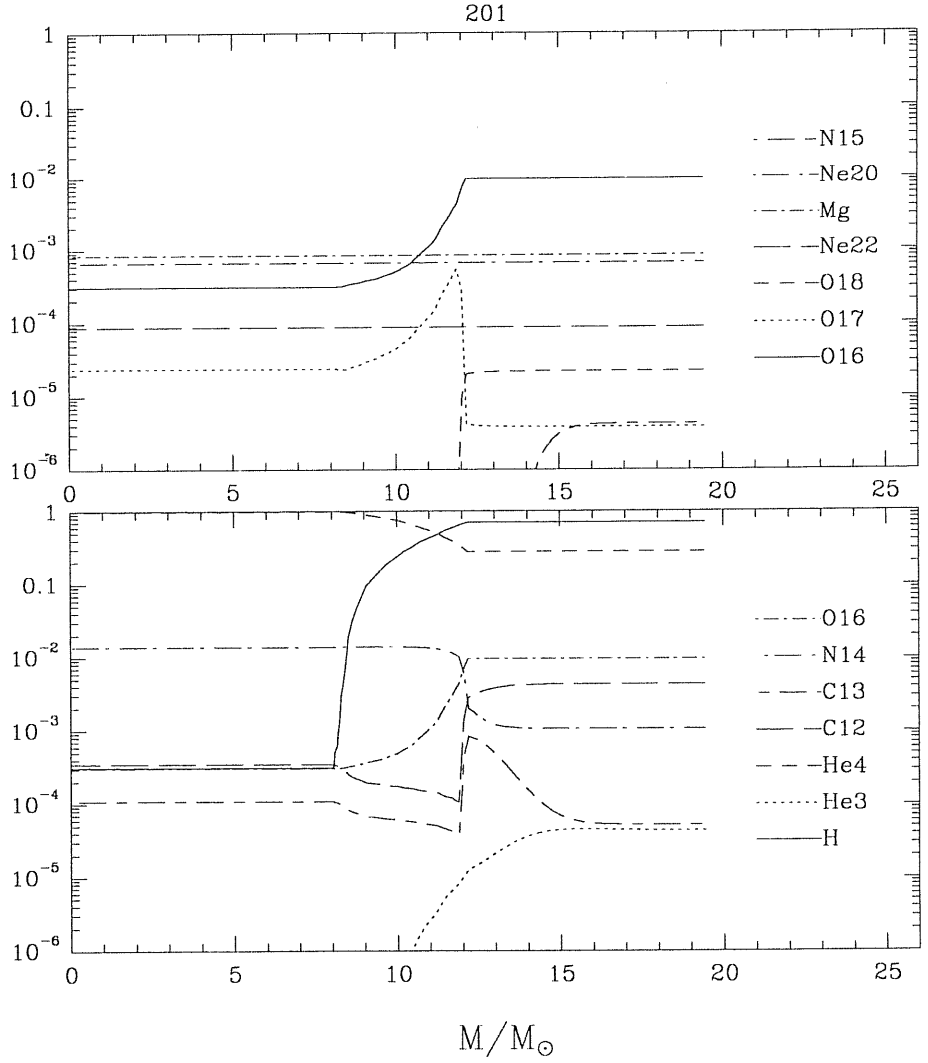
201
N15
Ne20
Mg
Ne22
O18
O17
O16
O16
N14
C13
C12
He4
He3
H
M/M⊙

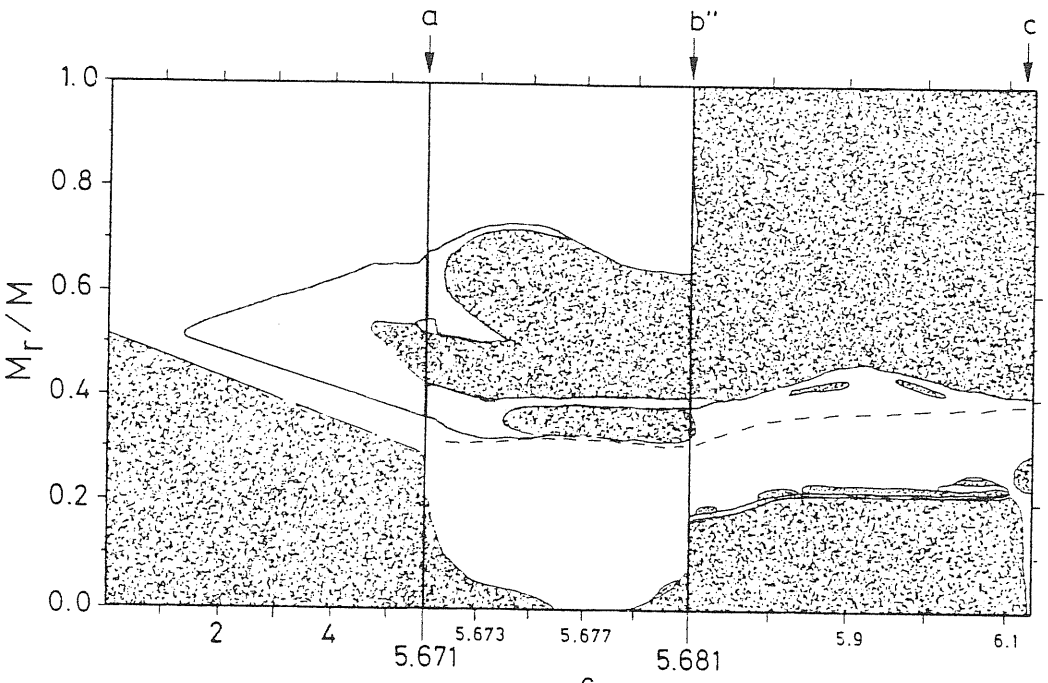

Fig. 10 c

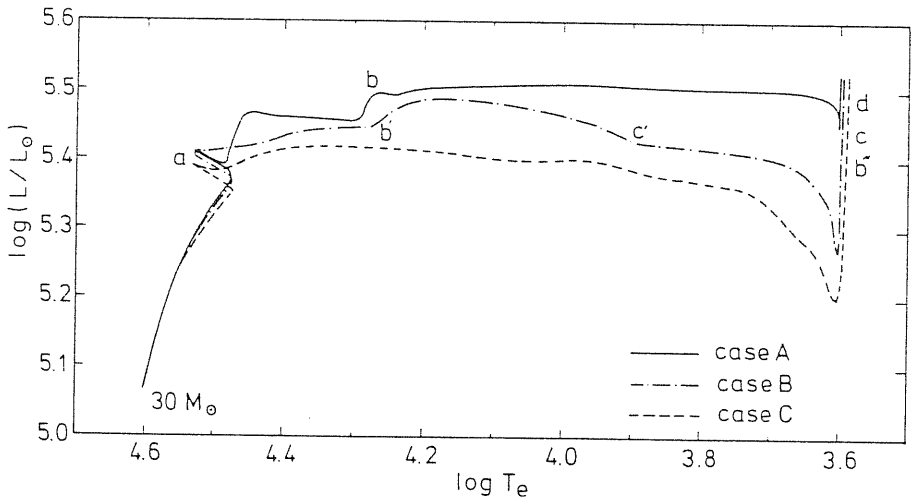

SC30 (1L)

TABLE ( ) CASE: SC30

MOD	eta	dt/t	LogL	LogTE	Mbol	gms	rate	comp	Xsup	Ysup	Csup	Osup	Nsup	Conv	qhel	qcarox
At ZAMS:																
1	0.000	0.000	5.0891	4.5732	-7.95	30.00	0.00	0.700	7.00E-01	2.80E-01	4.36E-03	9.63E-03	1.06E-03	0.5707	0.000	0.000
2	0.559	0.091	5.0992	4.5843	-7.98	30.00	0.00	0.686	7.00E-01	2.80E-01	4.36E-03	9.63E-03	1.06E-03	0.5626	0.000	0.000
3	0.631	0.103	5.1028	4.5938	-7.99	30.00	0.00	0.682	7.00E-01	2.80E-01	4.36E-03	9.63E-03	1.06E-03	0.5707	0.000	0.000
4	0.703	0.115	5.1057	4.5997	-7.99	30.00	0.00	0.678	7.00E-01	2.80E-01	4.36E-03	9.63E-03	1.06E-03	0.5786	0.000	0.000
5	0.812	0.132	5.1114	4.6038	-8.01	30.00	0.00	0.668	7.00E-01	2.80E-01	4.36E-03	9.63E-03	1.06E-03	0.5707	0.000	0.000
At lowest T_eff on MS:																
156	5.615	0.914	5.4176	4.4386	-8.77	30.00	0.00	0.020	7.00E-01	2.80E-01	4.36E-03	9.63E-03	1.06E-03	0.3144	0.000	0.000
At Central H-exhaustion:																
222	5.702	0.928	5.4603	4.4946	-8.88	30.00	0.00	0.000	7.00E-01	2.80E-01	4.36E-03	9.63E-03	1.06E-03	0.2034	0.000	0.000
223	5.702	0.928	5.4614	4.4954	-8.88	30.00	0.00	0.980	7.00E-01	2.80E-01	4.36E-03	9.63E-03	1.06E-03	0.1704	2.034	0.000
At Central He-ignition:																
251	5.712	0.930	5.4701	3.8386	-8.91	30.00	0.00	0.980	7.00E-01	2.80E-01	4.36E-03	9.63E-03	1.06E-03	0.1181	3.181	0.000
252	5.712	0.930	5.4615	3.8112	-8.88	30.00	0.00	0.979	7.00E-01	2.80E-01	4.36E-03	9.63E-03	1.06E-03	0.1271	3.236	0.000
At the bottom of RGB:																
257	5.713	0.930	5.3273	3.6887	-8.55	30.00	0.00	0.979	7.00E-01	2.80E-01	4.36E-03	9.63E-03	1.06E-03	0.1788	3.254	0.000
At first dredge-up:																
286	5.742	0.935	5.5874	3.6544	-9.20	30.00	0.00	0.959	6.34E-01	3.46E-01	3.03E-03	7.57E-03	4.28E-03	0.2320	3.576	0.000
At Half He burnt:																
599	5.946	0.968	5.4918	3.6537	-8.96	30.00	0.00	0.490	6.31E-01	3.49E-01	2.99E-03	7.48E-03	4.40E-03	0.2880	4.217	0.000
At some specific points:																
144	5.487	0.893	5.4066	4.4469	-8.75	30.00	0.00	0.050	7.00E-01	2.80E-01	4.36E-03	9.63E-03	1.06E-03	0.3291	0.000	0.000
223	5.702	0.928	5.4614	4.4954	-8.88	30.00	0.00	0.980	7.00E-01	2.80E-01	4.36E-03	9.63E-03	1.06E-03	0.1704	2.034	0.000
255	5.713	0.930	5.3795	3.7247	-8.68	30.00	0.00	0.979	7.00E-01	2.80E-01	4.36E-03	9.63E-03	1.06E-03	0.1619	3.254	0.000
402	5.836	0.950	5.5700	3.6551	-9.16	30.00	0.00	0.771	6.31E-01	3.49E-01	2.99E-03	7.48E-03	4.40E-03	0.2645	3.990	0.000
805	6.132	0.999	5.4920	3.6539	-8.96	30.00	0.00	0.255	6.31E-01	3.49E-01	2.99E-03	7.48E-03	4.40E-03	0.2994	4.290	0.000

** The SPECIFIC means the models to which the figures energy generation rate profile, chemical profile and temperature gradients profiles are given. (the same meaning works for all following tables)

Fig SC 30 1

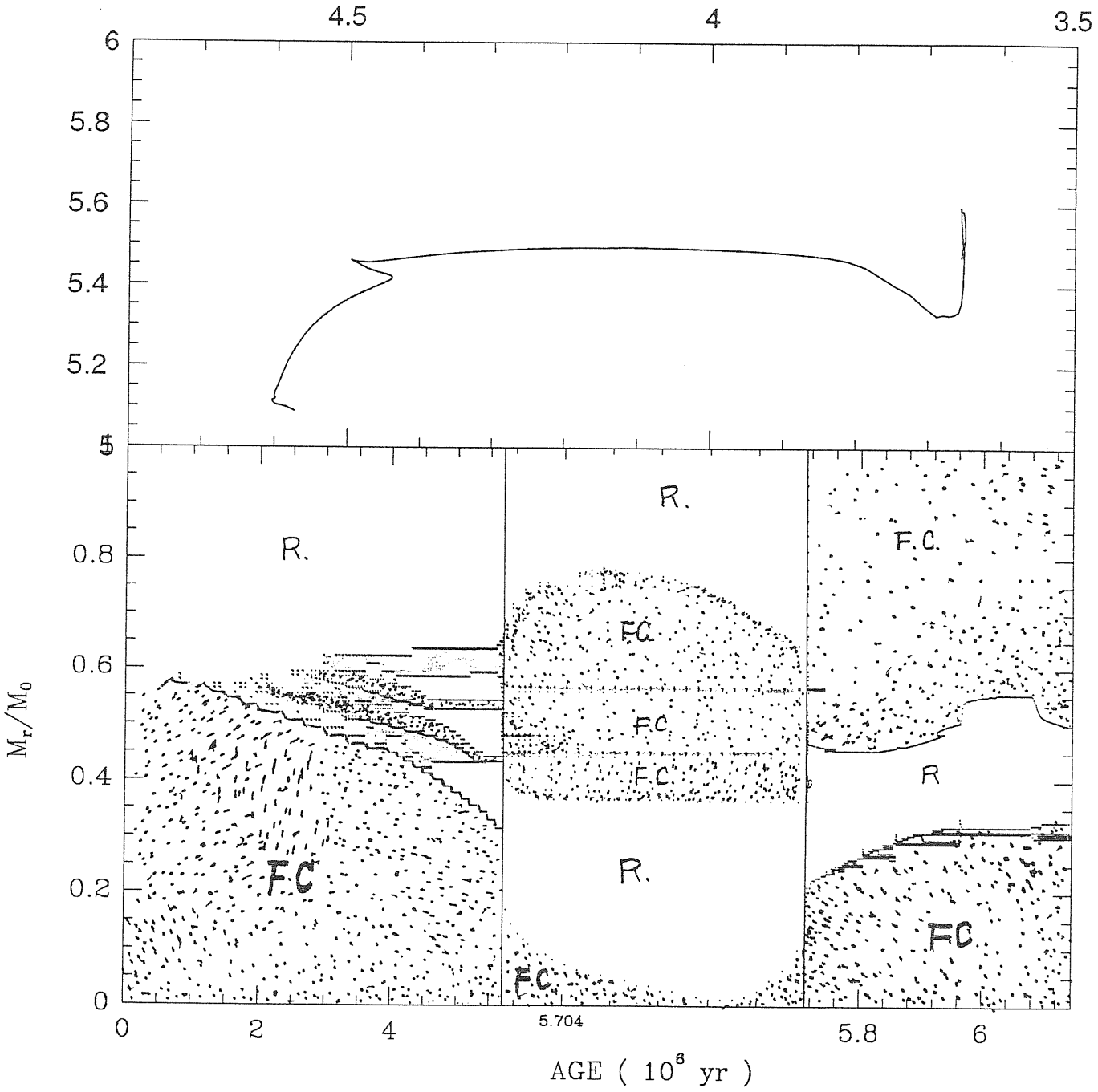
4.5
4
3.5
6
5.8
5.6
5.4
5.2
5
0.8
0.6
0.4
0.2
0
R.
R.
F.C.
F.C.
F.C.
F.C.
R
R.
F.C.
F.C.
F.C.
M_r/M_0
0
2
4
5.704
5.8
6
AGE (10^6 yr)

Fig SC30 3

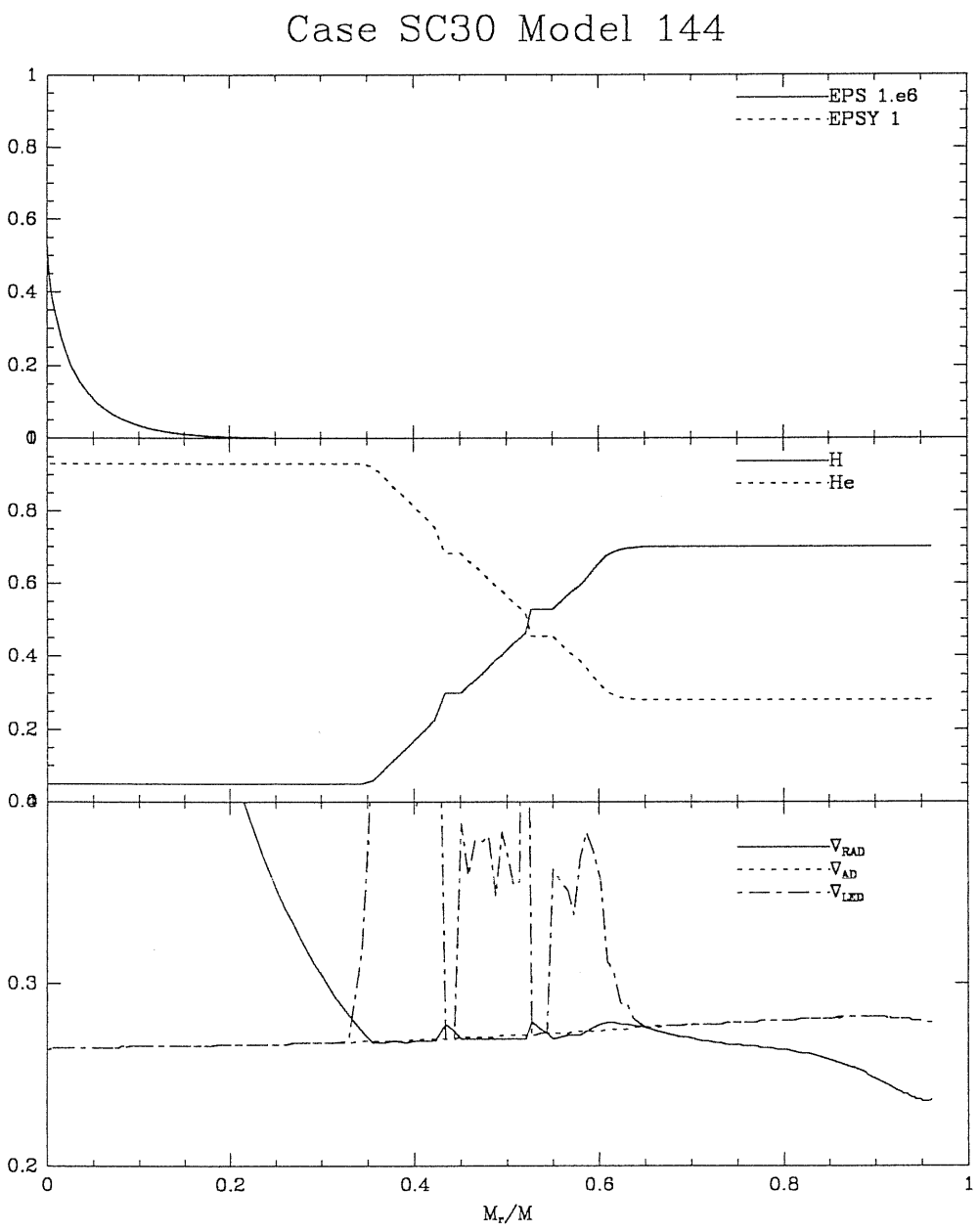
Case SC30 Model 144
EPS 1.e6
EPSY 1
H
He
∇_{RAD}
∇_{AD}
∇_{LED}
1
0.8
0.6
0.4
0.2
0
0.3
0.2
0
0.2
0.4
0.6
0.8
1
M_r/M

Fig SC30 4.

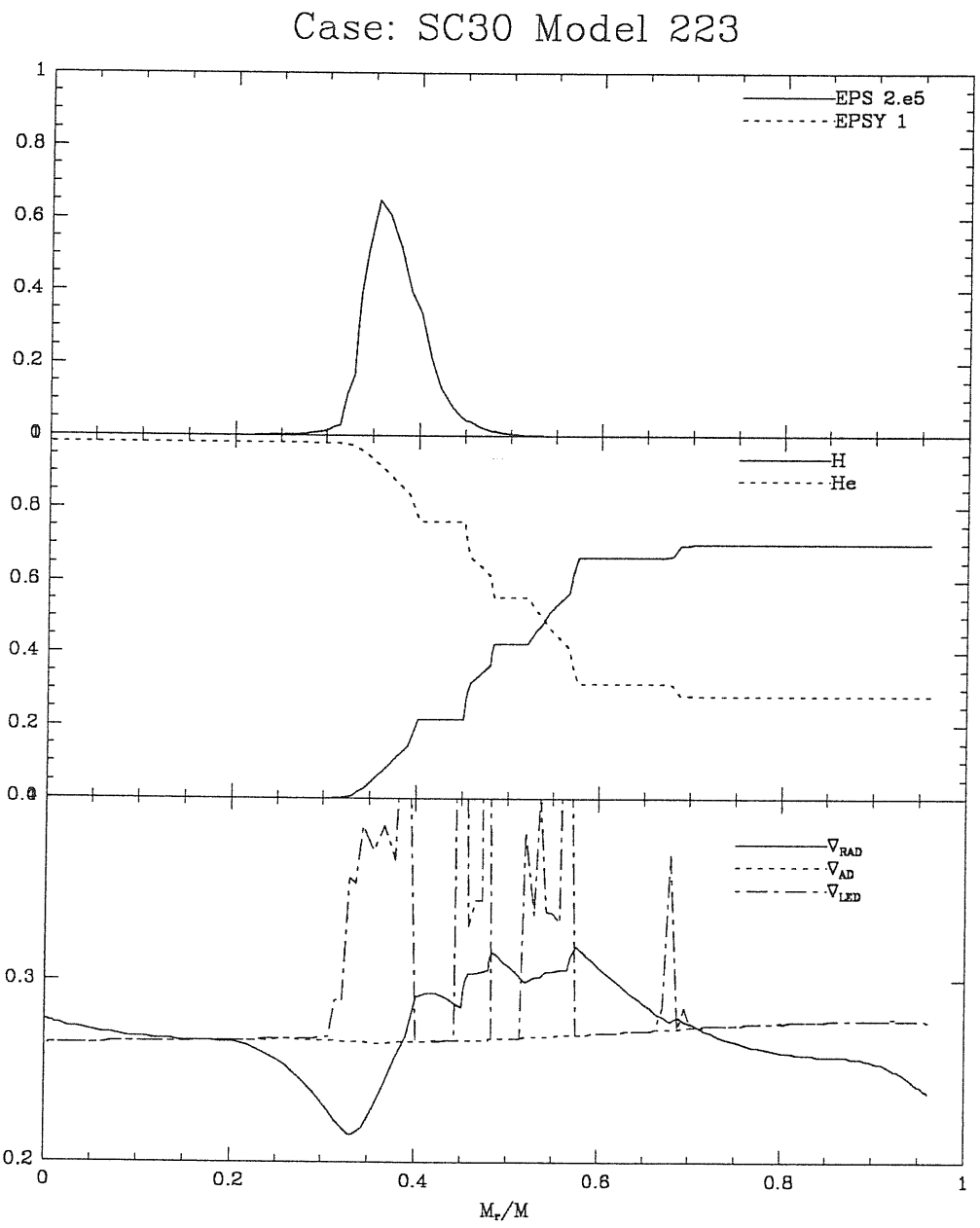
Case: SC30 Model 223
EPS 2.e5
EPSY 1
H
He
∇_{RAD}
∇_{AD}
∇_{LED}
1
0.8
0.6
0.4
0.2
0
0.3
0.2
0
0.2
0.4
0.6
0.8
1
M_r/M

Fig SC30 5.

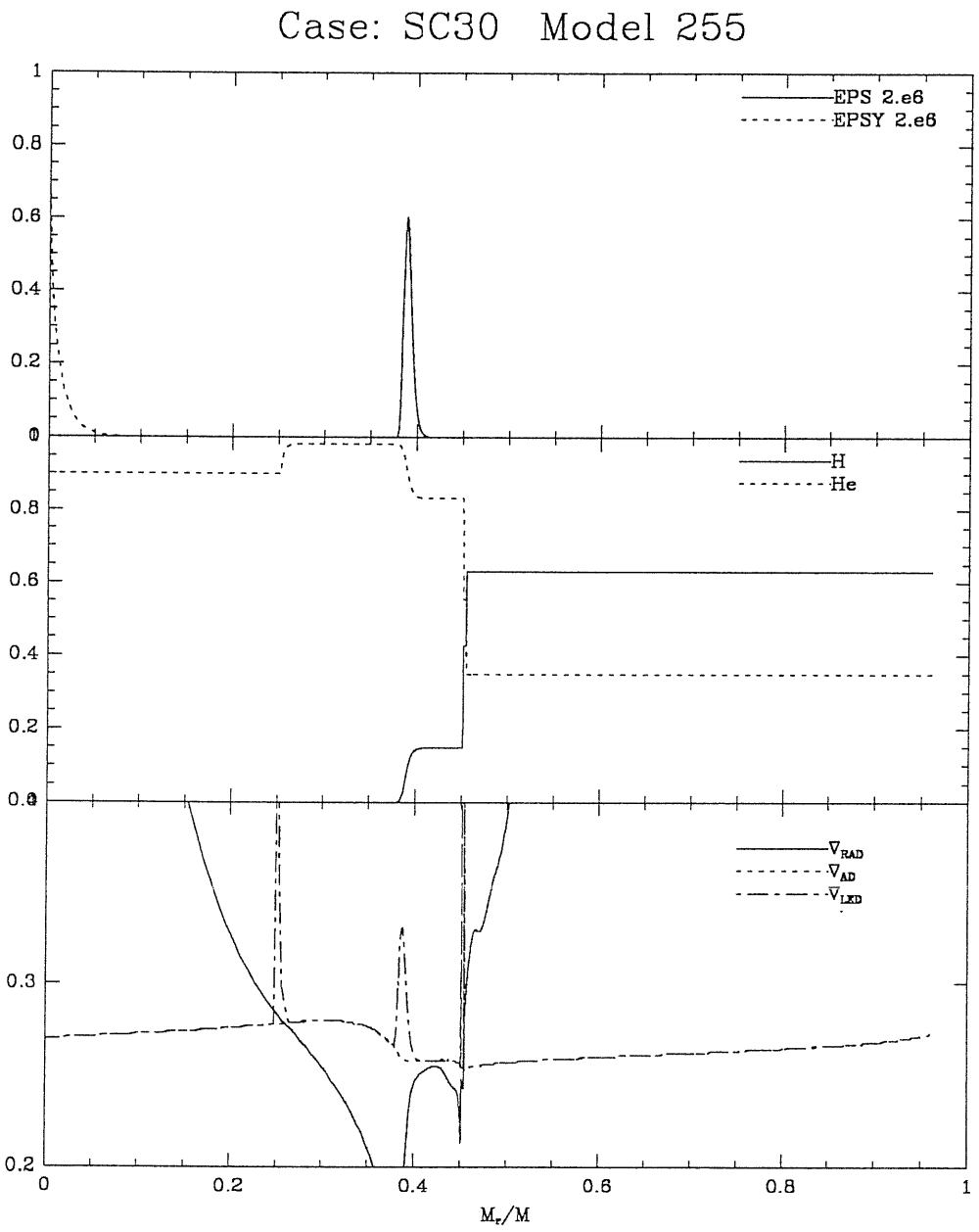
Case: SC30 Model 255
EPS 2.e6
EPSY 2.e6
H
He
∇_{RAD}
∇_{AD}
∇_{LED}
1
0.8
0.6
0.4
0.2
0
0.3
0.2
0
0.2
0.4
0.6
0.8
1
M_r/M

Fig SC30 6

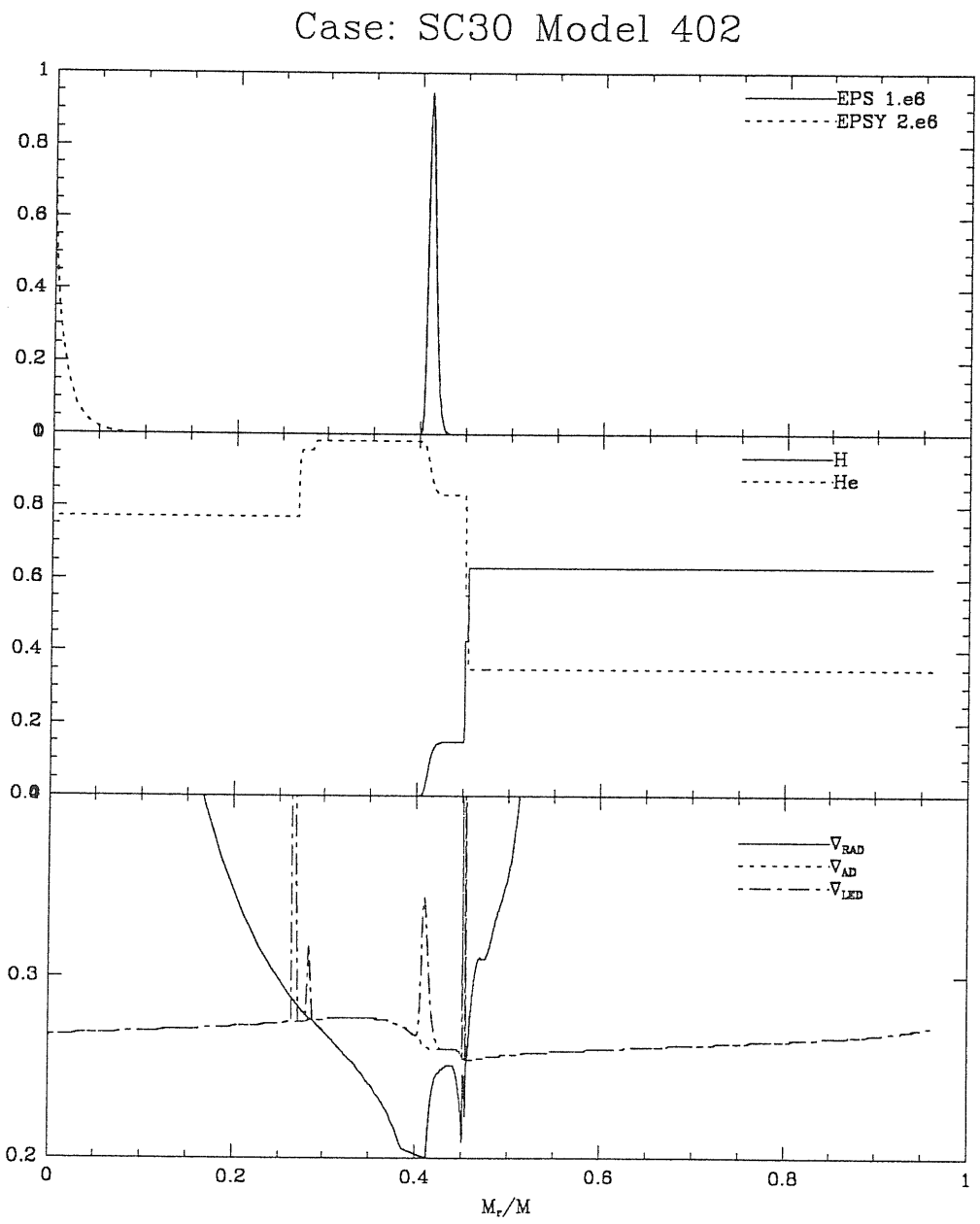
Case: SC30 Model 402
EPS 1.e6
EPSY 2.e6
H
He
∇_{RAD}
∇_{AD}
∇_{LED}
M_r/M

Fig SC30 7

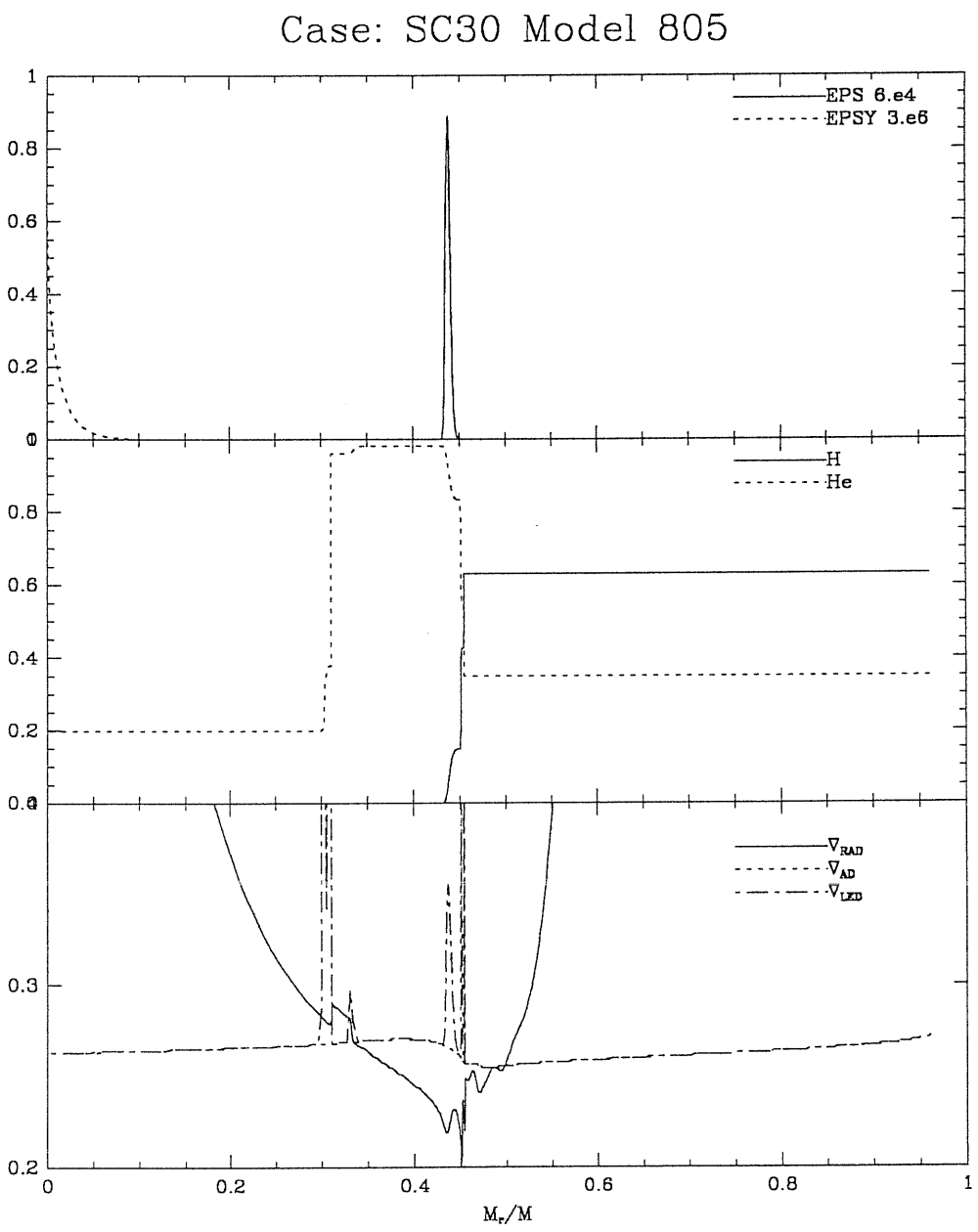
Case: SC30 Model 805
EPS 6.e4
EPSY 3.e6
H
He
∇_{RAD}
∇_{AD}
∇_{LED}
M_r/M

Table ( ) Case: DO4

MOD	eta	dt/t	LogL	LogTE	Mbol	gms	rate	comp	Xsup	Ysup	Csup	Osup	Nsup	Conv	qhel	qcarox
At ZAMS:																
1	0.000	0.000	4.6443	4.5102	-6.84	20.00	0.00	0.700	7.00E-01	2.80E-01	4.36E-03	9.63E-03	1.06E-03	5.332	0.000	0.000
2	0.559	0.057	4.6425	4.5184	-6.84	20.00	0.00	0.693	7.00E-01	2.80E-01	4.36E-03	9.63E-03	1.06E-03	5.922	0.000	0.000
3	0.634	0.064	4.6477	4.5286	-6.85	20.00	0.00	0.690	7.00E-01	2.80E-01	4.36E-03	9.63E-03	1.06E-03	5.941	0.000	0.000
4	0.706	0.071	4.6519	4.5370	-6.86	20.00	0.00	0.687	7.00E-01	2.80E-01	4.36E-03	9.63E-03	1.06E-03	5.941	0.000	0.000
5	0.790	0.080	4.6555	4.5411	-6.87	20.00	0.00	0.682	7.00E-01	2.80E-01	4.36E-03	9.63E-03	1.06E-03	5.941	0.000	0.000
At Lowest T_eff on MS:																
165	9.565	0.968	5.1552	4.3166	-8.12	20.00	0.00	0.013	7.00E-01	2.80E-01	4.36E-03	9.63E-03	1.06E-03	4.206	0.000	0.000
166	9.571	0.969	5.1561	4.3162	-8.12	20.00	0.00	0.012	7.00E-01	2.80E-01	4.36E-03	9.63E-03	1.06E-03	4.206	0.000	0.000
167	9.577	0.969	5.1568	4.3163	-8.12	20.00	0.00	0.011	7.00E-01	2.80E-01	4.36E-03	9.63E-03	1.06E-03	4.206	0.000	0.000
At Central H Exhausting:																
197	9.668	0.978	5.1994	4.3860	-8.23	20.00	0.00	0.000	7.00E-01	2.80E-01	4.36E-03	9.63E-03	1.06E-03	2.942	0.000	0.000
198	9.668	0.978	5.2009	4.3868	-8.23	20.00	0.00	0.980	7.00E-01	2.80E-01	4.36E-03	9.63E-03	1.06E-03	1.359	2.370	0.000
At Helium ignition:																
224	9.678	0.979	5.1301	3.7059	-8.06	20.00	0.00	0.980	7.00E-01	2.80E-01	4.36E-03	9.63E-03	1.06E-03	1.533	3.947	0.000
225	9.678	0.979	5.1217	3.6923	-8.03	20.00	0.00	0.979	7.00E-01	2.80E-01	4.36E-03	9.63E-03	1.06E-03	1.619	3.947	0.000
At the Base of RGB:																
228	9.679	0.979	5.0982	3.6603	-7.98	20.00	0.00	0.979	7.00E-01	2.80E-01	4.36E-03	9.63E-03	1.06E-03	1.788	3.981	0.000
At first Dredge-up:																
247	9.682	0.980	5.3486	3.6264	-8.60	20.00	0.00	0.977	6.37E-01	3.43E-01	3.21E-03	7.88E-03	3.78E-03	2.574	4.098	0.000
248	9.683	0.980	5.3482	3.6266	-8.60	20.00	0.00	0.976	6.37E-01	3.43E-01	3.20E-03	7.87E-03	3.79E-03	2.623	4.135	0.000
At Starting to Loop:																
549	9.836	0.995	5.2503	3.6500	-8.36	20.00	0.00	0.737	6.37E-01	3.43E-01	3.19E-03	7.86E-03	3.81E-03	3.213	4.654	0.000
At the Tip of the loop:																
1130	9.944	0.997	5.2961	3.8715	-8.47	20.00	0.00	0.516	6.37E-01	3.43E-01	3.19E-03	7.86E-03	3.81E-03	3.271	4.751	0.000
1131	9.944	0.997	5.2961	3.8709	-8.47	20.00	0.00	0.516	6.37E-01	3.43E-01	3.19E-03	7.86E-03	3.81E-03	3.271	4.751	0.000
At the End of the loop:																
1898	10.066	0.989	5.2488	3.6502	-8.35	20.00	0.00	0.298	6.37E-01	3.43E-01	3.19E-03	7.86E-03	3.81E-03	3.391	4.811	0.000
1899	10.067	0.989	5.2489	3.6499	-8.35	20.00	0.00	0.298	6.37E-01	3.43E-01	3.19E-03	7.86E-03	3.81E-03	3.391	4.811	0.000
At central exhaustion:																
3182	10.313	0.997	5.3373	3.6295	-8.57	20.00	0.00	0.000	6.37E-01	3.43E-01	3.14E-03	7.86E-03	3.85E-03	2.191	4.829	0.000
3183	10.313	0.997	5.3384	3.6295	-8.58	20.00	0.00	0.589	6.37E-01	3.43E-01	3.14E-03	7.86E-03	3.86E-03	0.000	4.829	2.191
At the Tip of RGB																
3270	10.339	1.000	5.5724	3.6209	-9.16	20.00	0.00	0.589	6.04E-01	3.76E-01	2.91E-03	7.42E-03	4.53E-03	0.000	4.641	3.634
At some specific Points:																
147	9.314	0.942	5.1296	4.3482	-8.05	20.00	0.00	0.050	7.00E-01	2.80E-01	4.36E-03	9.63E-03	1.06E-03	4.369	0.000	0.000
203	9.669	0.978	5.2094	4.3940	-8.25	20.00	0.00	0.980	7.00E-01	2.80E-01	4.36E-03	9.63E-03	1.06E-03	0.857	2.655	0.000
253	9.691	0.981	5.3310	3.6258	-8.56	20.00	0.00	0.971	6.37E-01	3.43E-01	3.19E-03	7.86E-03	3.81E-03	2.755	4.250	0.000
755	9.876	0.990	5.2629	3.6648	-8.39	20.00	0.00	0.658	6.37E-01	3.43E-01	3.19E-03	7.86E-03	3.81E-03	3.246	4.696	0.000
3116	10.267	0.993	5.2975	3.6328	-8.47	20.00	0.00	0.049	6.37E-01	3.43E-01	3.19E-03	7.86E-03	3.81E-03	3.630	4.825	0.000

Fig. D04 1.

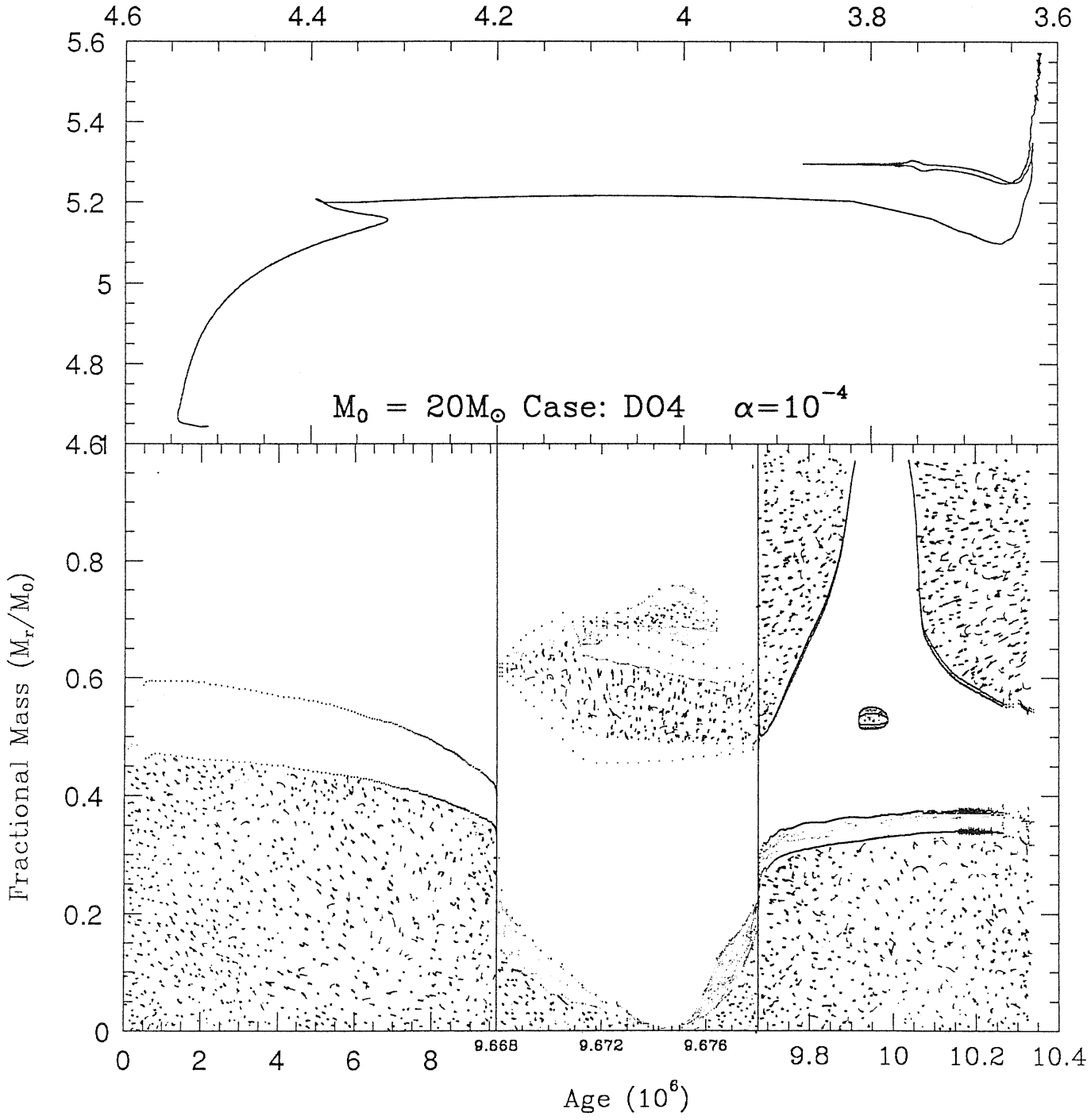
4.6
4.4
4.2
4
3.8
3.6
5.6
5.4
5.2
5
4.8
4.61
M_0 = 20$M_\odot$ Case: D04 $\alpha=10^{-4}$
0.8
0.6
0.4
0.2
0
Fractional Mass (M_r/M_0)
0
2
4
6
8
9.668
9.672
9.676
9.8
10
10.2
10.4
Age (10^6)

Fig D04 2

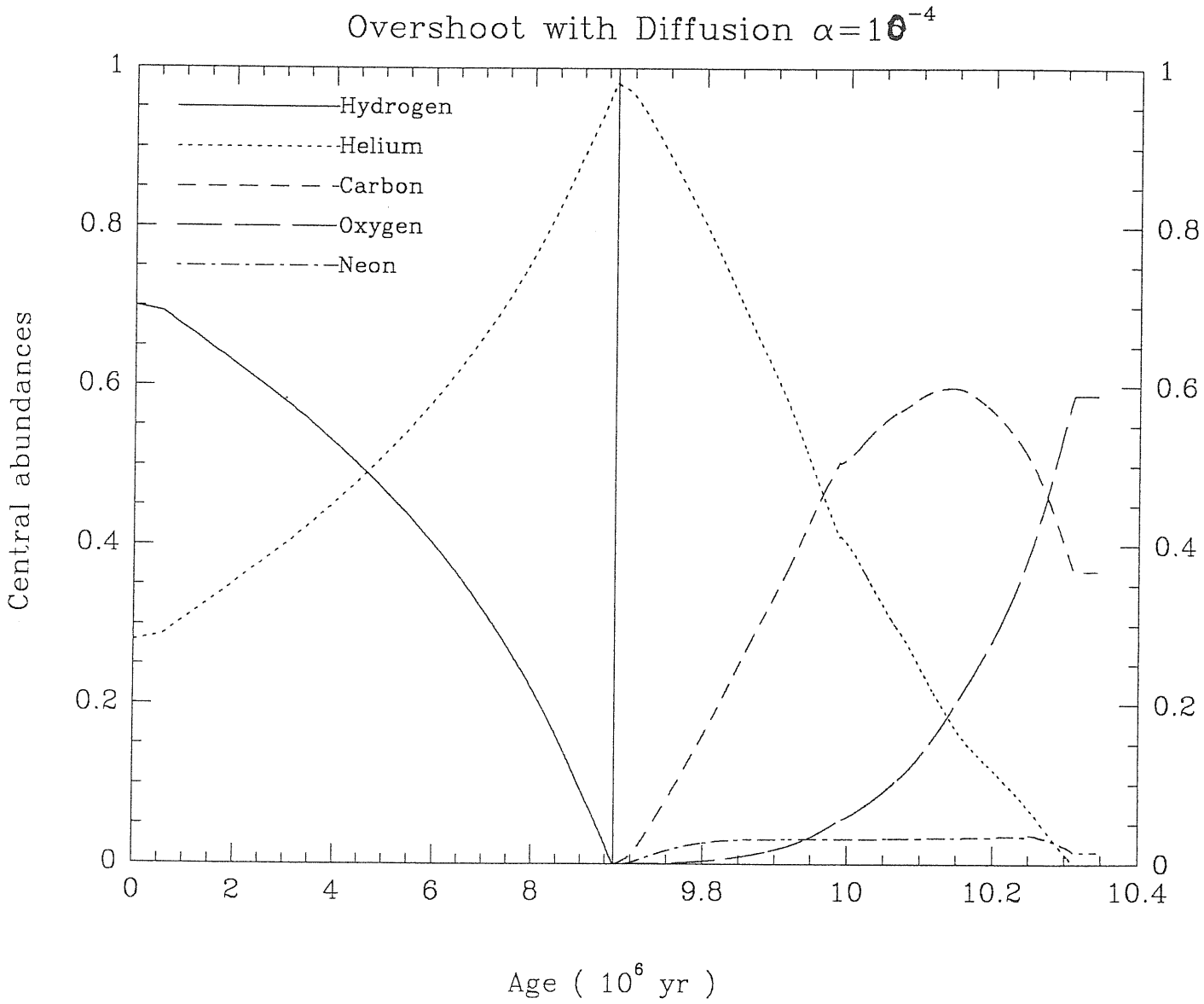
Overshoot with Diffusion $\alpha=10^{-4}$
Hydrogen
Helium
Carbon
Oxygen
Neon
Central abundances
0
0.2
0.4
0.6
0.8
1
0
2
4
6
8
9.8
10
10.2
10.4
Age (10^6 yr)

Fig D04 3

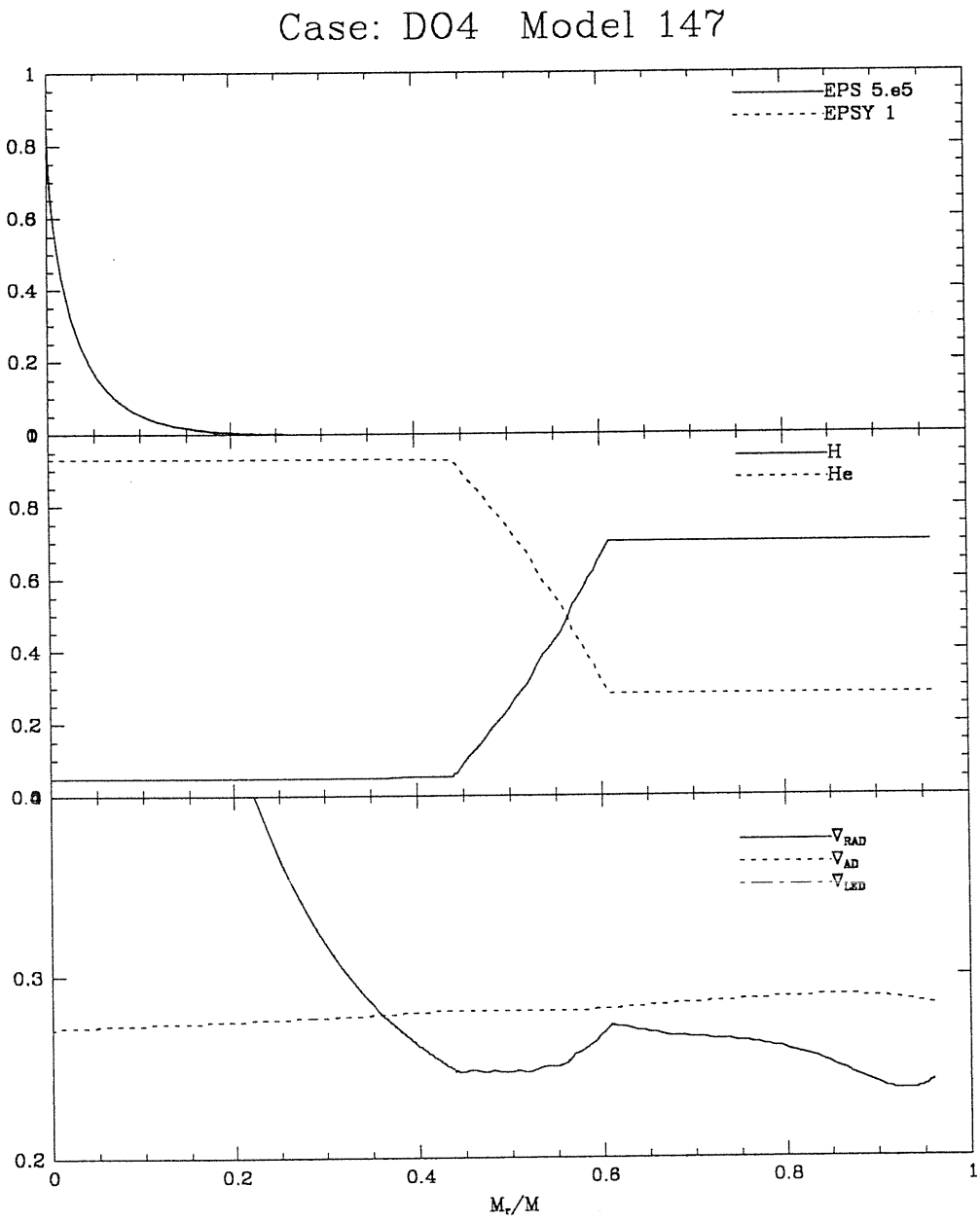
Case: D04 Model 147
EPS 5.e5
EPSY 1
H
He
∇_{RAD}
∇_{AD}
∇_{LED}
1
0.8
0.6
0.4
0.2
0
0.3
0.2
0
0.2
0.4
0.6
0.8
1
M_r/M

Fig D04 4

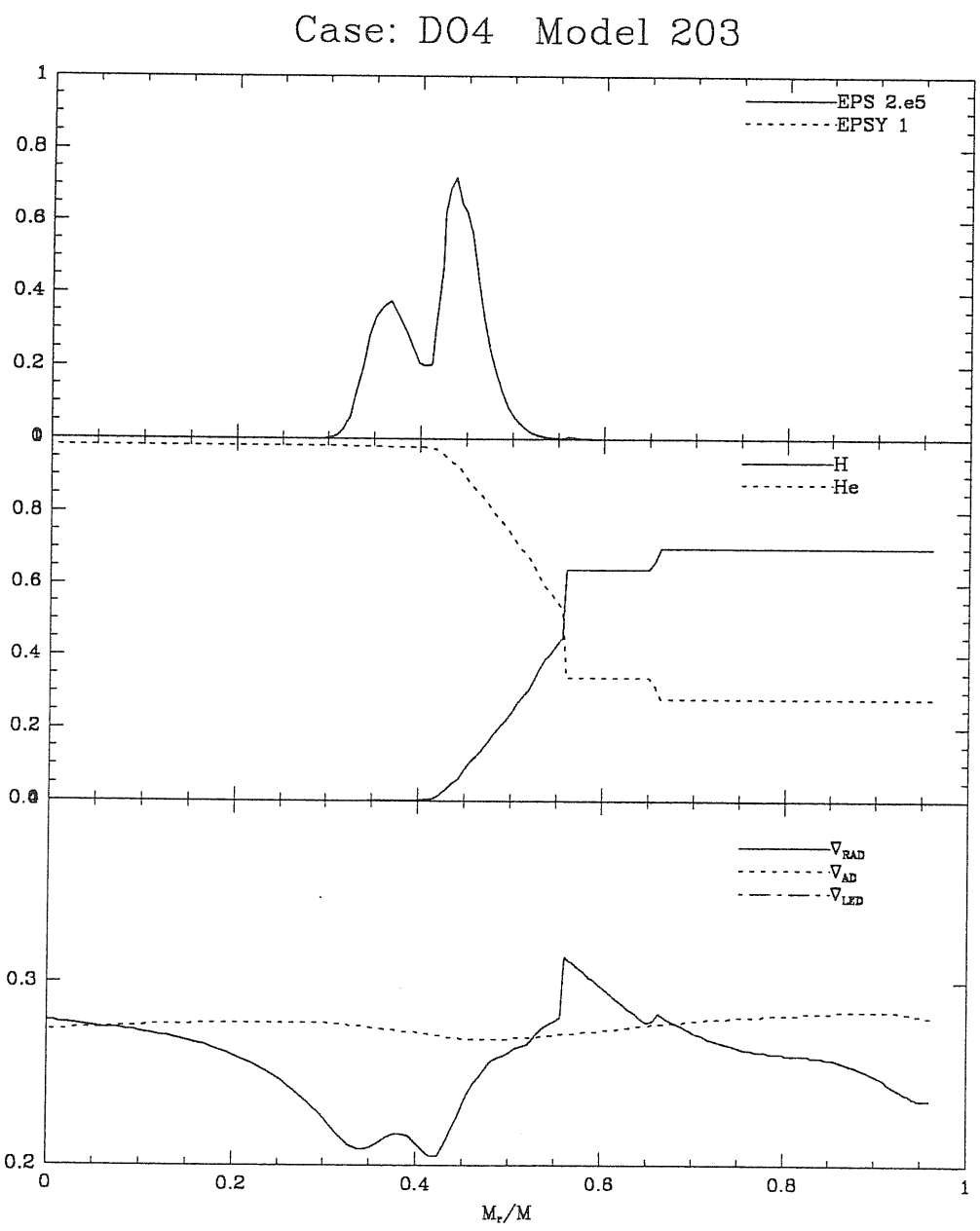
Case: D04 Model 203
EPS 2.e5
EPSY 1
H
He
∇_{RAD}
∇_{AD}
∇_{LED}
0
0.2
0.4
0.6
0.8
1
0.3
M_r/M

Fig D04 5

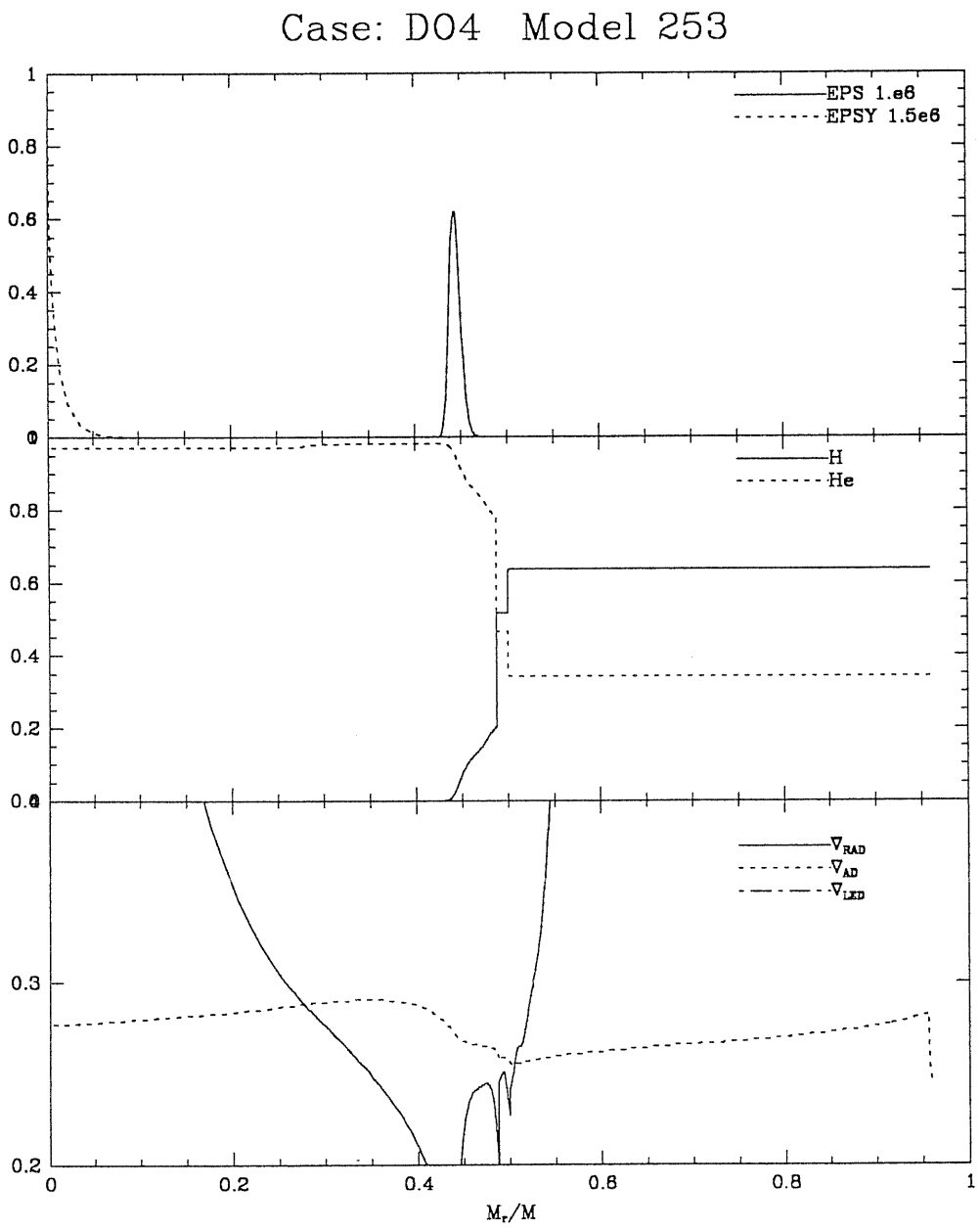
Case: D04 Model 253
EPS 1.e6
EPSY 1.5e6
H
He
∇_{RAD}
∇_{AD}
∇_{LED}
1
0.8
0.6
0.4
0.2
0
0.3
0.2
0
0.2
0.4
0.6
0.8
1
M_r/M

Fig D04 6

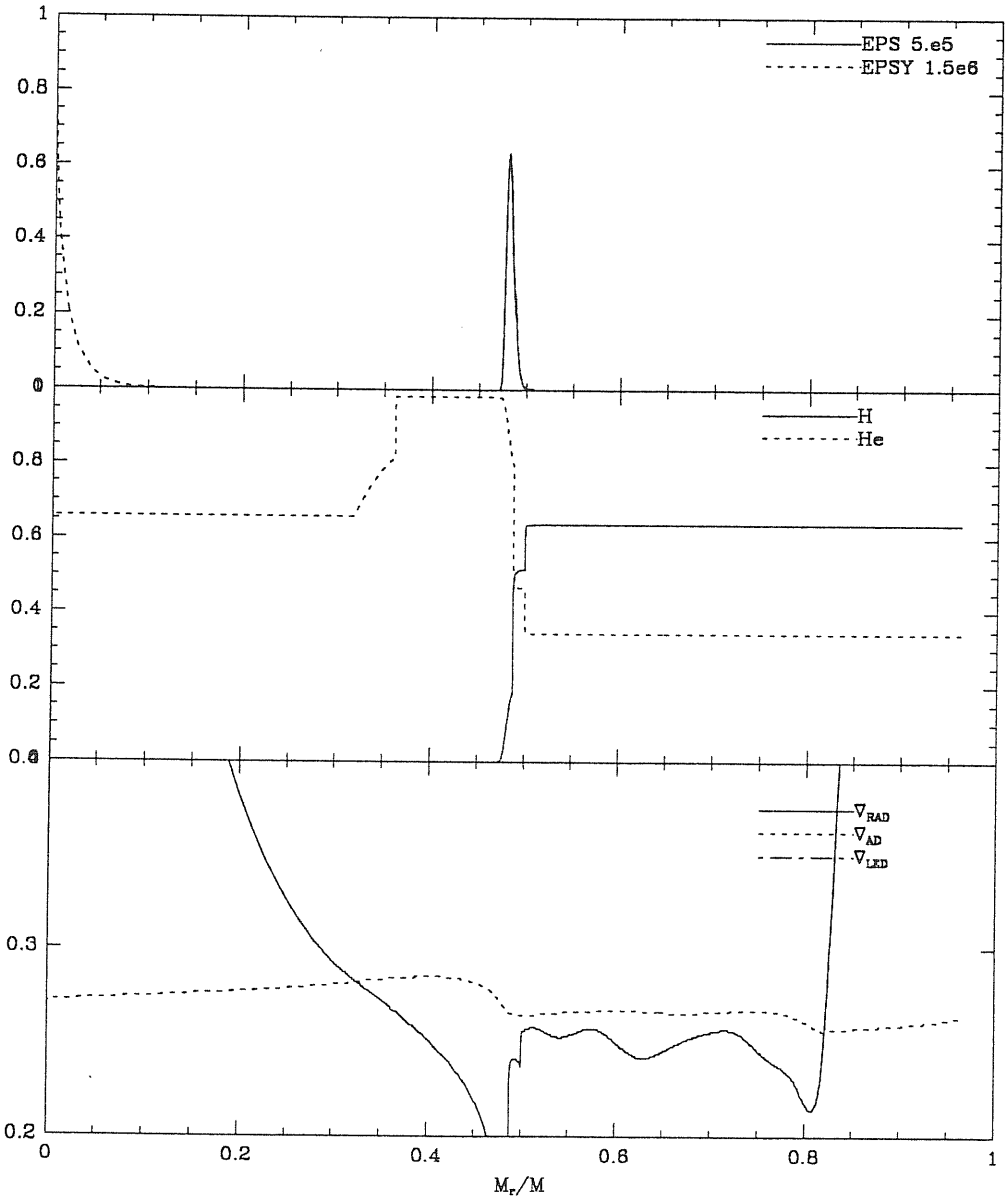
Case: D04 Model 755
EPS 5.e5
EPSY 1.5e6
H
He
∇_{RAD}
∇_{AD}
∇_{LED}
M_r/M

TABLE ( ) Case: D03

MOD	eta	dt/t	LogL	LogTE	Mbol	gms	rate	comp	Xsup	Ysup	Csup	Osup	Nsup	Conv	qhel	qcarox
At ZAMS:																
1	0.000	0.000	4.6443	4.5102	-6.84	20.00	0.00	0.700	7.00E-01	2.80E-01	4.36E-03	9.63E-03	1.06E-03	5.332	0.000	0.000
2	0.559	0.057	4.6425	4.5183	-6.84	20.00	0.00	0.693	7.00E-01	2.80E-01	4.36E-03	9.63E-03	1.06E-03	5.922	0.000	0.000
3	0.634	0.064	4.6474	4.5278	-6.85	20.00	0.00	0.690	7.00E-01	2.80E-01	4.36E-03	9.63E-03	1.06E-03	5.941	0.000	0.000
4	0.712	0.072	4.6521	4.5360	-6.86	20.00	0.00	0.686	7.00E-01	2.80E-01	4.36E-03	9.63E-03	1.06E-03	5.941	0.000	0.000
5	0.805	0.082	4.6564	4.5421	-6.87	20.00	0.00	0.682	7.00E-01	2.80E-01	4.36E-03	9.63E-03	1.06E-03	5.941	0.000	0.000
At lowest T-eff on MS:																
166	9.545	0.970	5.1575	4.3140	-8.12	20.00	0.00	0.012	7.00E-01	2.80E-01	4.36E-03	9.63E-03	1.06E-03	4.206	0.000	0.000
At the cetral H exhaustion:																
217	9.627	0.979	5.2035	4.3699	-8.24	20.00	0.00	0.000	7.00E-01	2.80E-01	4.36E-03	9.63E-03	1.06E-03	2.822	0.000	0.000
218	9.627	0.979	5.2050	4.3709	-8.24	20.00	0.00	0.980	7.00E-01	2.80E-01	4.36E-03	9.63E-03	1.06E-03	1.359	2.110	0.000
At central He ignition:																
244	9.637	0.980	5.1226	3.6908	-8.04	20.00	0.00	0.980	7.00E-01	2.80E-01	4.36E-03	9.63E-03	1.06E-03	1.640	4.008	0.000
245	9.637	0.980	5.1187	3.6802	-8.03	20.00	0.00	0.979	7.00E-01	2.80E-01	4.36E-03	9.63E-03	1.06E-03	1.740	4.008	0.000
At the bottom of RGB:																
248	9.637	0.980	5.1076	3.6582	-8.00	20.00	0.00	0.979	7.00E-01	2.80E-01	4.36E-03	9.63E-03	1.06E-03	1.922	4.040	0.000
At the first dredge-up:																
267	9.641	0.980	5.3459	3.6277	-8.59	20.00	0.00	0.977	6.38E-01	3.42E-01	3.22E-03	7.91E-03	3.75E-03	2.653	4.152	0.000
At starting to loop:																
543	9.795	0.996	5.2531	3.6500	-8.36	20.00	0.00	0.749	6.38E-01	3.42E-01	3.20E-03	7.89E-03	3.78E-03	3.393	4.678	0.000
At the tip of the loop:																
1276	9.931	0.993	5.2959	3.8218	-8.47	20.00	0.00	0.491	6.38E-01	3.42E-01	3.20E-03	7.89E-03	3.78E-03	3.369	4.789	0.000
At the end of the loop:																
1738	10.007	0.991	5.2538	3.6502	-8.36	20.00	0.00	0.350	6.38E-01	3.42E-01	3.20E-03	7.89E-03	3.78E-03	3.558	4.820	0.000
At central helium exhaustion:																
3132	10.267	0.997	5.3439	3.6295	-8.59	20.00	0.00	0.000	6.38E-01	3.42E-01	3.17E-03	7.89E-03	3.81E-03	2.281	4.847	0.000
3133	10.267	0.997	5.3451	3.6296	-8.59	20.00	0.00	0.570	6.38E-01	3.42E-01	3.16E-03	7.89E-03	3.81E-03	0.000	4.847	2.281
At the tip of RGB:																
3220	10.298	1.000	5.5797	3.6210	-9.18	20.00	0.00	0.570	6.07E-01	3.73E-01	2.94E-03	7.46E-03	4.47E-03	0.000	4.678	3.738
At some specific points:																
147	9.287	0.944	5.1311	4.3466	-8.06	20.00	0.00	0.050	7.00E-01	2.80E-01	4.36E-03	9.63E-03	1.06E-03	4.369	0.000	0.000
236	9.633	0.979	5.2126	4.2222	-8.26	20.00	0.00	0.980	7.00E-01	2.80E-01	4.36E-03	9.63E-03	1.06E-03	0.057	3.678	0.000
333	9.710	0.987	5.2652	3.6373	-8.39	20.00	0.00	0.900	6.38E-01	3.42E-01	3.20E-03	7.89E-03	3.78E-03	3.340	4.546	0.000
1203	9.917	0.992	5.2957	3.7967	-8.47	20.00	0.00	0.506	6.38E-01	3.42E-01	3.20E-03	7.89E-03	3.78E-03	3.473	4.783	0.000

Fig D03 1.

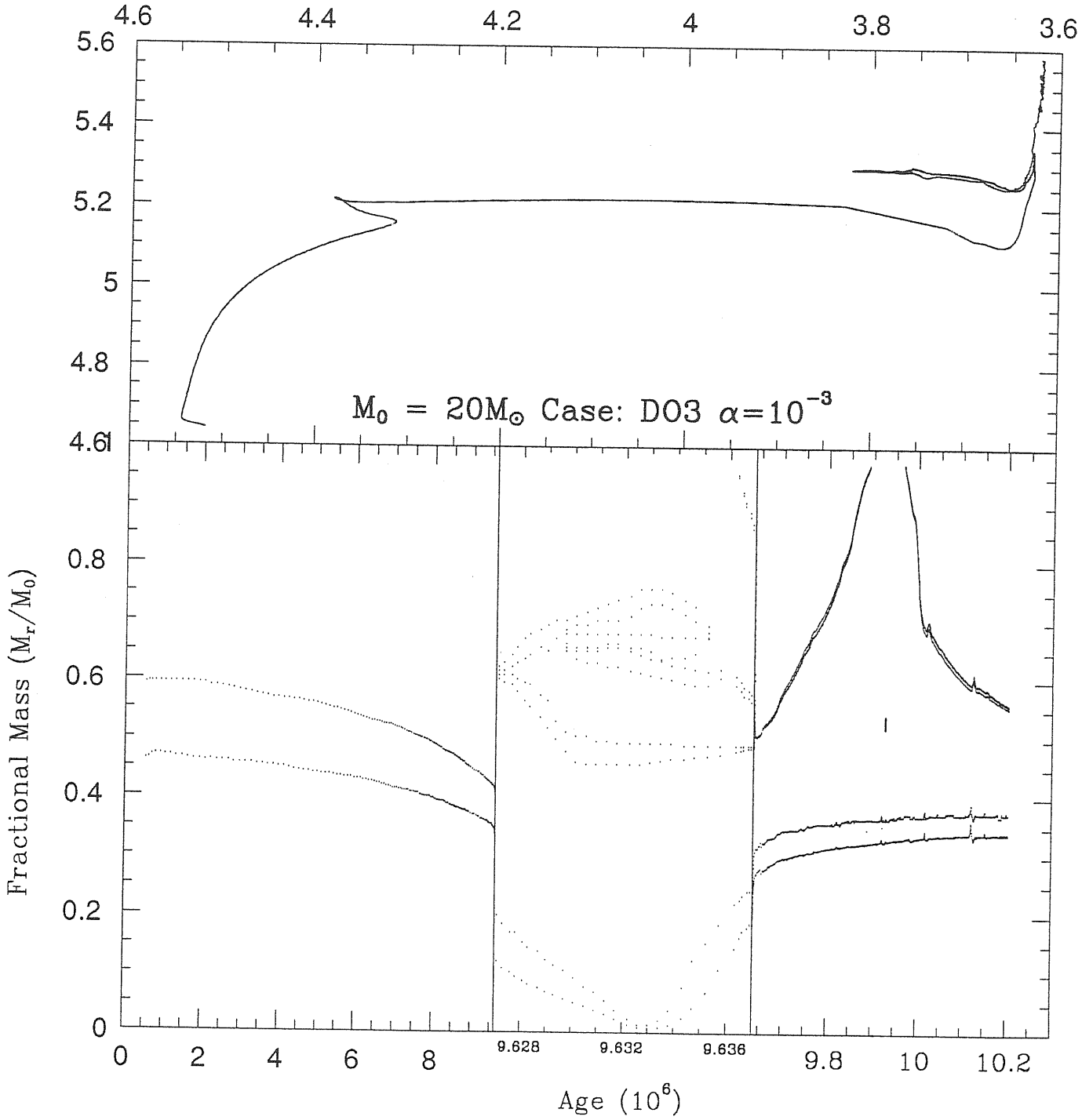
4.6
4.4
4.2
4
3.8
3.6
5.6
5.4
5.2
5
4.8
4.61
$M_0 = 20M_\odot$ Case: D03 $\alpha=10^{-3}$
0.8
0.6
0.4
0.2
0
Fractional Mass (M_r/M_0)
0
2
4
6
8
9.628
9.632
9.636
9.8
10
10.2
Age (10^6)

Fig D03 2

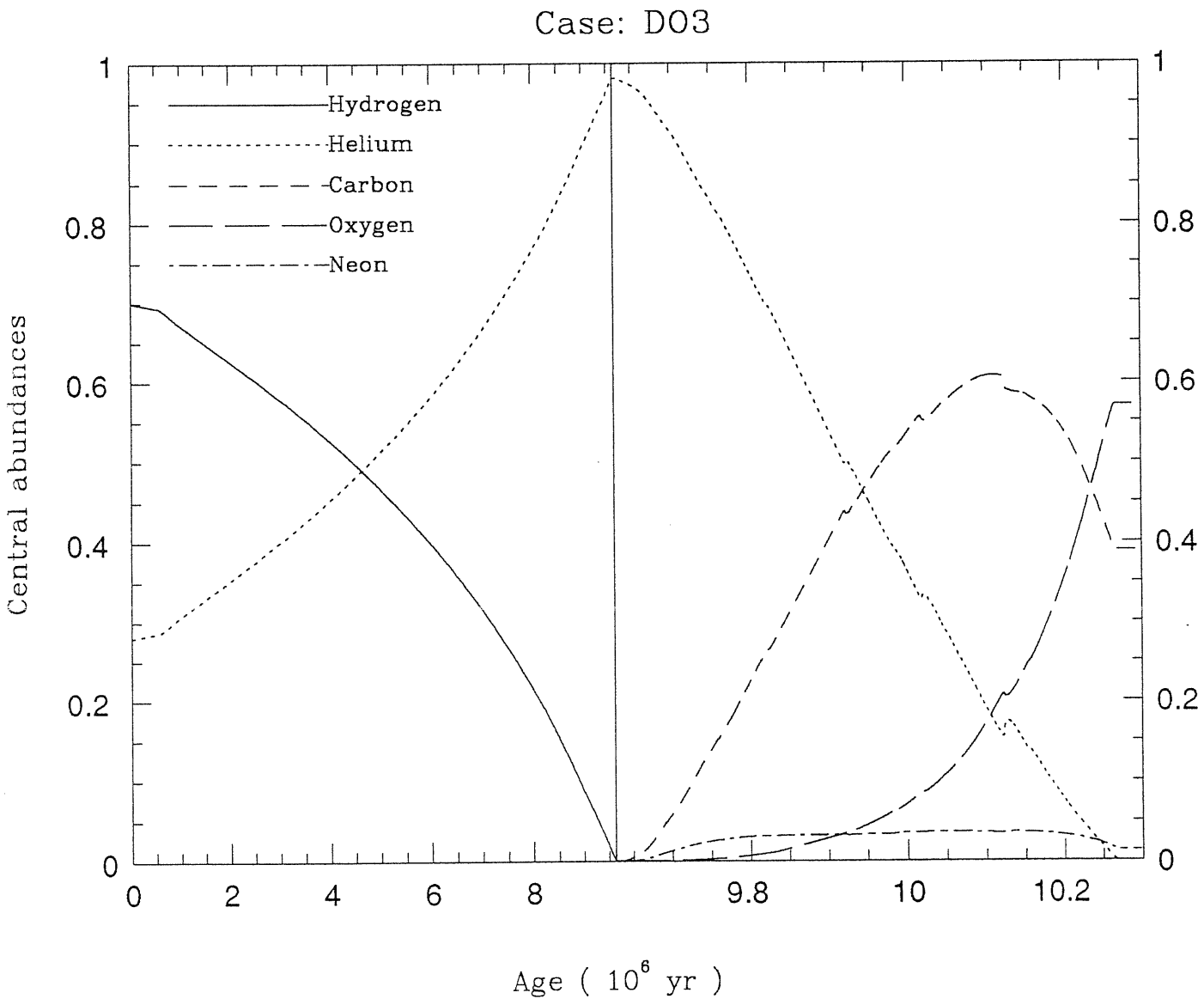
Case: D03
Hydrogen
Helium
Carbon
Oxygen
Neon
Central abundances
Age (10^6 yr)
0
0.2
0.4
0.6
0.8
1
0
2
4
6
8
9.8
10
10.2

Fig D03 3

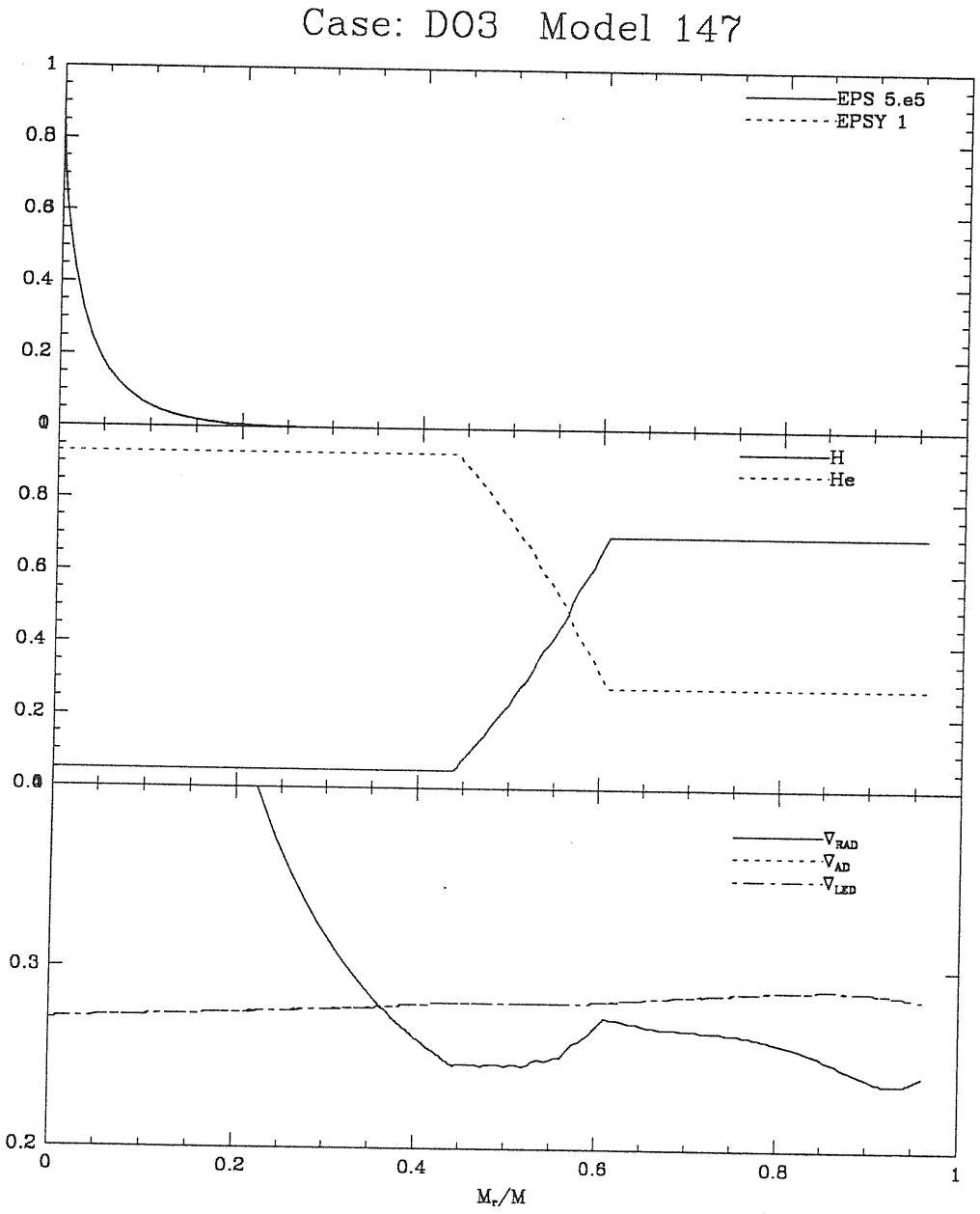
Case: D03 Model 147
EPS 5.e5
EPSY 1
H
He
∇_{RAD}
∇_{AD}
∇_{LED}
1
0.8
0.6
0.4
0.2
0
0.3
0.2
0
0.2
0.4
0.6
0.8
1
M_r/M

Fig D03 4

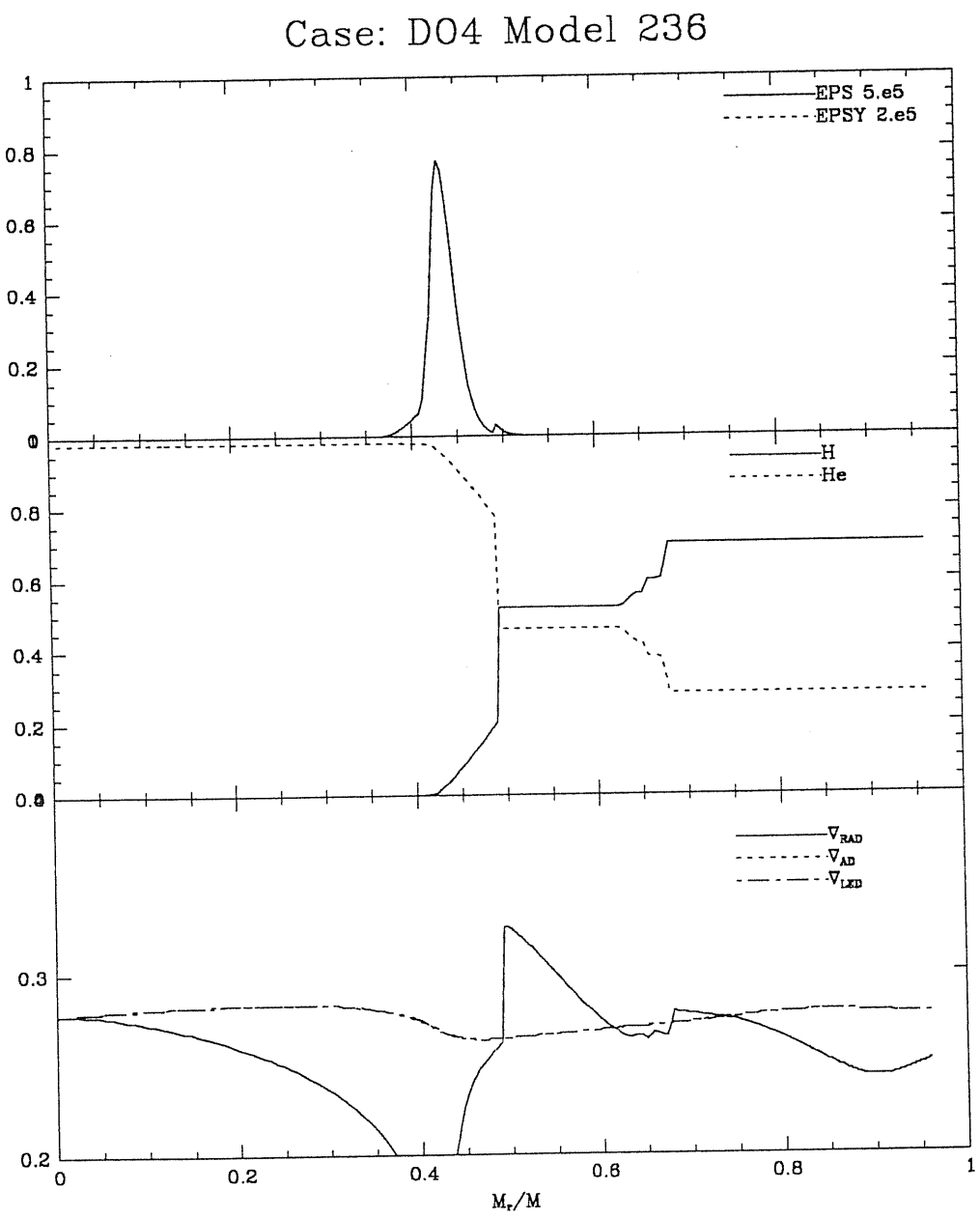
Case: D04 Model 236
EPS 5.e5
EPSY 2.e5
H
He
∇_{RAD}
∇_{AD}
∇_{LED}
1
0.8
0.6
0.4
0.2
0
0.3
0.2
0
0.2
0.4
0.6
0.8
1
M_r/M

Fig D03 5

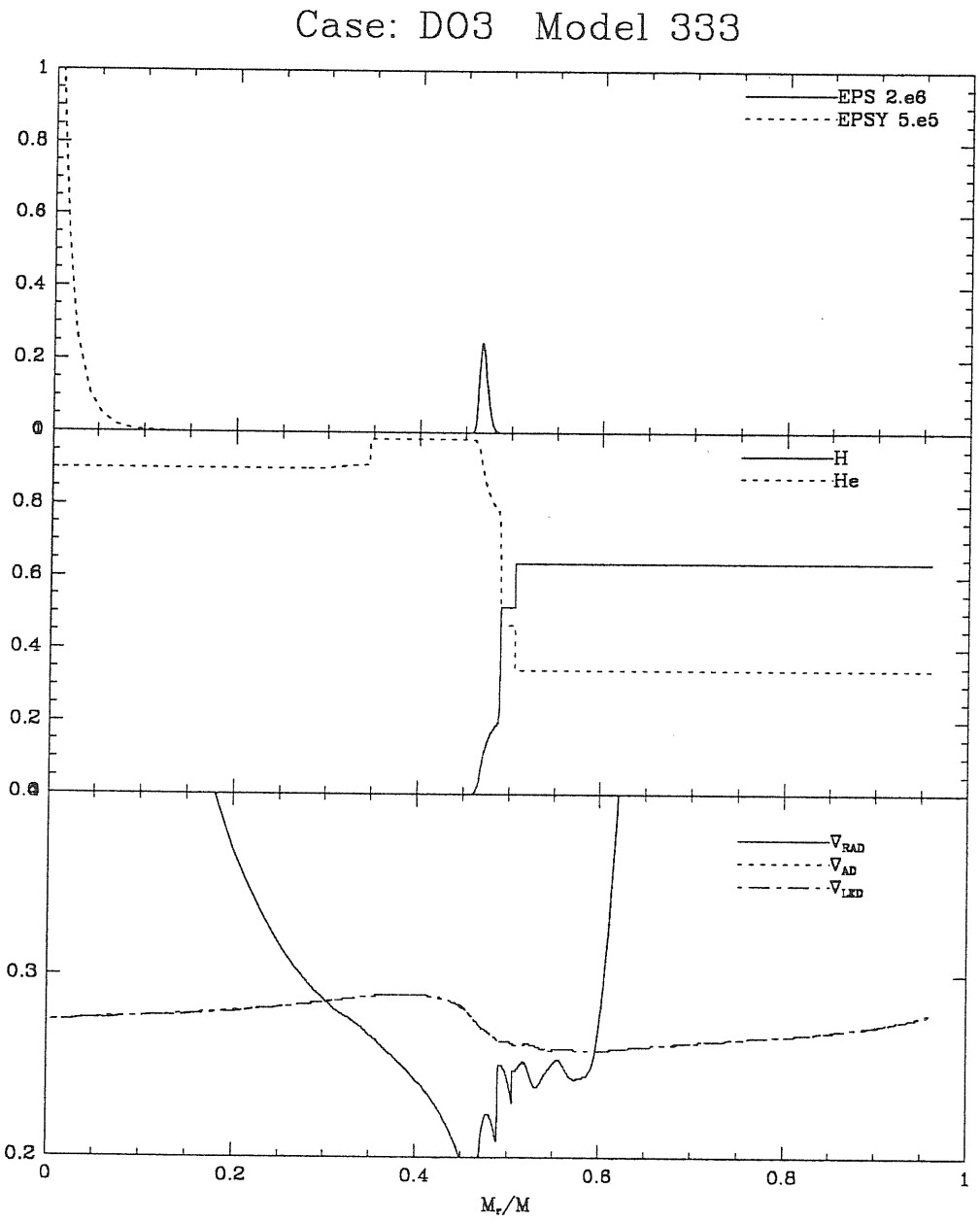
Case: D03 Model 333
EPS 2.e6
EPSY 5.e5
H
He
∇_{RAD}
∇_{AD}
∇_{LED}
1
0.8
0.6
0.4
0.2
0
0.3
0.2
0
0.2
0.4
0.6
0.8
1
M_r/M

Fig D03 6

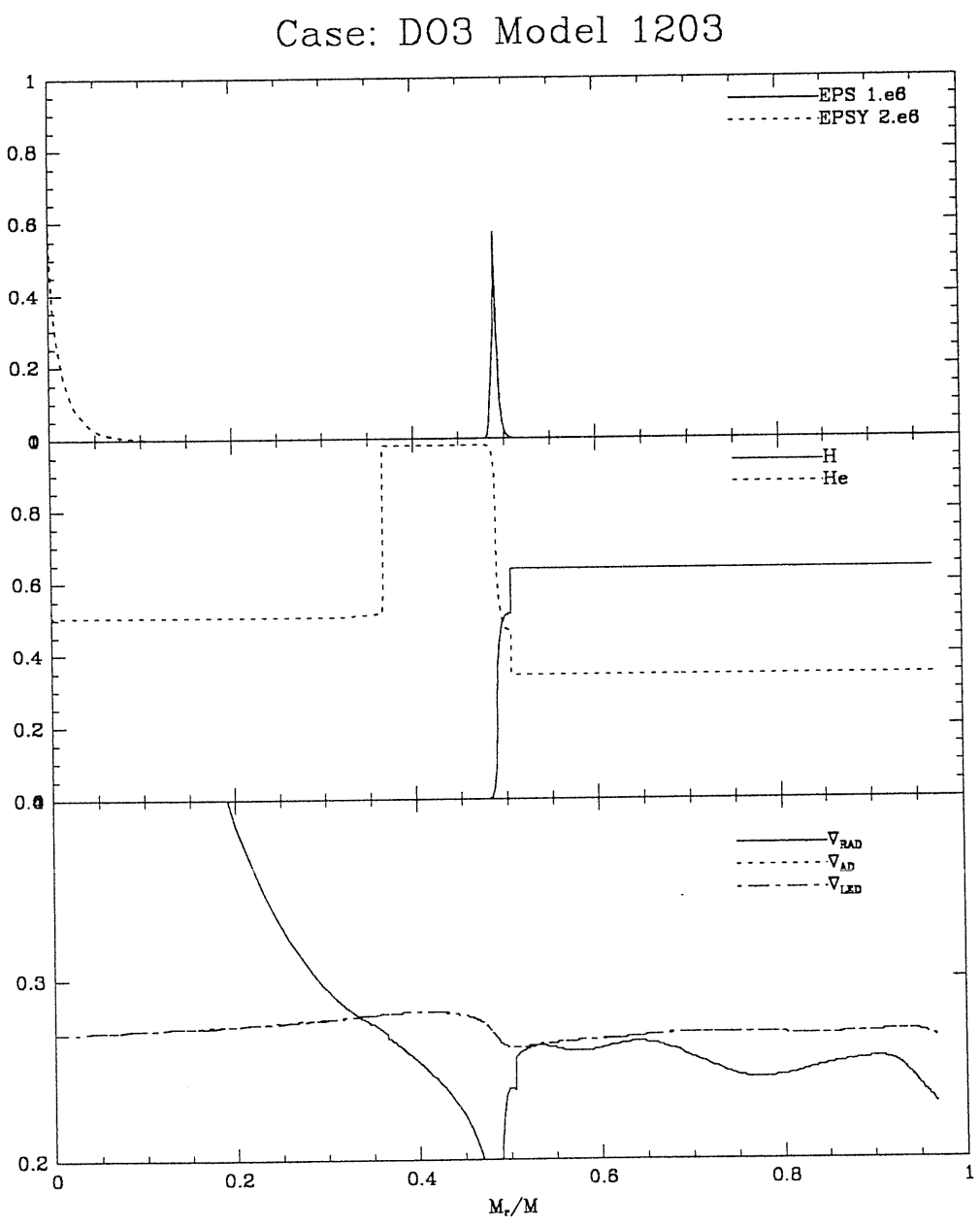
Case: D03 Model 1203
EPS 1.e6
EPSY 2.e6
H
He
∇_{RAD}
∇_{AD}
∇_{LED}
1
0.8
0.6
0.4
0.2
0
0.3
0.2
0
0.2
0.4
0.6
0.8
1
M_r/M

Table ( ) Case DO3ML

MOD	eta	dt/t	LogL	LogTE	Mbol	gms	rate	comp	Xsup	Ysup	Csup	Osup	Nsup	Conv	qhel	qcarox
At ZAMS:																
1	0.000	0.000	4.6443	4.5102	-6.84	20.00	-7.67	0.700	7.00E-01	2.80E-01	4.36E-03	9.63E-03	1.06E-03	5.332	0.000	0.000
2	0.559	0.056	4.6417	4.5182	-6.83	19.99	-7.66	0.693	7.00E-01	2.80E-01	4.36E-03	9.63E-03	1.06E-03	5.925	0.000	0.000
3	0.634	0.063	4.6465	4.5276	-6.85	19.99	-7.71	0.690	7.00E-01	2.80E-01	4.36E-03	9.63E-03	1.06E-03	5.945	0.000	0.000
4	0.712	0.071	4.6511	4.5359	-6.86	19.98	-7.76	0.686	7.00E-01	2.80E-01	4.36E-03	9.63E-03	1.06E-03	5.945	0.000	0.000
5	0.805	0.080	4.6553	4.5419	-6.87	19.98	-7.78	0.682	7.00E-01	2.80E-01	4.36E-03	9.63E-03	1.06E-03	5.946	0.000	0.000
At Lowerst T eff on MS:																
170	9.697	0.966	5.1367	4.2821	-8.07	18.77	-6.14	0.009	7.00E-01	2.80E-01	4.36E-03	9.63E-03	1.06E-03	4.340	0.000	0.000
171	9.702	0.966	5.1375	4.2820	-8.07	18.76	-6.14	0.008	7.00E-01	2.80E-01	4.36E-03	9.63E-03	1.06E-03	4.324	0.000	0.000
172	9.707	0.967	5.1382	4.2823	-8.08	18.76	-6.14	0.007	7.00E-01	2.80E-01	4.36E-03	9.63E-03	1.06E-03	4.325	0.000	0.000
At Central H Exhausting:																
218	9.760	0.972	5.1794	4.3350	-8.18	18.72	-6.10	0.000	7.00E-01	2.80E-01	4.36E-03	9.63E-03	1.06E-03	2.913	0.000	0.000
219	9.760	0.972	5.1809	4.3359	-8.18	18.72	-6.10	0.980	7.00E-01	2.80E-01	4.36E-03	9.63E-03	1.06E-03	1.310	2.173	0.000
At Central Ignition:																
256	9.769	0.973	5.2507	3.6336	-8.36	18.71	-5.67	0.980	6.97E-01	2.83E-01	4.15E-03	9.48E-03	1.34E-03	1.639	4.167	0.000
257	9.770	0.973	5.2672	3.6328	-8.40	18.71	-5.64	0.979	6.97E-01	2.83E-01	4.12E-03	9.46E-03	1.39E-03	1.776	4.167	0.000
At the base of RGB:																
246	9.768	0.973	5.0787	3.6688	-7.93	18.71	-5.97	0.980	7.00E-01	2.80E-01	4.36E-03	9.63E-03	1.06E-03	0.924	4.087	0.000
247	9.768	0.973	5.0743	3.6601	-7.92	18.71	-5.97	0.980	7.00E-01	2.80E-01	4.36E-03	9.63E-03	1.06E-03	1.018	4.087	0.000
248	9.769	0.973	5.0783	3.6534	-7.93	18.71	-5.97	0.980	7.00E-01	2.80E-01	4.36E-03	9.63E-03	1.06E-03	1.099	4.134	0.000
At First Dredge-up:																
268	9.775	0.973	5.3736	3.6275	-8.66	18.69	-5.40	0.977	6.42E-01	3.38E-01	3.16E-03	7.81E-03	3.88E-03	2.732	4.357	0.000
269	9.777	0.974	5.3724	3.6276	-8.66	18.68	-5.40	0.976	6.42E-01	3.38E-01	3.16E-03	7.80E-03	3.90E-03	2.767	4.384	0.000
At some specific points:																
147	9.407	0.937	5.1084	4.3271	-8.00	18.96	-6.23	0.050	7.00E-01	2.80E-01	4.36E-03	9.63E-03	1.06E-03	4.483	0.000	0.000
238	9.766	0.973	5.1836	4.0998	-8.19	18.72	-6.03	0.980	7.00E-01	2.80E-01	4.36E-03	9.63E-03	1.06E-03	0.046	3.822	0.000
334	9.846	0.981	5.3083	3.6307	-8.50	18.44	-5.53	0.900	6.42E-01	3.38E-01	3.16E-03	7.79E-03	3.90E-03	3.587	4.890	0.000
2005	10.186	1.000	5.2699	3.6436	-8.40	17.65	-5.63	0.279	6.42E-01	3.38E-01	3.16E-03	7.79E-03	3.90E-03	4.001	5.457	0.000

Fig D03ML 1

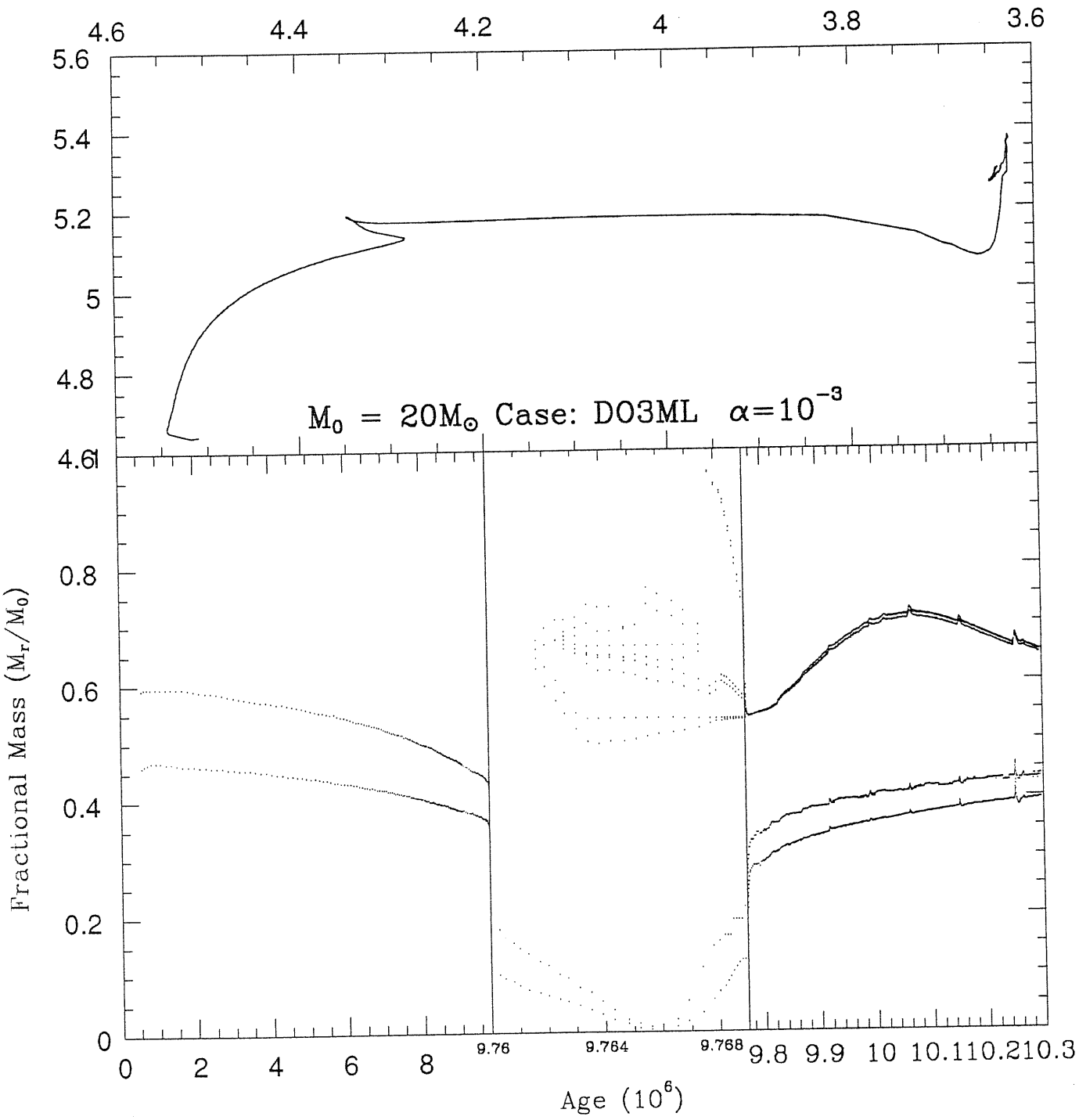
4.6
4.4
4.2
4
3.8
3.6
5.6
5.4
5.2
5
4.8
4.6
$M_0 = 20M_\odot$ Case: D03ML $\alpha=10^{-3}$
Fractional Mass (M_r/M_0)
0.8
0.6
0.4
0.2
0
0
2
4
6
8
9.76
9.764
9.768
9.8
9.9
10
10.1
10.2
10.3
Age (10^6)

Fig D03ML 2

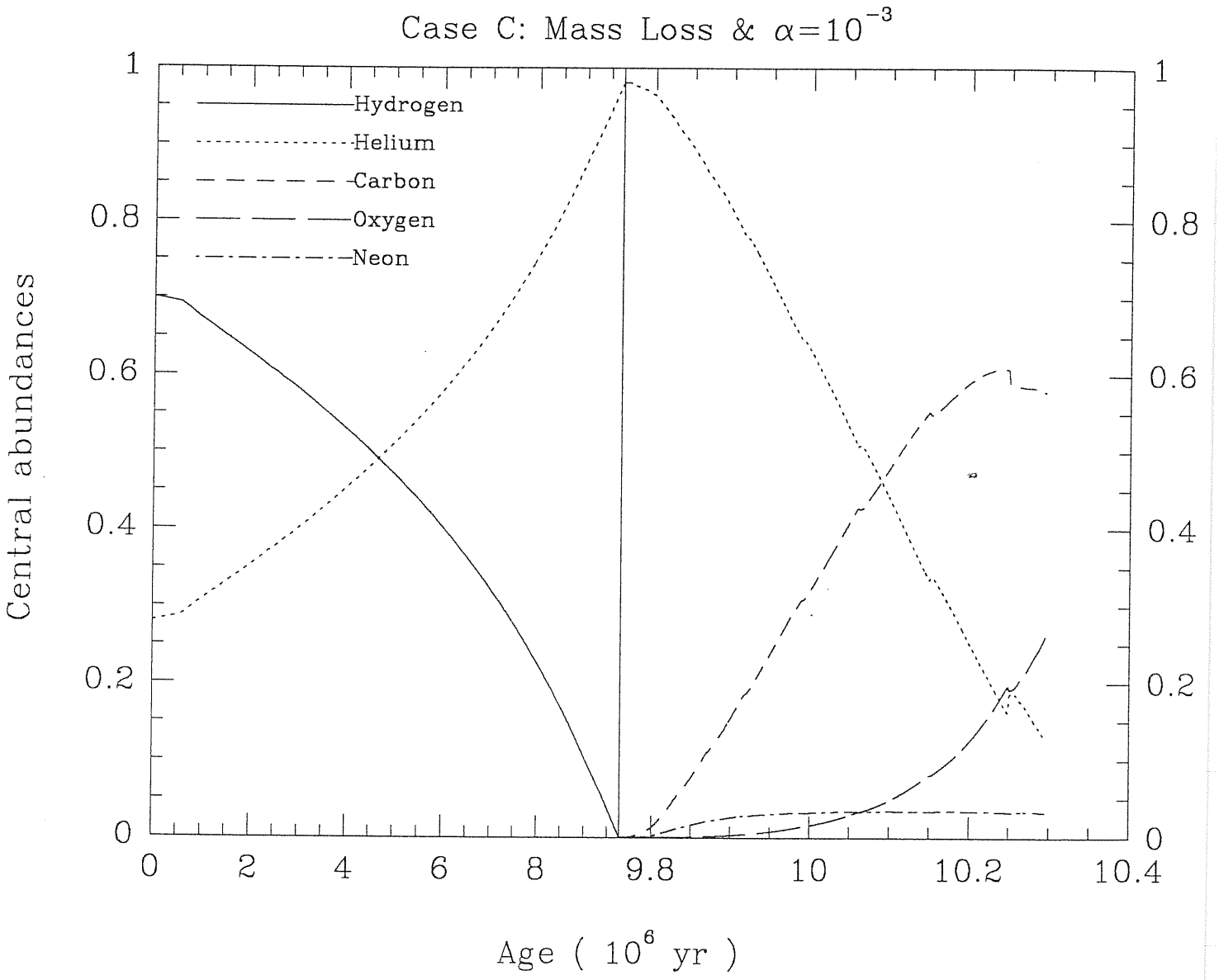
Case C: Mass Loss & $\alpha=10^{-3}$
Hydrogen
Helium
Carbon
Oxygen
Neon
Central abundances
Age (10^6 yr)
0
0.2
0.4
0.6
0.8
1
0
2
4
6
8
9.8
10
10.2
10.4

Table ( ) SC20

MOD	eta	dt/t	LogL	LogTE	Mbol	gms	rate	comp	Xsup	Ysup	Csup	Osup	Nsup	Conv	qhel	qcarox
At ZAMS:																
1	0.000	0.000	4.6455	4.5103	-6.84	20.00	0.00	0.700	7.00E-01	2.80E-01	4.36E-03	9.63E-03	1.06E-03	0.000	0.000	0.000
2	0.559	0.064	4.6529	4.5220	-6.86	20.00	0.00	0.692	7.00E-01	2.80E-01	4.36E-03	9.63E-03	1.06E-03	0.000	0.000	0.000
3	0.639	0.074	4.6572	4.5348	-6.87	20.00	0.00	0.689	7.00E-01	2.80E-01	4.36E-03	9.63E-03	1.06E-03	0.000	0.000	0.000
4	0.701	0.081	4.6590	4.5430	-6.88	20.00	0.00	0.687	7.00E-01	2.80E-01	4.36E-03	9.63E-03	1.06E-03	0.000	0.000	0.000
At the Lowest T eff on ZAMS:																
154	7.980	0.918	4.9928	4.4217	-7.71	20.00	0.00	0.029	7.00E-01	2.80E-01	4.36E-03	9.63E-03	1.06E-03	0.000	0.000	0.000
155	7.992	0.919	4.9937	4.4217	-7.71	20.00	0.00	0.027	7.00E-01	2.80E-01	4.36E-03	9.63E-03	1.06E-03	0.000	0.000	0.000
At Central H Exhausting:																
224	8.145	0.937	5.0433	4.4740	-7.84	20.00	0.00	0.000	7.00E-01	2.80E-01	4.36E-03	9.63E-03	1.06E-03	0.000	0.000	0.000
225	8.145	0.937	5.0435	4.4741	-7.84	20.00	0.00	0.980	7.00E-01	2.80E-01	4.36E-03	9.63E-03	1.06E-03	0.000	1.091	0.000
At He ignition:																
277	8.162	0.939	5.0350	3.9576	-7.82	20.00	0.00	0.980	7.00E-01	2.80E-01	4.36E-03	9.63E-03	1.06E-03	0.000	2.525	0.000
278	8.162	0.939	5.0278	3.9224	-7.80	20.00	0.00	0.979	7.00E-01	2.80E-01	4.36E-03	9.63E-03	1.06E-03	0.000	2.545	0.000
At the base of RGB:																
284	8.164	0.939	4.7157	3.6514	-7.02	20.00	0.00	0.979	7.00E-01	2.80E-01	4.36E-03	9.63E-03	1.06E-03	0.000	2.585	0.000
At the tip:																
322	8.219	0.945	5.1702	3.6089	-8.16	20.00	0.00	0.939	6.72E-01	3.08E-01	3.08E-03	8.57E-03	3.28E-03	0.000	2.980	0.000
At the end:																
880	8.696	1.000	5.1040	3.6140	-7.99	20.00	0.00	0.094	6.72E-01	3.08E-01	3.08E-03	8.57E-03	3.28E-03	0.000	3.587	0.000
At some specific points:																
148	7.882	0.906	4.9858	4.4242	-7.69	20.00	0.00	0.046	7.00E-01	2.80E-01	4.36E-03	9.63E-03	1.06E-03	0.000	0.000	0.000
225	8.145	0.937	5.0435	4.4741	-7.84	20.00	0.00	0.980	7.00E-01	2.80E-01	4.36E-03	9.63E-03	1.06E-03	0.000	1.091	0.000
253	8.159	0.938	5.0621	4.1461	-7.89	20.00	0.00	0.980	7.00E-01	2.80E-01	4.36E-03	9.63E-03	1.06E-03	0.000	2.423	0.000
454	8.375	0.963	5.1299	3.6091	-8.05	20.00	0.00	0.740	6.72E-01	3.08E-01	3.08E-03	8.57E-03	3.28E-03	0.000	3.322	0.000
760	8.614	0.991	5.0962	3.6144	-7.97	20.00	0.00	0.241	6.72E-01	3.08E-01	3.08E-03	8.57E-03	3.28E-03	0.000	3.543	0.000

Fig SC20 1

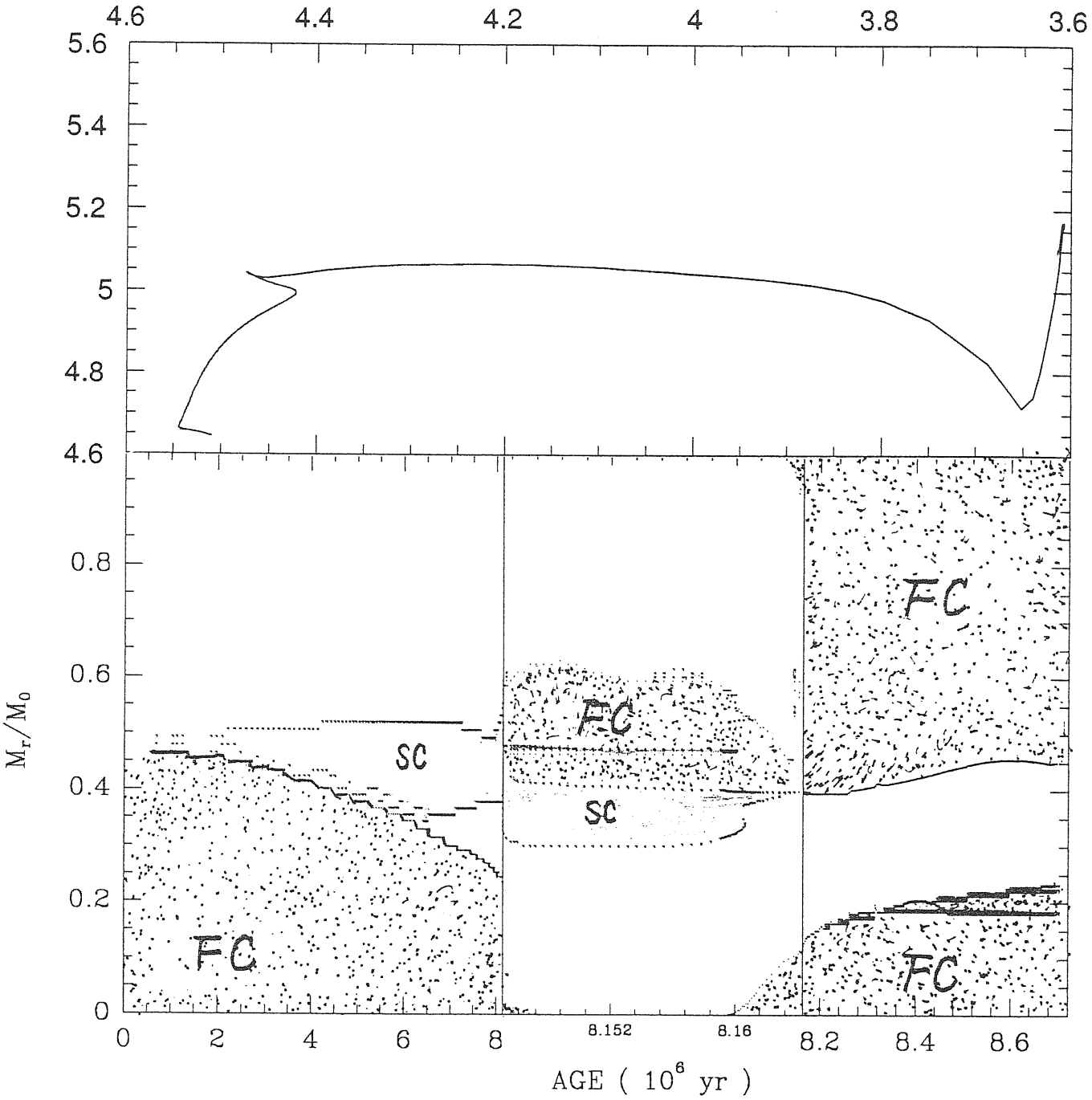
4.6
4.4
4.2
4
3.8
3.6
5.6
5.4
5.2
5
4.8
4.6
0.8
0.6
0.4
0.2
0
M_r/M_0
SC
FC
FC
SC
FC
FC
0
2
4
6
8
8.152
8.16
8.2
8.4
8.6
AGE (10^6 yr)

Fig SC20 8

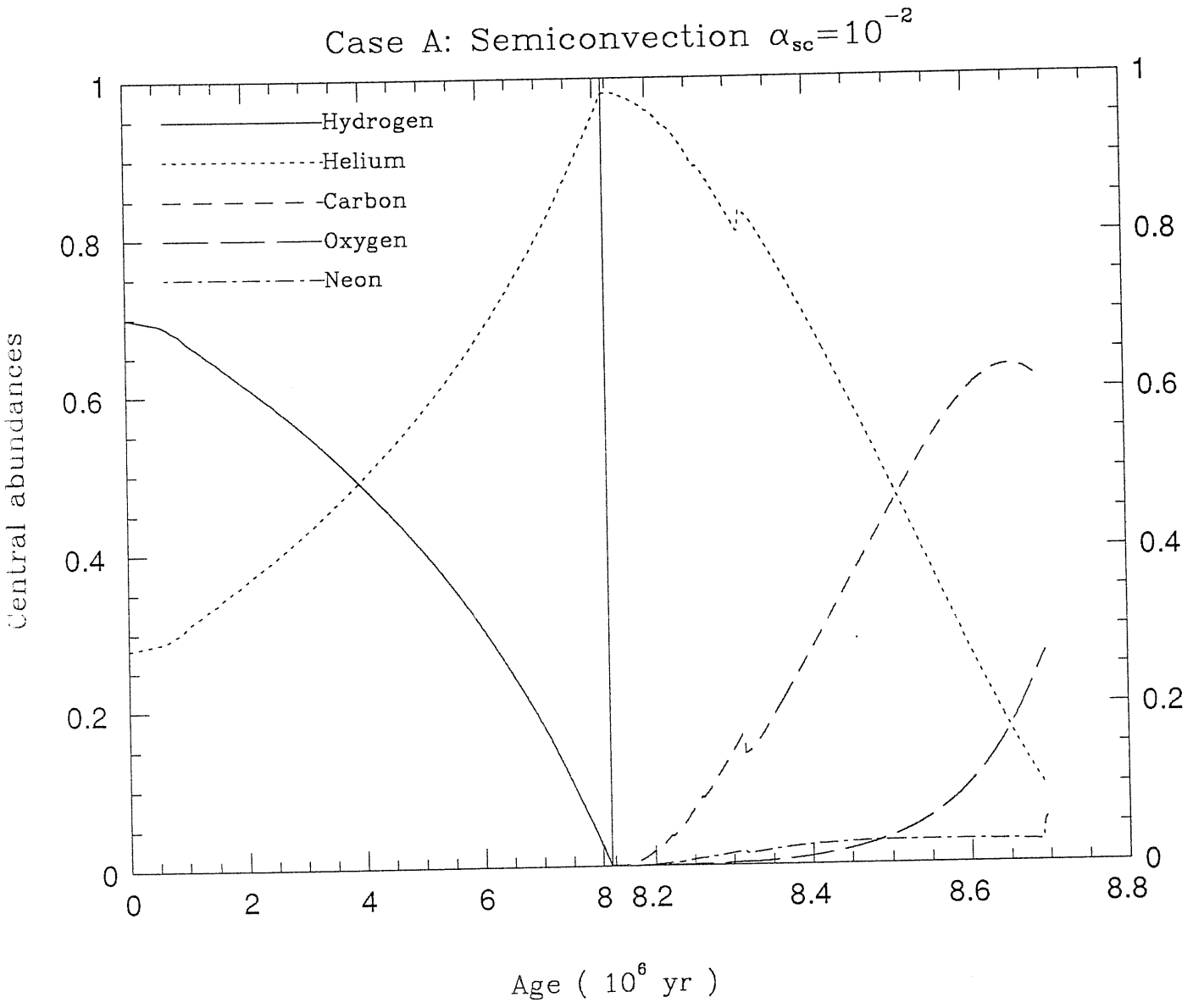
Case A: Semiconvection $\alpha_{sc}=10^{-2}$
Hydrogen
Helium
Carbon
Oxygen
Neon
Central abundances
Age (10^6 yr)
0
0.2
0.4
0.6
0.8
1
0
2
4
6
8
8.2
8.4
8.6
8.8

Fig SC20 3

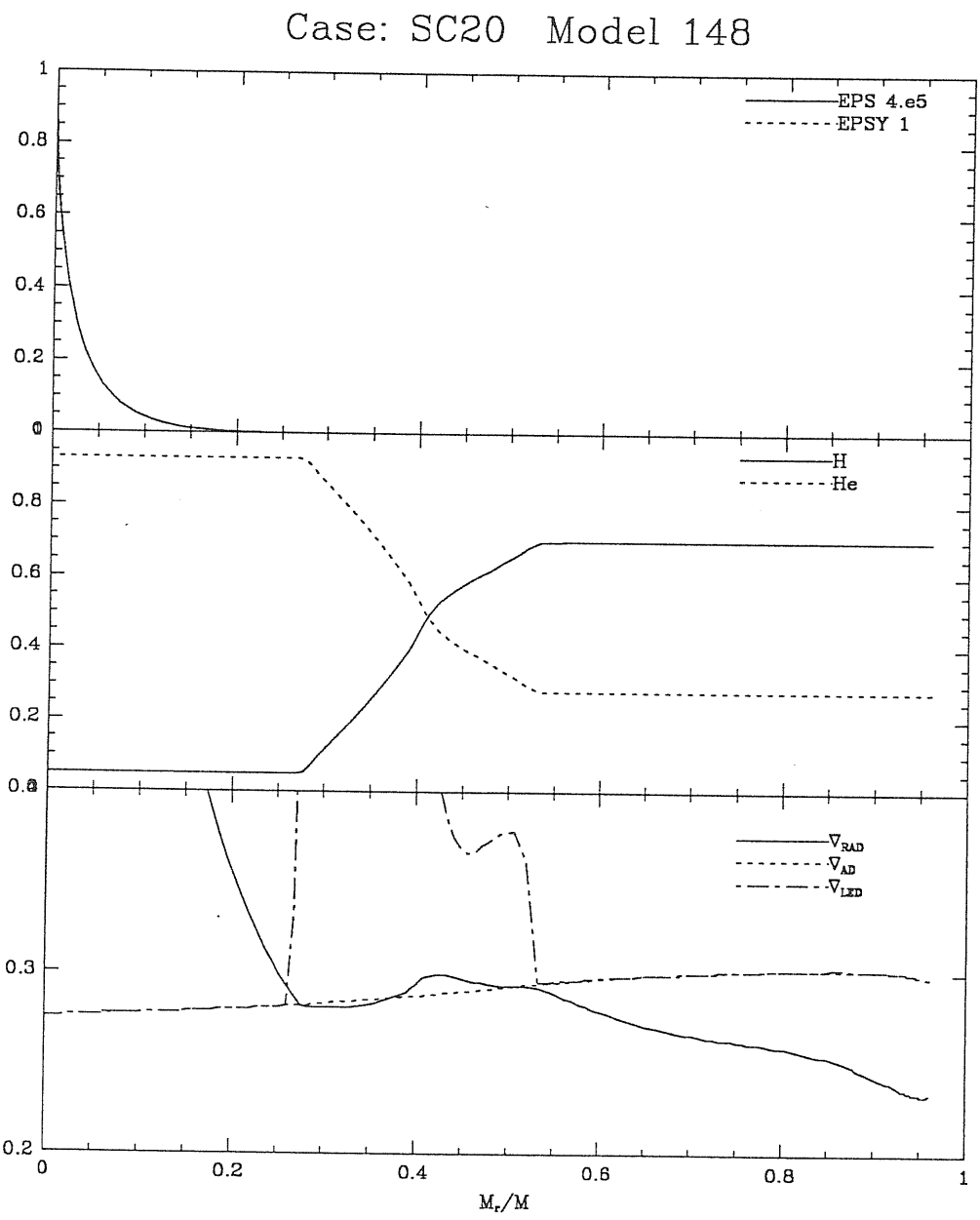
Case: SC20 Model 148
EPS 4.e5
EPSY 1
H
He
∇_{RAD}
∇_{AD}
∇_{LED}
1
0.8
0.6
0.4
0.2
0
0.3
0.2
0
0.2
0.4
0.6
0.8
1
M_r/M

Fig SC20 4

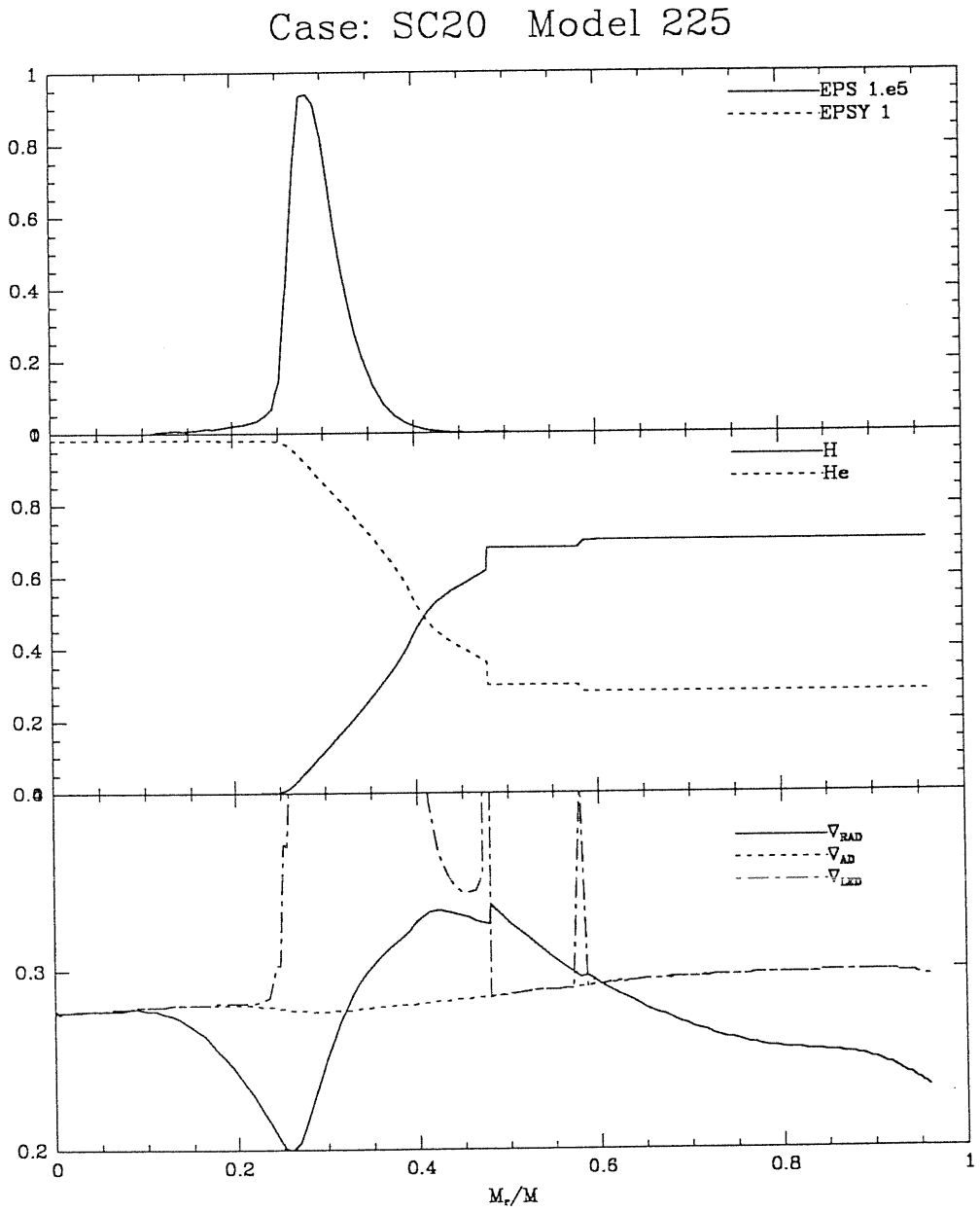
Case: SC20 Model 225
EPS 1.e5
EPSY 1
H
He
∇_{RAD}
∇_{AD}
∇_{LED}
0
0.2
0.4
0.6
0.8
1
0.3
M_r/M

Fig SC20 5

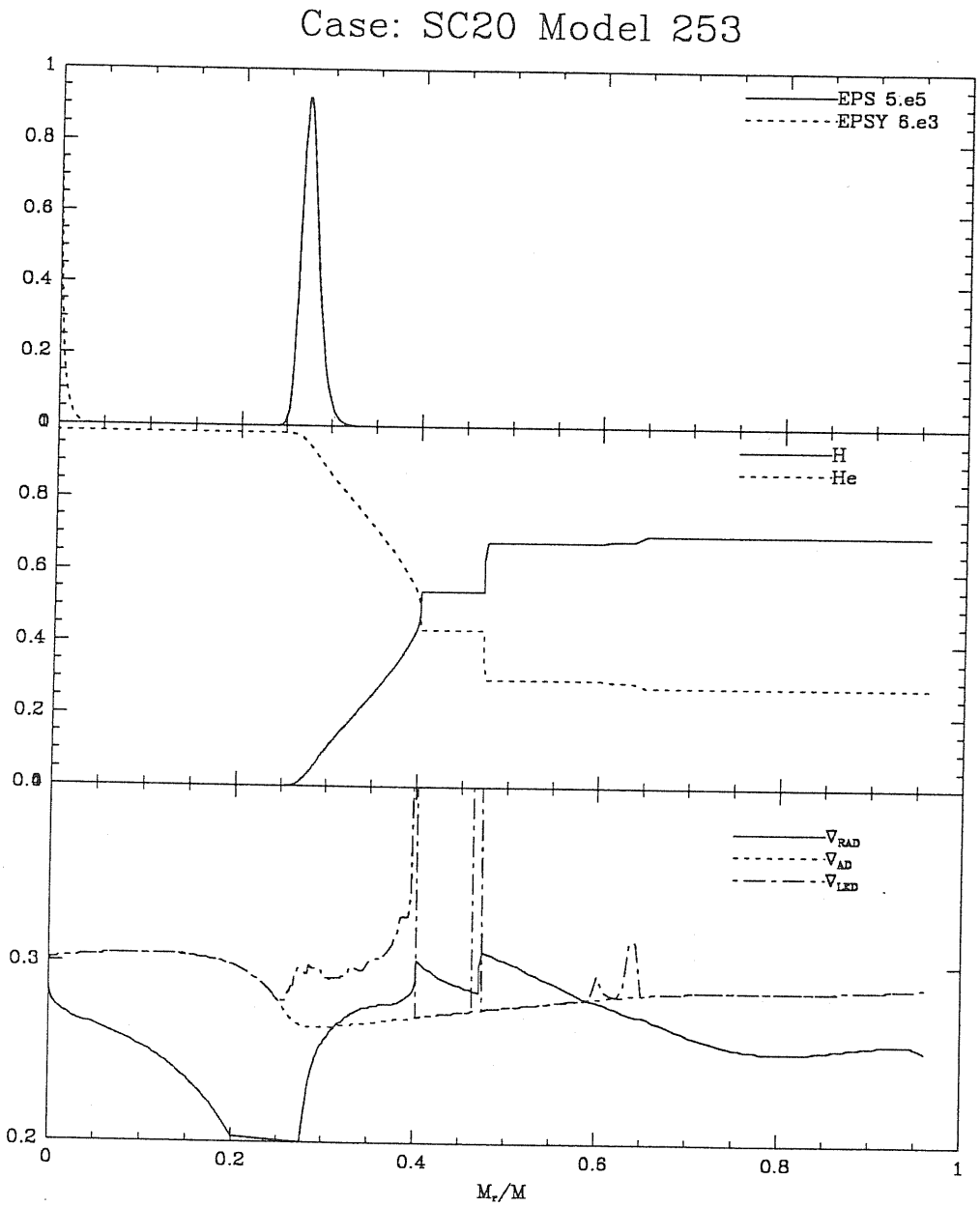
Case: SC20 Model 253
EPS 5.e5
EPSY 6.e3
H
He
∇_{RAD}
∇_{AD}
∇_{LED}
1
0.8
0.6
0.4
0.2
0
0.3
0.2
0
0.2
0.4
0.6
0.8
1
M_r/M

Fig SC20 6

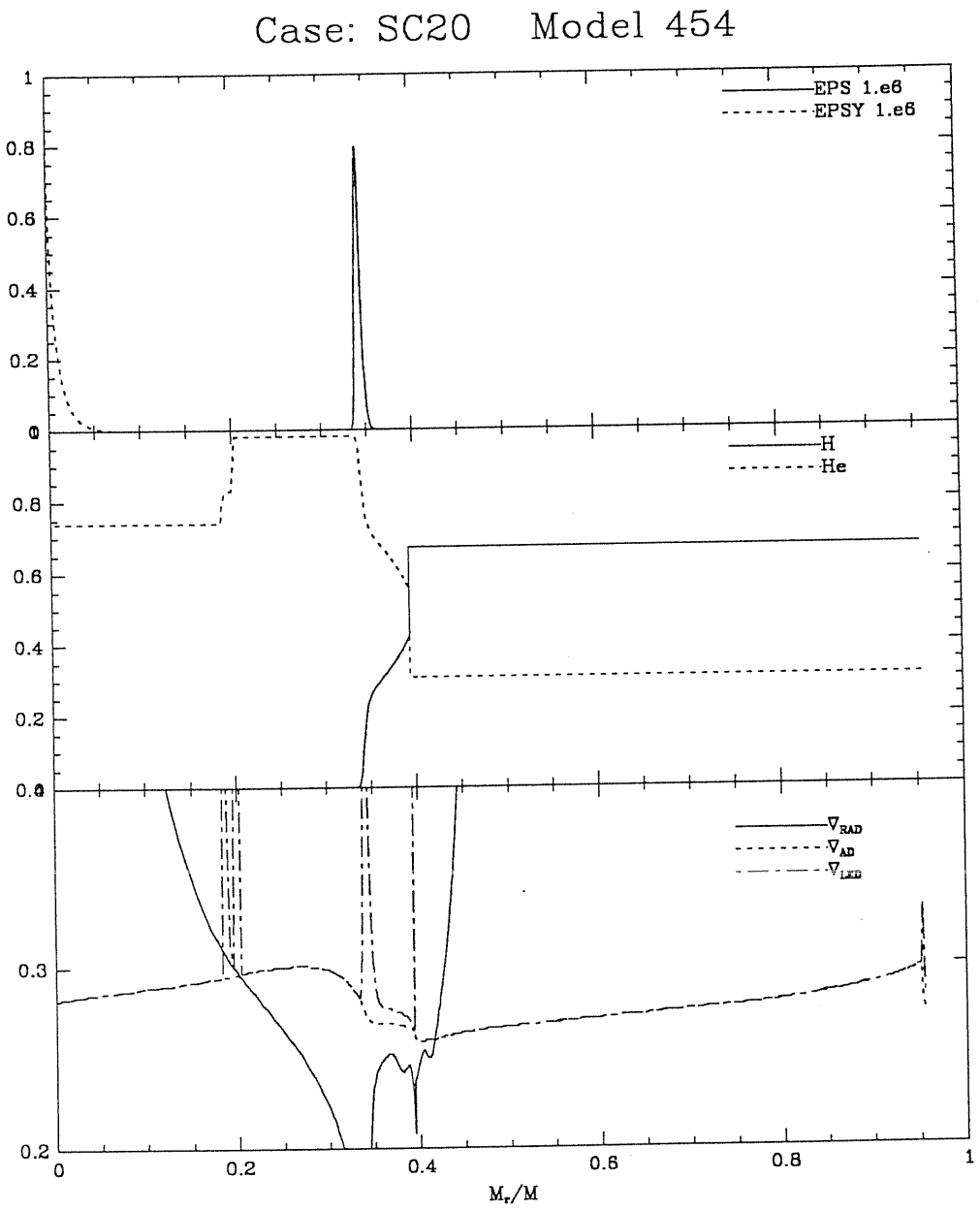
Case: SC20 Model 454
EPS 1.e6
EPSY 1.e6
H
He
∇_{RAD}
∇_{AD}
∇_{LED}
0
0.2
0.4
0.6
0.8
1
0.3
M_r/M

Fig SC 20 7

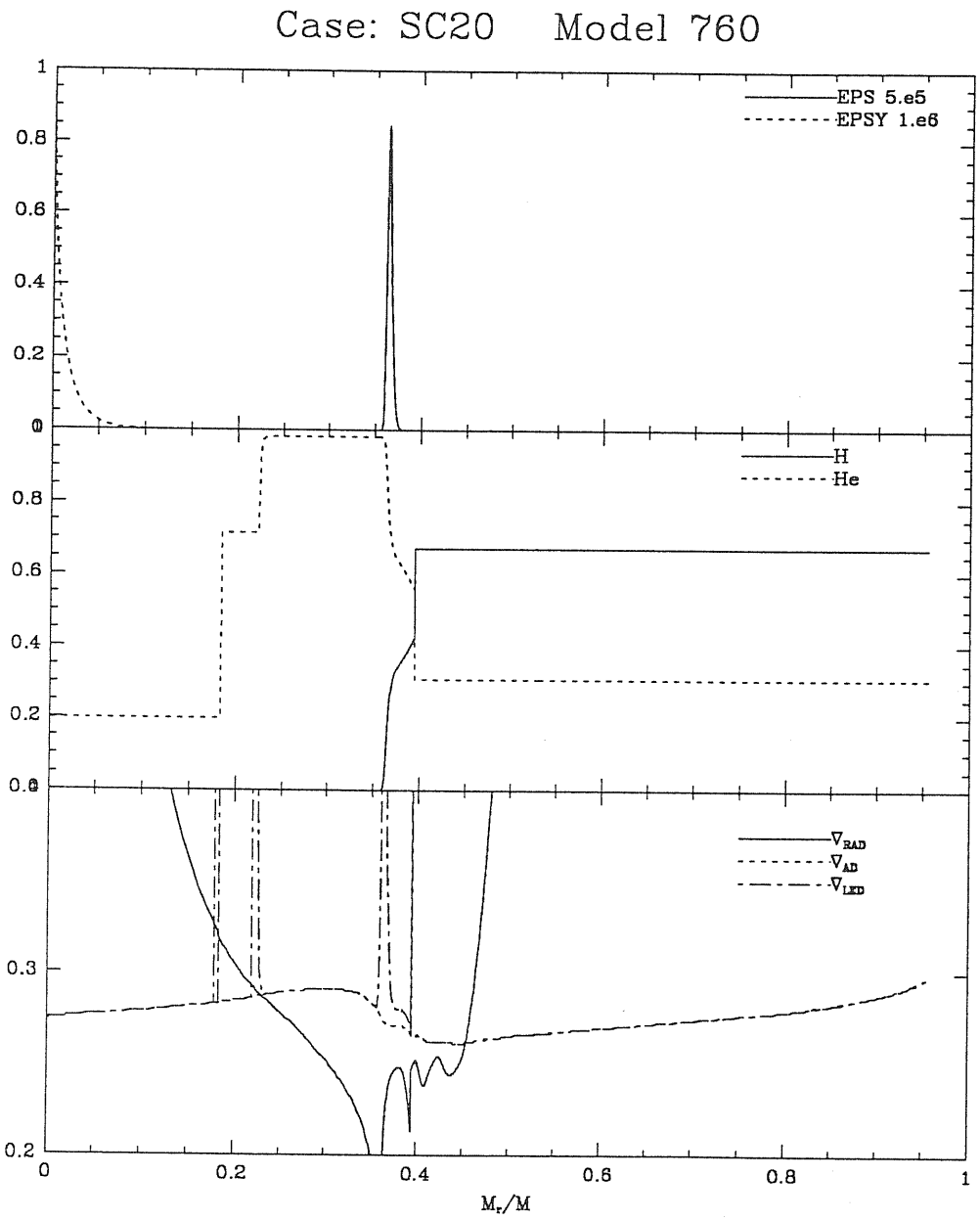
Case: SC20 Model 760
EPS 5.e5
EPSY 1.e6
H
He
∇_{RAD}
∇_{AD}
∇_{LED}
1
0.8
0.6
0.4
0.2
0
0.3
0.2
0
0.2
0.4
0.6
0.8
1
M_r/M

Chapter 6

Conclusion and future work

The present work is based on the assumption that overshooting can be treated as a diffusive mixing process. Models of a 20 solar mass star are constructed with the help of the code of the Padova stellar evolution group. To test the numerical method, models of the same diffusion scheme are made. Comparison shows our method is quite workable, despite some problems related to the link between the diffusive treatment of chemicals and the chemical routines in the main code, which lead to the failure near the end of helium burning.

Xiong' model with a large overshooting distance is modelled with our method. Comparative studies show that most of the features of Xiong's results on massive stars can be reproduced by introducing a large mixing extension in the core but some of them still remain. The radiative overshooting is to be tested in the future.

Our results at present are not ready for comparison with observation, but the preliminary models computed with our mixing scheme shows some interesting features on the evolutionary tracks in the HR diagram. For the assumed diffusive mixing for all possible mixing regions, our models perform a loop in the core helium burning phase. This may be able to account for the ledge. Current models with mass loss and core overshoot alone (Maeder and Meynet, 1987, 1988, 1989; Maeder 1990) cannot be used because they

ingnite and spend the whole core helium burning phase as red supergiant. Therefore, not only the ledge, but also the existence of stars in the middle of the HRD cannot be explained. The inclusion of overshoot at the base of the convective envelope (Alongi et al 1991) favours the extension of the loops. Our model with diffusive overshoot possesses the same advantages (main sequence width, star counts) of the overshoot model, and perform a loop, which is not found for the abundances used in this work for the instant overshoot model.

The semiconvection is a subject stimulated by the explosion of SN1987A. Observational evidence shows that the progenitor was a blue supergiant which came from the red side shortly before the explosion or a star even in the blue. A theoretical approach to the evolution of this progenitor by semiconvective models turns out to be very successful but those models cannot fit many other observations for the vast majority of stars. It will be a great puzzle in stellar evolution theory if it is shown that the blue progenitor is not a peculiar object. Current stellar evolution theory with overshooting could not account for such an evolutionary scenario. The general understanding of this problem is that the same evolutionary models must take into account the properties as well as of the population of supergiant stars. This makes a very interesting point to study. The code still has some problems for the treatment of mixing, and before we go further into this problem, this must be solved.

I also want to apply the diffusive mixing methods to low mass stars. The evolution of these stars is subject to intensive studies, and the observation gives a lot of interesting points related to the mixing treatment. The ratio of star counts in the horizontal branch to that of stars setting at higher luminosity than the horizontal branch gives a very sensitive indicator of the primodial helium abundance. This must be considered as a very good application and test of the mixing mechanisms.

REFERENCES

Alexander, D. R., 1975, Ap. J. Suppl. **29**, 363.

Alexander, D. R.,et al, 1983, Ap. J., **273**, 773.

Alongi, M., Bertelli, G., Bressan, A., Chiosi, C., 1991, A. Ap. **244** 95.

Backer, N.H., Kuhuβ, R., 1987, A. Ap., **185**, 117.

Bertelli, G., Bressan, A., Chiosi, C., 1984, **130**, 279.

Bessell, M.S. et al, 1989, AAS **77**, 1.

Biermann, L., 1976, Proceedings of IAU Colloquium No. 38, 4.

Böhm, 1976, Proceedings of IAU Colloquium No. 38.

Böhm-Vitense, 1958, Z. Astrophys., **46**, 108.

Bressan, A., 1984, Unpublished SISSA Thesis.

Bressan, A, 1989, Italian National School for Astronomy, proceedings, 1990

Bressan, A., Bertelli, G., Chiosi, C., 1981, A. Ap., **102**, 25.

Castor, J.I., Abbot, D.C., Klein, R.I., 1975, Ap.J., **195**, 157.

Caughlan, G. R., Fowler, W. A., Harris, M., Zimmermann, B. 1985, Atomic Data Nuc. Data Tables **32**, 197.

Chang, J. S., Cooper, G, 1970, J. Comp. Physics, **6**, 1.

Chiosi, C., Bertelli, G., Bressan, A., 1991, Ap. J.,(in press)

Chiosi, C., Maeder, A. 1986, Ann. Rev. A. Ap., **26**, 329.

Chiosi. C., Nasi, E., 1974, Astro. Space Sci., **56**, 431.

Chiosi, C., Nasi,E., Sreenivasan, S. R., 1978, AA. **63**, 103.

Chiosi, C., Wood, P. R., Bertelli, G., Bressan, A., Mateo, M.,1991, Ap. J., (in press).

Chiosi, C., Summa, C., 1970, Astr. Space Sci., **8**, 478.

Cloutman, L. D., Eoll, J. D., 1976, Ap. J., **206**, 548.

Cloutman, L. D., Whitaker, R. W., 1980, Ap. J., **237**, 900.

Cox, J.P., Giuli, R. T., 1968, *Stellar Structure.*

Cox, A. N., Stewart, J. N., 1970, Ap. J., **19** 243.

Cranck, J., 1986, *The Mathematics of Diffusion*, Clarendon Press.

Eggleton, P.P., 1971, M. N. R. A. S., **151**, 351.

Eggleton, P.P., 1972, M. N. R. A. S., **156**, 316.

Fowler, W. A., et al, 1975, Annu. Rev. Astron. Astrophys. **13** 69.

Gough, D. O., 1969, J. Atmos. Sci., **26**, 448.

Greggio, L. 1984, *In Observational Tests of the Stellar Evolution Theory*, ed. A. Maeder, A. Renzini, p. 329.

Jost, W., 1960, *Diffusion in Solids, Liquids, Gases.*

Kato, S., 1966, Publ. Astron. Soc. Japan, **18**, 374.

Kettner, K. U. et al 1982, Z. Phys. A-Atoms and Nuclei **308**, 73.

Kippenhahn, R., Wiegert, A., 1991, *Stellar Structure and Evolution*, Springer-Verlag.

Kippenhahn,R., Weigert, A., Hofmeister, E., 1967, Meth. Com. Phys., **7**, 129.

Landau and Lifshitz, 1987, *Fluid Mechanics*, Pergamon Press.

Langer, N., 1989a, AA **210**, 93.

Langer, N., 1989b, AA **220**, 135.

Langer,N., El Eid, M.F., Fricke, K.J., 1985, A. Ap., **145**, 179.

Langer,N., Sugimoto,D., Fricke,K.J., 1983, A. Ap.,**126**, 207.

Ledoux,P., 1947, Ap.J., **105**, 205.

Maeder, A., 1975, A. Ap. **164**, 45.

Maeder, A., 1983, A. Ap. **120**, 113.

Maeder, A., Meylan, G., 1989, A. Ap., **210**, 155.

Mermoiloid, J.C., Maeder, A., 1982, A. Ap., **189**, 34.

Meylan, G., Maeder, A., 1982, A. Ap., **108**, 148.

Munakata, H., et al, 1985, Ap. J., **295** 197.

Parildrach, A., Puls, J., Kudrizki, R.P., 1986, A. Ap., **164**, 86.

Renzini,A., 1987, A. Ap., **188**, 49.

Roxbough, I., 1965, M.N.R.A.S., **130**, 223.

Sakashita,S., Hayashi,C., 1961 Prog. Theor. Phys. Kyoto, **26**, 942.

Saslow, W.C., Schwarzschild, M., 1965, Ap.J., **142**, 1468.

Schwarzschild, M., Härm, R., 1958, Ap.J., **128**, 348.

Shariv, G., Salpeter, E.E., 1973, Ap.J., **184**, 191.

Simpson, E.E., 1971, Ap.J., **188**, 166.

Spiegel, E.A., 1960, Ap.J., **132**, 716.

Spiegel, E.A., Veronis, 1960, Ap.J., **131**, 442.

Seecnivansan, S.R., Wilson, W.J.F., 1978, Astro. Space Sci. **53**, 193.

Stothers, R., 1970, M.N.R.A.S., **151**, 65.

Ulrich, R.K., 1970, Astro. Space Sci., **7**, 183.

Unno, W., 1967, Publ. Astron. Soc. Japan, **18**, 40.

Vitense, E., 1953, Z. Astrophys., **46**, 108.

Weaver, T.A.,Woosley, G.B., 1978, Ap.J. **225**, 1021.

Weiss, A., 1989, Ap. J., **339** 365.

Woosley, S. E., 1988, Ap. J.,**330**, 218.

Xiong, D., 1985, A. Ap., **150** 133.

Xiong, D., 1986, A. Ap., **167**, 239.

Xiong, D., 1990, A. Ap., **232**, 31.

ACKNOWLEDGEMENTS

First of all I am very grateful to Profs. Chiosi and Sciama who offered me the chance to be here in Trieste. I want to express my gratitude to Dr. A. Bressan for all the continuous encouragement, help and enormous discussions during the work for this thesis. Of course, I would like to say " Xie Xie !" to all of my friends here in SISSA who offered me so great favour.